

# **Visual and Auditory Perceptual Decision-Making in The Human Brain as Investigated by fMRI and Lesion Studies**

Dissertation

for the award of the degree

“Doctor rerum naturalium (Dr. rer. nat.)”

of the Georg-August-University Göttingen

within the doctoral program Neuroscience

of the Georg-August University School of Science (GAUSS)

Submitted by

Ahmad M. Nazzal

from Amman, Jordan

Göttingen

March 2017

## **Thesis Committee Members**

Prof. Dr. Melanie Wilke  
Dept. of Cognitive Neurology  
University Medical Center Goettingen

Prof. Dr. Mathias Bähr  
Dept. of Neurology  
University Medical Center Goettingen

Prof. Dr. Tobias Moser  
Institute for Auditory Neuroscience & InnerEarLab  
University Medical Center Goettingen

## **Members of the Examination Board**

Referee: Prof. Dr. Melanie Wilke  
Dept. of Cognitive Neurology  
University Medical Center Goettingen

2<sup>nd</sup> Referee: Prof. Dr. Mathias Bähr  
Dept. of Neurology  
University Medical Center Goettingen

## **Further members of the Examination Board**

Prof. Dr. Tobias Moser  
Institute for Auditory Neuroscience & InnerEarLab  
University Medical Center Goettingen

Dr. Igor Kagan  
Decision and Awareness Group  
German Primate Center

Pooresmaeili, Arezoo, MD, PhD  
Perception and Cognition Group  
European Neuroscience Institute, Göttingen, Germany

PD Dr. Peter Dechent  
Dept. of Cognitive Neurology  
University Medical Center Goettingen

Date of oral examination: 26<sup>th</sup>. May. 2017

## **Acknowledgments**

Foremost, I would like to express my sincere gratitude to my advisor Prof. Dr. Melanie Wilke for her inspiring commitment towards science, and the freedom she gave me to develop my own scientific interest. I would like to thank the rest of my thesis committee members: Prof. Dr. Mathias Bähr and Prof. Dr. Tobias Moser for their insightful comments and guidance. My deepest thanks go to Carsten Schmidt-Samoa and Dr. Jeffrey C Erlich for being generous with their time, knowledge, and expertise. It would have never been possible to finish this work without their valuable comments and feedback. I thank my fellow lab members in the cognitive neurology department: Laura Geurts, Marie Dewenter, Yian Liaw, Yuranny Cabral-Calderin, Eva Poland, Kathleen Williams, Kristina Miloserdov, Severin Heumüller, Dr. Iris Steinmann, and Dr. Peter Dechent for stimulating discussions and friendship. Many thanks to Dr. Igor Kagan for his comments and questions. Countless thanks to the lab technicians Ilona Pfahlert, who made the lab feels like home, and Britta Perl for their support in imaging data acquisition. I thank Regina Vinnen for her support in administrative issues. I am grateful to Prof. Dr. Michael Hörner for his wisdom and advice. I appreciate Dr. Zsolt Turi for his friendship and motivation. I wholeheartedly thank my sister Ranah Nazzal for her unconditional support and love. Finally, I am most grateful to my wife Haneen Eid for believing in me.

## Table of contents:

|   |    |
|---|----|
| Abstract.....   | 1  |
| 1. General Introduction.....  | 3  |
| 1.1 Perceptual decision-making.....   | 4  |
| 1.2 Tasks in the study of perceptual decision-making.....   | 6  |
| 1.3 Theoretical background and models.....  | 10 |
| 1.3.1 Signal detection theory.....  | 10 |
| 1.3.2 Sequential probability ratio theory.....  | 12 |
| 1.3.3 Biophysically plausible models: Integrate-and-fire<br>attractor models.....                   | 14 |
| 1.4 Bridging the gap between neural processes and behavioral<br>outcome.....                        | 16 |
| 1.5 Neural correlates of sensory evidence accumulation in the non-<br>human primate literature..... | 17 |
| 1.6 Sensory evidence accumulation: signals and task difficulty....                                  | 19 |
| 1.7 Blood oxygen level dependent signal .....   | 20 |
| 1.8 Neural correlates of sensory evidence accumulation from<br>human fMRI.....                      | 22 |
| 2. Confidence in the decision.....  | 28 |
| 2.1 Definition of confidence in the decision.....   | 28 |
| 2.2 Confidence rating measures .....  | 29 |
| 2.3 Methods for quantifying confidence.....   | 31 |

|      |   |    |
|------|---|----|
| 2.4  | The study of confidence in animals .....  | 32 |
| 2.5  | Neural correlates of confidence in animals .....  | 33 |
| 2.6  | Architecture of confidence forming network .....  | 34 |
| 2.7  | Neural correlates of confidence in human fMRI .....   | 36 |
| 2.8  | Efforts to disentangle neural correlates of confidence in the<br>decision from neural correlates of sensory evidence<br>accumulation in humans..... | 37 |
| 2.9  | Methods in investigating confidence using fMRI.....   | 38 |
| 3.   | Spatial decision-making .....   | 40 |
| 3.1  | Anatomy of sound localization .....   | 40 |
| 3.2  | Functional anatomy of sound localization from human<br>neuroimaging studies.....  | 41 |
| 3.3  | Functional anatomy of visual-spatial processes.....   | 42 |
| 3.4  | Lateralization of spatial processes as a multi-modal property of<br>the brain.....  | 43 |
| 3.5  | Hemispatial neglect syndrome as a model for studying causal<br>contribution of lesions in spatial decision-making deficits....                      | 44 |
| 3.6  | Neglect and extinction.....   | 45 |
| 3.7  | Deficits in sound localization from the literature on neglect...  | 46 |
| 3.8  | Theories in neglect.....  | 47 |
| 3.9  | Causality and the study of lesions.....   | 49 |
| 3.10 | Issues in the study of lesions effect on cognitive tasks.....   | 50 |

|       |  |     |
|-------|--|-----|
| 3.11  | Voxel-based lesion-symptom mapping.....  | 51  |
| 4.    | The scope of the manuscript.....   | 52  |
| 5.    | Empirical studies.....   | 53  |
| 5.1   | Modality-specific neural signatures of perceptual evidence<br>accumulation: a model-based fMRI approach.....                                       | 54  |
| 5.2   | Dissociated neural signature of visual sensory evidence<br>accumulation and decision-monitoring.....   | 100 |
| 5.3   | Voxel-based lesion-symptom mapping of the effect of cortical<br>and subcortical lesions on auditory and visual perceptual decision-<br>making..... | 142 |
| 6.    | General discussion.....  | 175 |
| 6.1   | How the studies are related to each other .....  | 176 |
| 6.2   | Relations of our studies to the literature on perceptual decision-<br>making .....   | 178 |
| 6.2.1 | Rodents .....  | 178 |
| 6.2.2 | Non-human primates .....   | 180 |
| 6.2.3 | Human neuroimaging .....   | 183 |
| 6.3   | Dealing with crisis of reproducibility and interpretability...   | 184 |
| 6.4   | General limitations .....  | 189 |
| 6.5   | Closing remarks and outlook .....  | 190 |

|                           |     |
|---------------------------|-----|
| 7. Appendix .....         | 191 |
| 7.1 Figures list .....    | 191 |
| 7.2 Tables list .....     | 192 |
| 8. References .....       | 193 |
| 9. Curriculum Vitae ..... | 211 |

**Abstract:**

Perceptual decision-making refers to the act of choosing one option from a set of alternatives based on the available sensory information. In this manuscript, we used model-based functional magnetic resonance imaging and lesions studies to investigate auditory and visual perceptual decision-making.

In the first study, we demonstrated that spatially-specific sensory evidence, when decoupled from motor plans, accumulates in modality-specific sensory cortices: Occipital regions showed signals correlated to spatially-specific accumulated visual sensory evidence, and superior temporal regions showed signals correlated with spatially-specific accumulated auditory evidence. On the other hand, signals in the frontal and parietal regions were modulated by the level of accumulated sensory evidence in a spatially non-specific manner for both modalities; when the level of evidence was low, the signal in the frontal and parietal regions was stronger regardless of the sensory modality. Thus, the well-known signatures of evidence accumulation observed in frontal and parietal cortices described in the literature might reflect secondary decision processes such as saliency.

In the second study, we investigated the neural correlates of visual confidence in the decision. We used model-based fMRI to investigate the neural correlates of visual perceptual decision-making and devised criteria based on predictions from integrate-and-fire attractor models to identify neural correlates of



confidence in the decision. We managed to disentangle the neural correlates of sensory evidence accumulation from neural correlates of decision monitoring; confidence in the decision and error detection. We found that the signal in the occipital cortex was modulated by visual sensory evidence accumulation while the frontal and midbrain regions had signals suggestive of decision monitoring.

In the third study, we investigated the effect of cortical and subcortical lesions on auditory and visual perceptual decision-making. We formulated an fMRI-driven hypothesis based on the findings from our fMRI studies. We used voxel-based lesion-symptom mapping to investigate the role of lesions on patients' behavior in a voxel-by-voxel manner. Data from the patients suggests a role of the right parietal cortex in auditory task performance as predicted by the fMRI study.

Together, our results help to reveal the neural correlates of auditory and visual perceptual decision-making in human beings, explore neural correlates of visual decision-monitoring, and provide insights into the underlying mechanisms of the auditory and visual hemispatial neglect syndrome.

## **1. General introduction:**

On a daily basis, people make hundreds of decisions. Imagine, for example, the decision to cross a street. Superficially such a decision might sound trivial. However, it has been shown that deciding when it is safe to cross a street based on potential gaps in the traffic is a complex everyday task involving several functional abilities (Tournier, 2016). In identifying a crossing-gap one has to wait, look around, gather visual and auditory information, and evaluate input, and then make the decision to cross. If it is foggy, it will be more difficult to make safe street-crossing decisions, and one might take longer to decide. Moreover, it is important to be able to determine how confident one is in the decision. A correct estimation of the confidence in the decision allows one to collect more information in case of uncertainty. This plays an important role in the optimization of decisions in general (Schwartenbeck, 2015). As such, forming even trivial decisions and evaluating the level of confidence in decisions are intricate, complex cognitive processes that are hard to study and crucial to understand.

## 1.1 Perceptual decision-making

Perceptual decision-making refers to the act of choosing one option from a set of alternatives based on available sensory information (Heekeren, 2008). Making a perceptual decision involves several highly collinear parallel cognitive processes (Cisek, 2012) (**Figure 1.1**).

### 1. Task stage (observable)

---

|  |                     |                |                               |
|--|---------------------|----------------|-------------------------------|
|  | Sensory processing  | Categorization | Sensory evidence accumulation |
| <b>2. Decision formation stage</b><br>(unobservable) | Reward              | Attention      | Effort                        |
|  | Decision monitoring | Uncertainty    | Preference                    |
|  | Motor preparation   | Expectations   | Response selection            |

---

### 3. Motor response stage (observable)

Figure 1.1. **Outline for studying perceptual decisions.** (1) Task stage: stimuli designed by the experimenter are presented to the participant (2) Decision formation stage: several collinear cognitive processes are computed in the participant's brain. (3) Motor response stage: the participant responds by hand movement, eye movement, or verbal response, which can be recorded by the examiner. (Modified from Hebart, 2014)

Perceptual decision-making processes can be categorized into core decision-making processes (Erlich, 2015), and secondary decision-making processes (Katz, Yates, Pillow, & Huk, 2016) (**Figure 1.2**). One core decision-making strategy is sensory evidence accumulation. Brains reconstruct the external world on the basis of input from sensory receptors; this input is the sensory evidence. When choosing between two alternatives in the case of forming perceptual decisions the brain has to be able to retain the memory of previous sensory evidence favoring one alternative and has to have the ability to add new sensory evidence over time which supports that alternative; hence accumulation. This is the origin of the term “sensory evidence accumulation”. However, in order to disentangle the neural correlates of core decision-making processes such as sensory evidence accumulation from secondary decision-making processes such as saliency, or confidence in the decision is a challenging task (Gold & Shadlen, 2007). To do so in a laboratory setup, we simulate complex reality using simple tasks involving controlled stimuli, record motor outputs, and record neural signals.

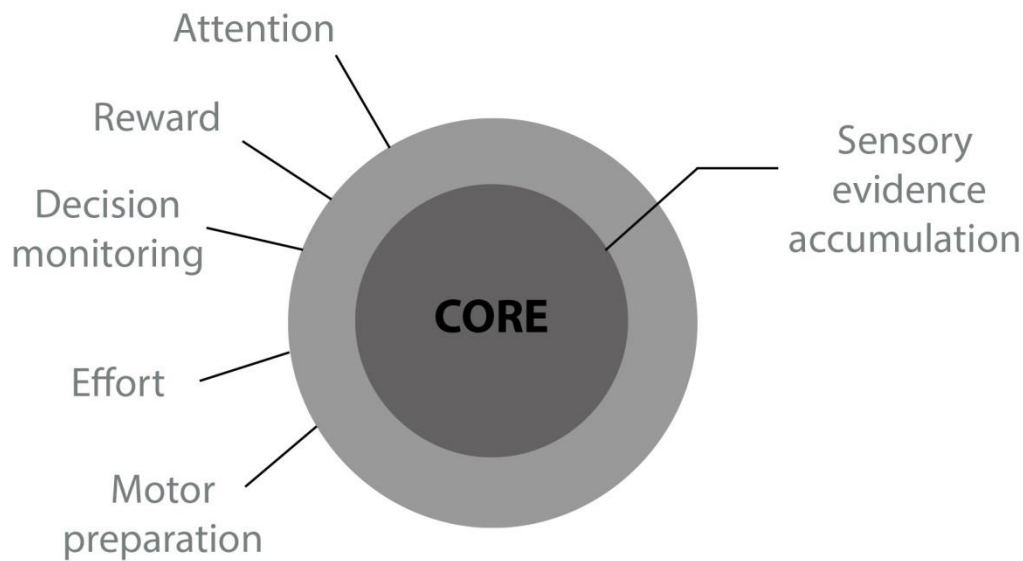


Figure 1.2. **Taxonomy of processes in perceptual decision-making.** Perceptual decision-making processes can be categorized into core decision-making process such as sensory evidence accumulation and secondary decision-making process that can influence the decision making process such as attention, reward, and effort. Cognitive processes involved in decision formation are collinear and computed in parallel (Modified from Hebart, 2014).

### ***1.2 Tasks in the study of perceptual decision-making:***

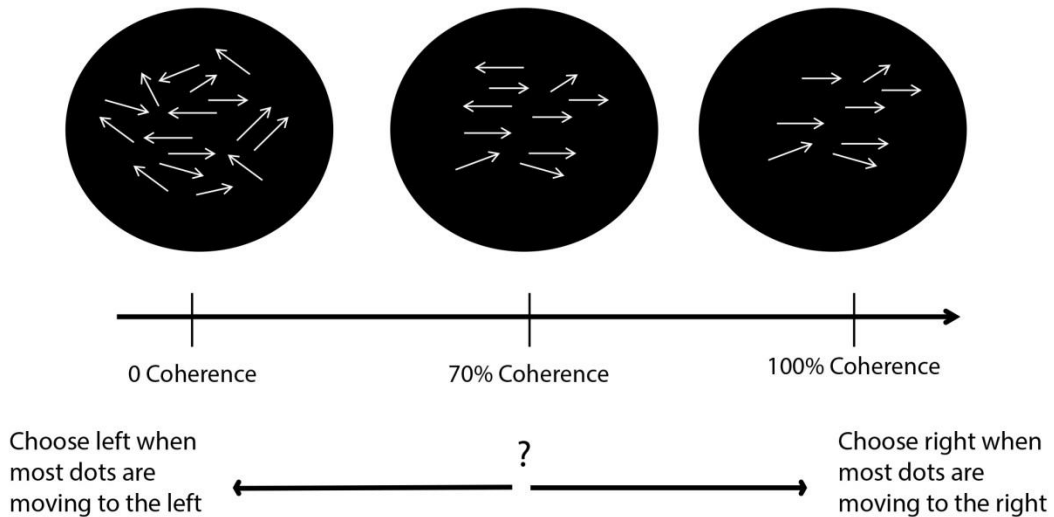
Several tasks that allow controlled experimental manipulation were developed to study perceptual decision-making (Gold & Shadlen, 2007; Heekeren, 2008). Such tasks share their ability to test a subject's performance with regard to accuracy and reaction time. The tasks used in the study of perceptual decisions are often visual tasks. In the visual domain, popular tasks are random dot motion (RDM) (Newsome & Pare, 1988) or feature distinction tasks involving faces and houses (Heekeren et al., 2004). One of the most successful tasks in the perceptual decision-making literature is the random dot motion (RDM) task (Newsome & Pare, 1988). In the RDM the subjects view a cloud of moving dots

which can move to the right or the left (**Figure 1.3A**). Typically, a few dots move in the same direction from one frame to the next while the rest serve as noise. If for example, ninety percent of the dots moved to the right the trial is considered to have high coherency. If sixty percent of the dots moved to the right, the trial has low coherency. Subjects are required to report the direction of motion. The reason for the test's popularity is that motion is a well-studied function of the visual system. Also, the neural basis of motion detection has been well characterized in primate and human studies. Moreover, the duration of the stimuli can be varied. This allows one to test free-response paradigms (reaction time paradigms) that study accuracy-speed tradeoffs, as well as delayed paradigms that target the role of working memory in perceptual decision-making.

On the other hand, there are fewer tasks available to test other sensory modalities, i.e. somatosensory (Romo, 1998), olfactory (Uchida & Mainen, 2003) and auditory modalities (Binder, 2004). In the Binder study, the auditory task was a syllable detection task. The subjects had to press a button indicating whether a syllable had been presented first or second. As such, this task is not ideal for specifically studying sensory evidence accumulation. Recently, an accumulator model, auditory two-alternative forced-choice task was developed to study the ability of rats to accumulate sensory evidence (Brunton, 2013) (**Figure 1.3B**). The rats were trained to fixate their head, during which time spatially segregated trains of clicks drawn from a Poisson distribution were

presented discretely over time and space. The clicks were presented when the rats fixated. When the clicks stopped, the rats were trained to turn towards the side from which the most clicks had been presented after variable delay period. Afterward, the rats were rewarded for correct decisions. Fitting the rats' behavioral data to a descriptive model showed that the rats were able to accumulate sensory evidence and use all the information presented over the duration of the stimulus to form the decision. Rats were not impulsive or forgetful; they did not rely on early or late trains of clicks to form the decision but used information presented over the duration of the entire trial. Thus, the study concluded that the rats used an accumulation strategy to form the decision similar to human subjects tested using the same task. This task is relevant for the current manuscript for the following reasons: (1) It is transferable to different species, which allow one to test non-human primates and humans. (2) It is easily performed and can be used to test patients. (3) It allows the fitting of behavioral data to descriptive models that has the potential to provide insights into the accumulation process dynamics on a behavioral and neural level (Brunton, 2013). Therefore, we adopted this task for all the empirical studies describe below and implemented a visual variant of the task. A detailed description of the stimuli and the task is provided in Chapter 5, which discusses empirical studies.

(A)



(B)

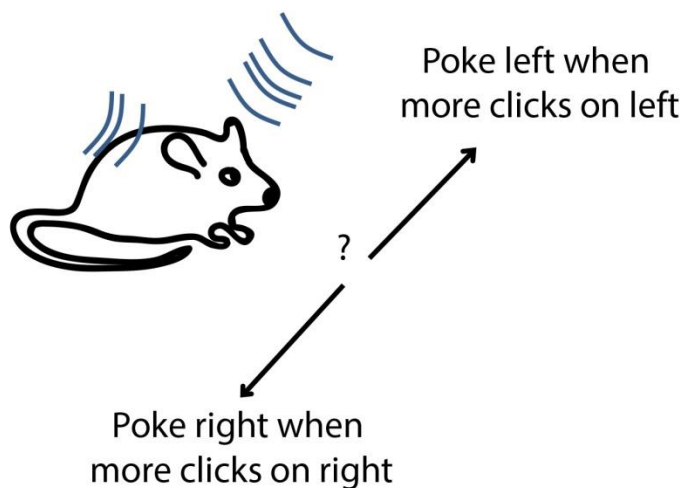


Figure 1.3. **Tasks in the study of perceptual decision-making** (A) Random dot motion paradigm description. A subject views a cloud of moving dots. The dots move in different directions with variable levels of coherency. Subjects have to decide towards which side most of the dots are moving. (B) The Poisson clicks task. Trains of spatially segregated clicks are presented to the rats once the rat fixates its head. The rat has to accumulate evidence and form a decision on which side there had been more clicks. The rat responds with body orientation and is rewarded if the decision was correct.



### ***1.3 Theoretical background and models:***

In recent years, the field of perceptual decision-making benefited from the development of phenomenologically and biophysically plausible models of perceptual decision-making.

#### ***1.3.1 Signal detection theory***

Signal detection theory (SDT) arose from research on radar during the Second World War. It specifies the optimal observation and decision process for detecting electronic signals against a background of random noise (Marcum 1948). SDT was applied to psychophysics for situations in which the human observer tries to discriminate between similar signals since this is viewed as a problem of inference (Green & Swets, 1966; Macmillan & Creelman, 2005). SDT introduced the analytical technique referred to as the receiver operating characteristic (ROC). ROC is a graphical technique that allows the measurement of two independent aspects of detection performance: (1) the decision criterion that represents the location of the observer's cut-off point. (2) The observer's ability to discriminate between signal-plus-noise and noise alone referred to as observer's sensitivity. In a 'yes-no' paradigm, the measure of discrimination performance or observer's sensitivity was denoted  $d'$  ( $d$  prime), which is defined as the difference between the means of two implicit, overlapping, normal (Gaussian) functions of equal variance for signal (A) and noise (B). The

separation between these two distributions indicates the sensitivity to discriminate A from B (Green & Swets, 1966).

$$d' = P(s/A) - P(s/B)$$

$d'$  is the  $d$  prime (sensitivity measure),  $s$  is sensory evidence,  $P$  is probability density function.

In two-alternative forced-choice paradigms (2AFC),  $d$  prime can be calculated from the percentage correctly identified (percent correct) (Green & Swets, 1966; Macmillan & Creelman, 2005).

$$d' = \sqrt{2} \cdot z(pc)$$

where  $z(pc)$  is the  $z$ -score transformation of percent correct.

However, SDT fails to capture the development of sensory evidence towards a decision over time. Therefore, SDT is limited to measures of performance but cannot account for reaction time behavior (Gold & Shadlen, 2007). To address the temporal limitations of SDT, psychologists benefited from sequential probability ratio theory (**Figure 1.4**).

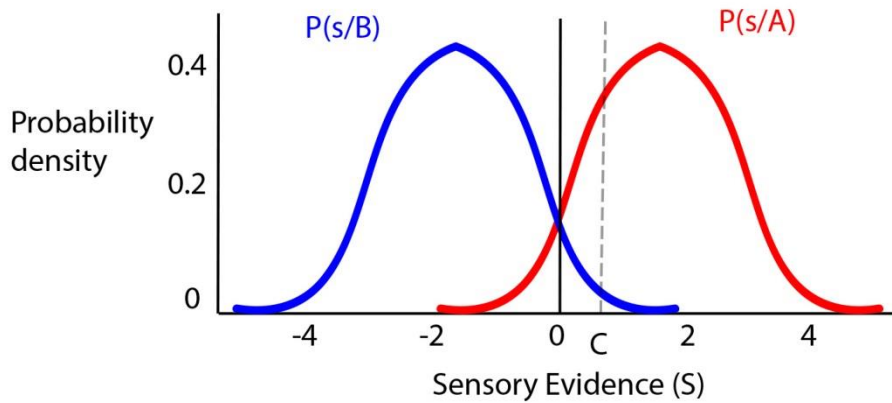


Figure 1.4. **Signal detection theory framework.** Curves represent probability density functions of sensory evidence for signal A, or noise B. The less overlap between the two probability density functions, the easier the discrimination. The subject has to infer the probability of the stimulus given the sensory evidence (S). The subject places a decision criterion (C) along the evidence axis. The decision is A if  $S > C$ .

### 1.3.2 Sequential probability ratio theory (SPRT):

Sequential probability ratio theory (SPRT) was developed as a classified military project by Abraham Wald in the mid-1940s. A major motivation for its development was to test whether the military equipment would satisfy a certain quality criterion. The advantage of the theorem application is that the sampling number does not have to be predetermined before testing the hypothesis, allowing the testing process to be terminated once a criterion is met. This reduces the time required for testing and makes it possible to include “time” as a dimension of the testing process. This characteristic motivated psychologists to implement SPRT in the field of perceptual decision-making. Models based on assumptions of SPRT were referred to as sequential sampling decision-making (SSDM) models. SSDMs have been implemented in the field of mathematical psychology since the 1960s (Stone, 1960). All models assume that evidence

gradually accumulates and that a decision is made whenever the evidence reaches a threshold (e.g., the diffusion model, (Ratcliff, 1978); and the linear ballistic accumulator model [LBA], (Heathcote & Love, 2012). However, the models differ according to whether there are one or two boundaries, and whether the boundaries are independent, i.e. whether they are assumed to be leaky or sticky. (e.g., (Ratcliff & Smith, 2004; Teodorescu & Usher, 2013). Such models have three central parameters: the *drift rate*, a measure of how fast evidence accumulates, a *threshold* that measures how much evidence needs to accumulate before a decision is made, and *non-decision time*, which is time taken up by processes not related to the decision-making process, e.g., the time needed to push a response button (Heathcote, Wagenmakers, & Brown, 2014). The first models of decision-making in humans or animals were accumulator models, often referred to as race models. In these models, evidence accumulates separately for each possible outcome. However, race models were not able to explain the response times for free-response paradigms, partially because the race models posit that there is no interaction between the different accumulators for the different options (Forstmann, Ratcliff, & Wagenmakers, 2016). These inconsistencies led to wider acceptance of Ratcliff's drift-diffusion model (DDM) (Ratcliff, 1978). In the DDM the accumulation process follows a Wiener process with two absorbing boundaries. Importantly, the DDM successfully captured two key aspects of the behavioral data; the shape of response time distributions and the covariation of mean response times and response accuracy

with task difficulty (Ratcliff & McKoon, 2008). DDM was developed further by adding different parameters. Among later iterations were the leaky competing accumulator models (LCA). The LCA were proposed to correspond better with neural data as suggested by (Usher & McClelland, 2001). In the LCA a ‘leaky’ parameter was introduced which represents a decay to baseline when new evidence input is lacking. The ‘competition’ means that evidence for one variable can reduce the evidence for other variables (**Figure 1.5**).

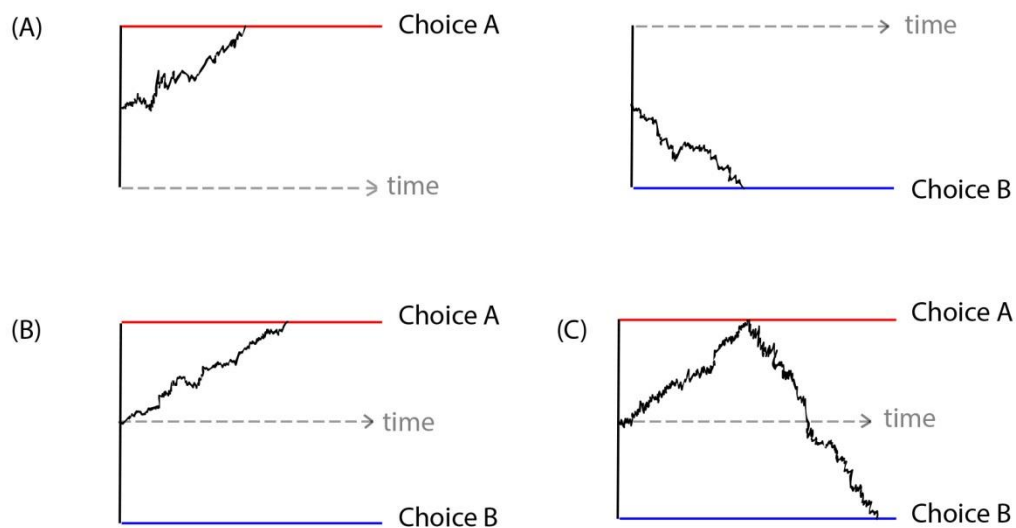


Figure 1.5. **Sequential models.** Decision boundaries A in red, B in blue. Thick black line is decision variable (A) Race models assumes independent boundaries. (B) Drift-diffusion models assume two sticky boundaries; once threshold is met a decision is reached. (C) Leaky competing accumulator models boundaries are not sticky; the decision could change even after a threshold had been reached.

### 1.3.3 Biophysically plausible models: integrate-and-fire attractor models.

Previously discussed abstract, mathematical ‘phenomenological’ models provided a rich theoretical, descriptive background of processes involved in forming perceptual decisions. However, sequential sampling decision-making

did not provide details on the cellular, or network dynamics involved in decision-making. Thus, biophysically plausible models were developed to bridge the gap between the descriptive models, behavioral data, and the neural code underlying decision-making. Recently, biophysically driven network models have been developed and applied to various experimental paradigms, including perceptual tasks that involve both decision-making and working memory, action selection and preparation, and metacognition (Rolls & Deco, 2010; Wang, 2002, 2008). Such models share similar basic assumptions: (1) “Attractor states” which is a mathematical term referring to synaptic excitation that is sufficiently strong to generate stable steady states in neural populations representing categorical choices, (2) Reverberating excitation that gives rise to long ramping neural activity over time allowing the network to have a slow transient dynamics providing a neural mechanism of information accumulation, (3) Feedback inhibition that provides competitive dynamics underlying the formation of a categorical choice, and (4) Highly irregular spiking activity of neurons that makes it possible to capture neural dynamic underlying generating stochastic choice behavior (Wang, 2008). The “integrate-and-fire” attractor model was further implemented to explain behavioral and neural data in perceptual decision-making paradigms (Deco & Rolls, 2006; Rolls & Deco, 2010) (**Figure 1.6**).

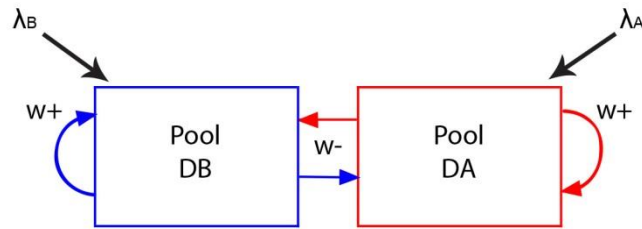


Figure 1.6. **Architecture of the integrate-and-fire attractor model decision network.** The network starts with spontaneous activity. High firing in pool DA represents decision A and high firing in pool DB represents decision B. Pool DA receives sensory input  $\lambda_A$  and pool DB receives input  $\lambda_B$ . Sensory input biases the attractor networks, which have an internal feedback produced by recurrent excitatory connections ( $w_+$ ). Pools DA, DB compete through inhibitory interneurons ( $w_-$ ). Noise in the network is the result of neurons randomly spiking. Noise makes the decision probabilistic (Insabato et al., 2010).

#### ***1.4 Bridging the gap between neural processes and behavioral outcome:***

Previously described abstract and biophysically plausible models represent an important attempt to bridge the gap between the neural process and the observed behavioral outcome. Such models help translate behavioral outputs related to accuracy and reaction times into cognitive processes (Ratcliff & McKoon, 2008). In 1996, Hanes and Schall showed that the activity in single cells in the rhesus monkey motor cortex represented a specific link between the movement initiated and the activity of those neurons and they evaluated a model to describe the neural processes underlying reaction time behavior (Hanes & Schall, 1996). This was possibly one of the first attempts to explain the underlying neural processes involved in developing overt behavioral output with the help of descriptive models, although there had been earlier attempts (Newsome, Britten, & Movshon, 1989). One finding from that the Hanes and Schall study was that

movement occurred if the firing rate of the recorded neurons reached a threshold and remained at that threshold. This finding encouraged researchers to apply the principles of the drift-diffusion model (DDM) in order to understand the underlying neural processes of perceptual decision-making. The DDM proposes that evidence accumulates over time until a threshold is met. Shadlen and Gold in 2000 were able to show that the firing rate of single cells in decision-related areas reach a maximum and, as such, mimics the expectations of the DDM that sensory evidence accumulates towards a threshold.

### *1.5 Neural correlates of sensory evidence accumulation in non-human primates:*

Electrophysiology studies investigating perceptual decision-making in primates suggest that the lateral intraparietal (LIP) region is a strong candidate for coding sensory evidence accumulation. LIP is defined as parietal region that projects to brain structures involved in the control of eye movements (Andersen, Asanuma, Essick, & Siegel, 1990). LIP receives input from the visual areas and the pulvinar, and its neurons can maintain activity for durations up to seconds when an animal is trained to withhold a saccade to a target (Gnadt & Andersen, 1988). A variant of random dot motion (RDM) with delayed saccade was tested in monkeys, and recordings from LIP showed that neural activity signaled the monkeys' choice (Gold & Shadlen, 2007), i.e. the neurons signaled the intended saccade. Moreover, MT activity showed constant firing rates over time while



firing rate in LIP increased with time. Furthermore, activity in the LIP was dynamically modulated by choice difficulty as predicted by the DDM (Roitman & Shadlen, 2002). Additionally, electrical microstimulation of LIP led to a systematic bias towards ipsilesional choices but did not lead to saccade initiation, which suggests that activity in LIP is not motor-related (Hanks, Ditterich, & Shadlen, 2006). However, the role of LIP in the accumulation of sensory evidence is still under debate. It was recently shown that LIP activity correlates to evidence accumulation but has no causal contribution in the accumulation process once inactivated; suggesting a role of LIP in secondary decision-making processes (Katz et al., 2016). On the other hand, prefrontal cortex (Hunt et al., 2012) including frontal eye fields (FEF; (Kim & Shadlen, 1999)), striatum (Ding & Gold, 2012), and superior colliculus (Horwitz & Newsome, 1999) exhibited activity that correlated with sensory evidence accumulation. However, it is hard to investigate auditory perceptual decision-making in monkeys (Gold & Shadlen, 2007). A study investigating sound discrimination in rhesus monkeys found that activity in prefrontal regions was modulated by the monkey's choice, and activity in the anterior superior temporal gyrus reflected representations of sensory evidence (Tsunada, Lee, & Cohen, 2011). In the somatosensory domain, a study investigating the ability of monkeys to discriminate vibrotactile frequencies identified neural correlates of somatosensory evidence accumulation in prefrontal regions (Romo, 1998).

### ***1.6 Sensory evidence accumulation: signals and task difficulty***

In studies of the neural correlates of sensory evidence accumulation using single unit recordings it was observed that neural activity reached threshold earlier in easy trials than in hard trials (Kim and Shadlen 1999). However, it remains debatable whether easy or hard trials are better suited for investigating neural correlates of sensory evidence accumulation. Simulations of neural activity from “integrate-and-fire” attractor models provide various explanations as to why neural activity during easy trials would be related to sensory evidence accumulation (Rolls, Grabenhorst, & Deco, 2010): (1) the network falls into its decision attractor faster on easy decisions, (2) the mean firing rate of a network that has settled into the correct decision attractor is higher with easy decisions compared to hard ones, or (3) the variability of the firing rate is greater with hard trials, suggesting that the network might have not even reached the attractor state in those trials. Based on the observations made by IFA one can conclude that neural signal during easy trials reflect sensory evidence accumulation.

### ***1.7 Blood oxygen level dependent signal***

In electrophysiology, one can investigate the minute dynamics of recorded signals in fine-tuned temporal and spatial resolution. In contrast, functional magnetic resonance imaging (fMRI) allows one to visualize brain activity in human beings while they perform tasks but doesn't exhibit fine-tuned temporal and spatial resolution (Logothetis, 2008). Neuronal activity induces hemodynamic changes via feed-forward neurovascular coupling and causes changes in blood inflow. Changes in blood inflow lead to changes in blood outflow, blood volume and deoxyhemoglobin content. Changes in blood volume and deoxyhemoglobin content are then visualized by the blood oxygen level dependent (BOLD) response (Havlicek et al., 2015) (**Figure 1.7**). Thus, it is challenging to infer the underlying neural processes of sensory evidence accumulation using the BOLD signal.

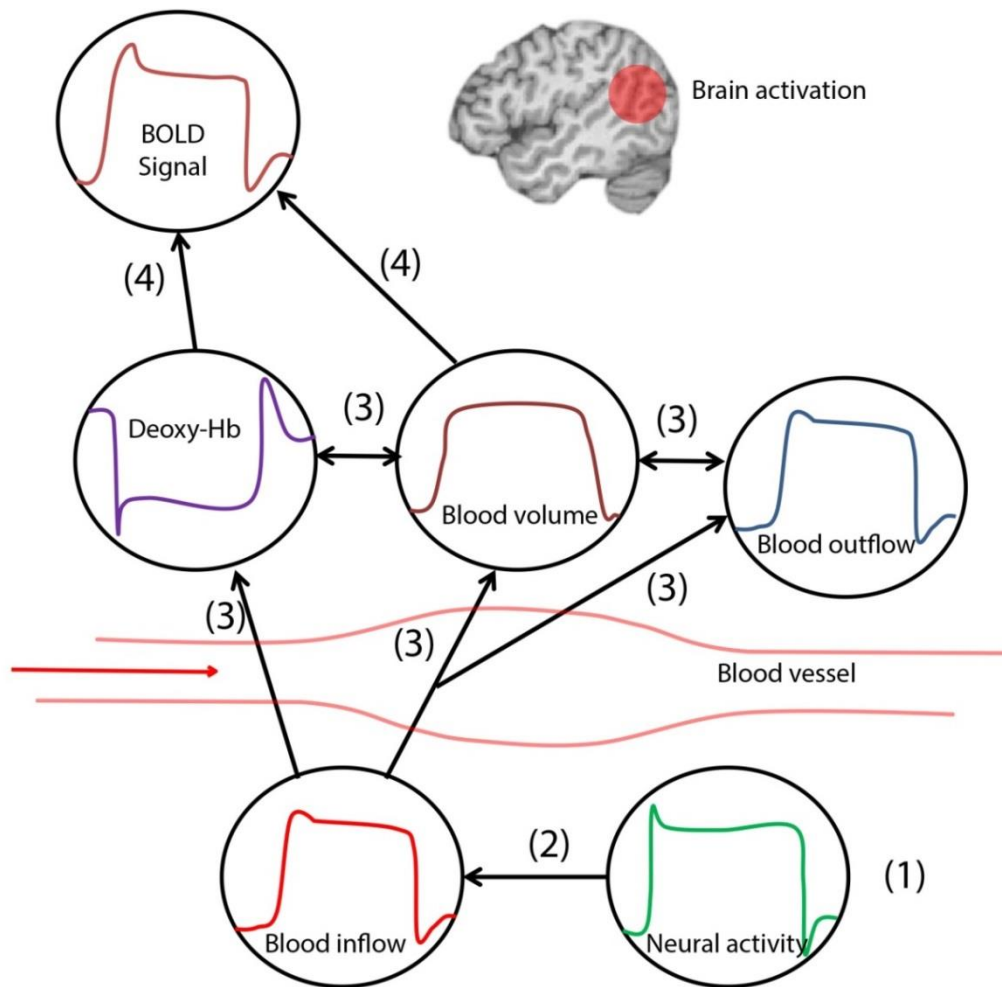


Figure 1.7. **Schematic illustration of the neuronal activity and BOLD signal relationship.** Neural activity (1) evokes hemodynamic changes via feed-forward neurovascular coupling (2) and causes changes in blood inflow. Changes in blood inflow lead to changes in blood outflow, blood volume, and deoxyhemoglobin content (3). Changes in blood volume and deoxyhemoglobin content are seen in the BOLD signal (4). Modified from (Havlicek et al., 2015).

### ***1.8 Neural correlates of sensory evidence accumulation from human fMRI:***

As discussed in the earlier chapter, the firing characteristics of the neural population involved in sensory evidence accumulation are: (1) the threshold was met faster with easy decisions compared to hard decisions, and (2) the ramp-up of neural activity continued until a decision was reported. However, understanding of the BOLD responses related to the neural activity of sensory evidence accumulation is challenging due to the subtle nature of the BOLD signal (check previous chapter). Therefore, trying to understand BOLD signal related to sensory evidence accumulation gave rise to two schools of thought in the neuroimaging literature. The first of these suggests that easy trials will result in a stronger BOLD signal in accumulator regions (Filimon, 2013; Hebart, Donner, & Haynes, 2012; Heekeren, 2004; Philiastides & Sajda, 2007; Rolls et al., 2010), while the second suggests that hard trials will result in a stronger BOLD signal in accumulator regions (Ho & Brown, 2009; Liu & Pleskac, 2011) (**Figure 1.8**). However, it seems the field is agreeing on easy trials to be more suitable for investigating neural correlates of evidence accumulation (Forstmann, Ratcliff, & Wagenmakers, 2016).

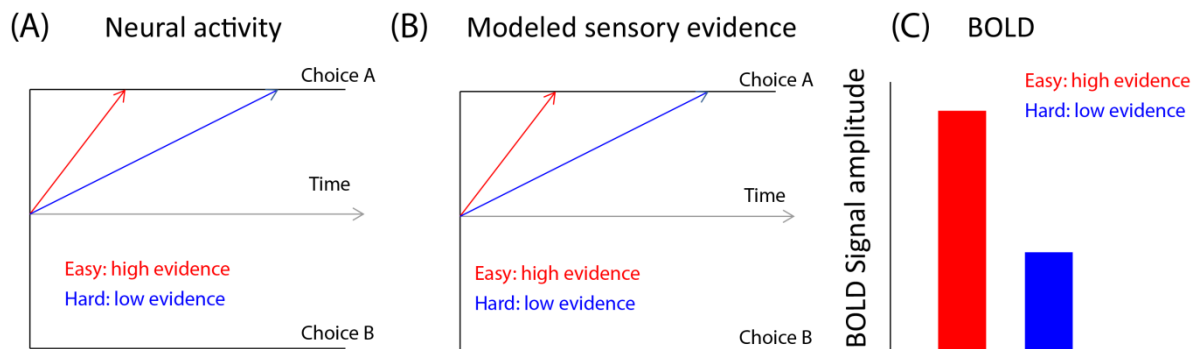


Figure 1.8. **BOLD signal related to difficulty.** (A) Electrophysiology studies showed that maximum neural activity is reached later with the difficult task (Gold & Shadlen, 2007). (B) Drift-diffusion models show that the threshold is met faster in easy trials (Forstmann, Ratcliff, & Wagenmakers, 2016). (C) Signal of sensory evidence accumulation correlates with stronger BOLD signal in easy trials (Rolls et al., 2010).

One of the first studies that applied assumptions from the accumulator models to investigate sensory evidence accumulation using fMRI reported a stronger BOLD signal in the dorsolateral prefrontal cortex (DLPFC) with easier decisions (Heekeren, 2004). In their study, Heekeren et al. proposed that the signal in the DLPFC represented a general mechanism for perceptual decision-making. Using effective connectivity analysis they showed that the DLPFC integrates information from early sensory cortices. Also, the lateral occipital cortex (Christophel, Hebart, & Haynes, 2012; Philiastides & Sajda, 2007), insular cortex (Ho & Brown, 2009), frontal eye field (FEF), and intraparietal sulcus (IPL) (Liu & Pleskac, 2011) were claimed to show accumulation signals. In light of the various regions found to correlate with evidence accumulation, it

seems reasonable to contemplate upon reasons for this discrepancy in the literature. One of the reasons proposed was that different studies used different tasks, and thus the sensory evidence accumulation signal is task-dependent, (ref. previous chapter). According to another reason, the identified sensory evidence signal could depend on the motor modality tested. One study investigated how embodied the signal of sensory evidence accumulation was by asking subjects to respond to a face vs house discrimination task using either the eyes or the hands. It found that when eye and hand motor preparation is disentangled from perceptual decisions, the parietal regions are not involved in accumulating sensory evidence. Rather increased effective connectivity between inferior frontal gyrus and sensory regions represents the evidence (Filimon, 2013). In a third proposal, the use of different response protocols, i.e. delay response versus free-response could be responsible for the discrepancy. A recent study comparing signals of evidence accumulation in delayed tasks and the free-response paradigm hypothesized that signals of evidence accumulation would be stronger for hard decisions compared to easy decisions in the free-response paradigm, while this would be reversed in the delayed paradigm, i.e. the signals would be stronger with easy decisions. They found that visual evidence accumulation is probably implemented in frontal and insular regions while the choice maintenance regions span frontal, temporal, and occipital cortices (Pedersen, 2015). Another reason is that decision signal is sensory modality dependent. However, there are fewer studies available that investigated the

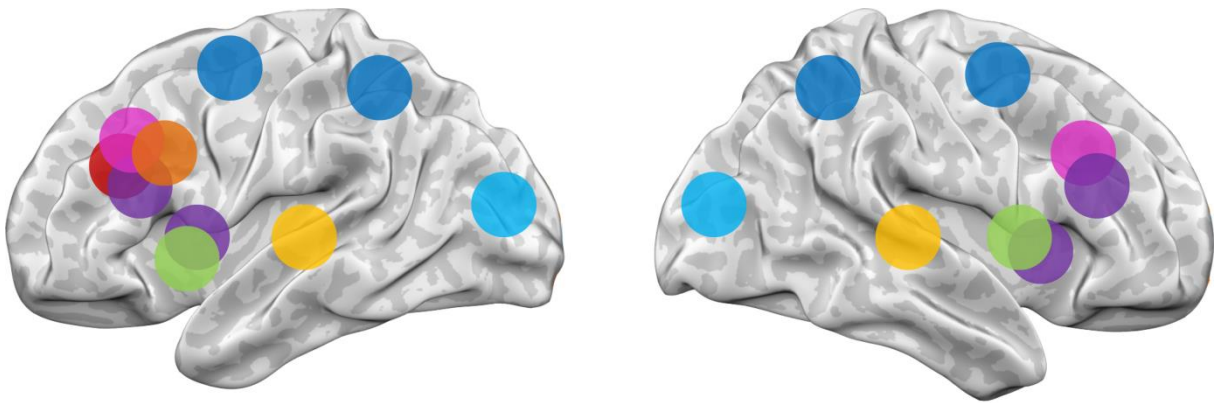
sensory evidence accumulation signature for sensory modalities other than the visual modality. In an auditory fMRI study, Binder et al (2004) used fMRI to scan human participants while they performed an auditory discrimination task. Words were masked by varying level of noise resulting in different degrees of difficulty. Accuracy and reaction times were used to investigate the behavior and decision components of the auditory perceptual system. They found that the anterior superior temporal gyrus was involved in accuracy, while the inferior frontal gyrus was involved in response times. They interpreted the results as indicating a role of the superior temporal gyrus in object identification; thus involved in forming the decision, with a role of inferior frontal gyrus in the motor preparation of the speech response. In another study using magnetic encephalography participants were asked to report if two consecutive syllables were different and to identify the location of syllables (Kaiser & Lutzenberger, 2004). Kaiser et al found that activity in the gamma frequency band in the left inferior frontal gyrus was higher for the discrimination part and activity in the inferior parietal lobule was higher for the spatial part of the task. Importantly, the level of activity was higher for easy tasks compared to harder ones (Kaiser & Lutzenberger, 2004). However, the stimuli used in those previous studies were not explicitly designed to study auditory sensory evidence accumulation per se. In the somatosensory domain, inspired by the vibrotactile frequency discrimination task used to investigate somatosensory perceptual decision-



making in monkeys, Pleger et al. found correlates of tactile decision-making in the dorsolateral prefrontal cortex (Pleger et al., 2006).

**Table 1.1 Neuroimaging studies of sensory evidence accumulation**

| Study                               | Task                               | Sensory modality | Response modality | Protocol   | Number of subjects | Regions  | Statistical threshold  |
|-------------------------------------|------------------------------------|------------------|-------------------|------------|--------------------|--|------------------------|
| (Heekeren, 2004)                    | Face vs house                      | Visual           | Manual            | Delay      | 12                 | Dorsolateral prefrontal cortex   | p<0.001 uncorrected    |
| (Philiastides & Sajda, 2007)        | Face vs cars, color discrimination | Visual           | Manual            | Delay      | 12                 | Occipital  | P<0.05 FDR corrected   |
| (Ho & Brown, 2009)                  | RDM                                | Visual           | Manual Saccade    | Free       | 12                 | Insula   | P<0.05 FDR corrected   |
| (Liu & Pleskac, 2011)               | RDM                                | Visual           | Manual Saccade    | Delay      | 9                  | Frontal eye field, intraparietal sulcus, insula, and inferior frontal sulcus     | P<0.005 FWE corrected  |
| (Filimon, 2013)                     | Face vs house                      | Visual           | Manual Saccade    | Delay      | 19                 | Inferior frontal cortex  | P<0.001 FWE corrected  |
| (Pedersen, Endestad, & Biele, 2015) | Face vs house                      | Visual           | Manual            | Delay Free | 20                 | Dorsomedial prefrontal cortex, right inferior frontal gyrus and bilateral insula | P<0.05 FWE corrected   |
| (Binder, 2004)                      | Syllable discrimination            | Auditory         | Manual            | Delay      | 18                 | Superior temporal gyrus  | P<0.1 uncorrected      |
| (Pleger et al., 2006)               | Frequency discrimination           | Somatosensory    | Manual            | Delay      | 10                 | Dorsolateral prefrontal cortex   | p = 0.0001 uncorrected |



(Heekeren, 2004)

(Philiastides & Sajda, 2007)

(Ho & Brown, 2009)

(Liu & Pleskac, 2011)

(Filimon, 2013)

(Pedersen, Endestad, & Biele, 2015)

(Binder, 2004)

(Pleger et al., 2006)

Figure 1.9. Schematic illustration showing an overview of brain regions involved in perceptual decision-making as identified in seminal studies.

From the detailed review of neuroimaging literature, we can conclude that most of what we know about perceptual decision-making stems from investigations of visual perceptual decision-making. Thus, it is not clear how different types of information are accumulated: Is a region involved in the accumulation of visual sensory evidence expected to accumulate auditory evidence as well?

## **2. Confidence in the decision**

In the street-crossing example, we explained that it is important to evaluate how sure we are of our decision that it is now safe to cross the street in order to cross safely. Such reflection allows us to gather more information, if necessary, when uncertain, and to optimize the decision, thus preventing accidents in this example we are discussing.

### ***2.1 Definition of confidence in the decision***

Confidence in perceptual decision making is defined as a subjective estimate of the accuracy of the decision (Mamassian, 2016). As such, confidence can be viewed as thinking of a thinking process and thus belongs to the metacognitive processes (Metcalf & Shimamura, 1994). Recent evidence suggests that confidence in a decision is estimated similarly across tasks (Gardelle & Mamassian, 2014), across sensory modalities (Gardelle, Corre, & Mamassian, 2016) and across observers (Bahrami et al., 2010).

## *2.2 Confidence rating measures*

Investigating confidence in a decision dates back to more than a hundred of years. In 1885 Peirce and Jastrow asked participants to discriminate between pressures applied to their finger and to rate how confident they were in their discrimination on a four-point scale. They found that confidence rating correlated with pressure discriminations. Studies consistently showed correlations between perceptual accuracy and confidence ratings (Vickers & Packer, 1982, Sandberg, 2010). Since the work of Peirce and Jastrow in 1885, it is common to ask participants to assess their confidence in a decision on a rating scale. Using confidence ratings (CR) has several advantages: (1) they are easy to obtain after the first decision, (2) they are easy for participants to understand, and (3) they are easy to analyze, as it is possible to simply plot correlations between decision accuracy and confidence ratings (Nelson 1984). Another paradigm for measuring confidence is to give the participants the opportunity to opt-out if they are uncertain (Gherman & Philiastides, 2015; Kiani & Shadlen, 2009). The major advantage of such a paradigm is that it is widely used to study confidence in animals. However, the opt-out paradigm could be viewed as a three-alternative forced-choice. The subject must decide if it was clearly stimulus A, clearly stimulus B, or somewhere between A and B. A further paradigm is post-decision wagering (PDW) (Persaud, McLeod, & Cowey, 2007). In PDW, participants are asked to bet on the outcome of the decision. If the participant is more confident that the decision is correct, then he will bet

more. However, it is important and challenging to set the reward matrix in the proper way to reward good bets and penalize bad one (Clifford, Arabzadeh, & Harris, 2008). An alternative paradigm is the perceptual awareness scale (PAS) (Ramsøy & Overgaard, 2004). In the PAS paradigm, the participants are free to create their own scale to describe the quality of their experience. Interestingly, participants ended up using a four-point scale. Participants described scales differently but they agreed on a similar definition of each level of the scale (Sandberg, 2010). However, this paradigm is particularly prone to the subjects' capability for introspection. A systematic comparison of the confidence rating (CR), post-decision wagering (PDW), and perceptual awareness (PAS) paradigms was conducted by Sandberg 2010. Sandberg compared how sensitive and exhaustive each of the measures was by studying the 'zero correlation criterion' and the 'guessing criterion' (Dienes, 1995). Results have shown PAS is the most exhaustive and most sensitive scale, while PDW, despite claims that it is most objective scale, was the worst. It was the least sensitive scale in variations and promoted binary decisions with respect to accuracy. CR was shown to be reasonably sensitive and exhaustive scale with which participants could rate their confidence.

### *2.3 Methods for quantifying confidence*

As described in the previous chapter, many paradigms have been developed to measure confidence in a decision. Here we will focus on methods proposed for quantifying confidence in perceptual decisions: (1) Metacognitive sensitivity, also known as metacognitive accuracy, type 2 sensitivity, discrimination reliability (2) The confidence-accuracy correlation. Both measures give insights to how accurately subjects rate their performance accuracy (Fleming, 2014). Metacognitive sensitivity can be measured based on signal detection theory (SDT). SDT assumes that both perceptual choices and perceptual confidence are based on the continuous evaluation of accumulated evidence over time in favor of one perceptual interpretation of a stimulus (Gold & Shadlen, 2007; Green & Swets, 1966; Macmillan & Creelman, 2005). One makes a categorical choice (e.g., “motion left” vs. “motion right”) by comparing the sensory evidence against a criterion, and one generates his choice-independent confidence based on the absolute distance of sensory evidence to this criterion (meta  $d'$ ) (**Figure 1.4**). It is important to distinguish between metacognitive sensitivity and metacognitive bias; a subject reporting high confidence all the time has a high metacognitive bias but no discriminability between correct and erroneous decisions, and thus low metacognitive sensitivity (Fleming, 2014). On the other hand, the confidence-accuracy correlation is easier to calculate and more intuitive to understand, and makes it possible to understand the development of conscious awareness as function of stimuli levels (Koch & Preuschoff, 2007;

Sandberg, 2010). However, this analysis should be approached carefully due to the variability in the subjects' confidence rating (Fleming, 2014).

#### ***2.4 The Study of confidence in animals***

It is arguably challenging to train an animal to report confidence in the decision, and to interpret that as a subjective rating by the animal. In an influential study, (Kepecs, Uchida, Zariwala, & Mainen, 2008) investigated confidence in the decision in rats. The rats were trained to categorize two odors A and B as well a range of mixtures between the two. Accuracy in categorizations increased as the distance of odor mixture to the stimulus category boundary increased. To investigate the metacognitive ability of the rats the study measured how long the animals were willing to wait for a reward. The longer the rat waited for reward meant the surer the rat was that they would get the reward, meaning the rat was confident that it had made a correct choice. The rats were able to be more confident for correct decisions in easy tasks but less so for incorrect decisions in the same tasks. It is easy to understand why the rat would show a higher degree of confidence for correct decisions in easy trials, but hard to imagine the reason for their behavior when they erred in easy trials. Kepecs et al (2008) proposed that since confidence and decision-making are probabilistic in nature, the probability that the rat would make an error in the easy condition is low. If the rat made an error in the easy condition, the probability is low for it to be confident.

In primates the opt-out paradigm is popular. The animal is given the option not to choose any category if it is uncertain. If the animal used the opt-out choice when the task was difficult, for small but sure reward, the researchers would assume that it had the ability to monitor its uncertainty. A study into the metacognitive ability of capuchin monkeys found that they only opted-out if the opt-out option was rewarded regardless of the difficulty; in easy and difficult trials. The study, therefore, concluded that capuchin monkeys have no metacognitive abilities, and that it is important to determine how the animal should be rewarded in opt-out paradigms (Beran, Smith, Coutinho, Couchman, & Boomer, 2009). In a seminal study, Kiani and Shadlen (Kiani & Shadlen, 2009) trained rhesus macaque monkey on a random dot motion task. In half of the trials a sure target was present that the monkey could choose for safe and sure reward. The monkeys opt-out (choose the sure target) more often in hard trials. The Kiani study therefore concluded that monkeys do have metacognitive abilities.

### ***2.5 Neural correlates of confidence in animals***

As described in a previous chapter, advances in task design have made it possible to study confidence in decision-making in animals. Recordings from animals suggest that several brain regions show neural correlates of confidence in the decision; the orbitofrontal cortex in rats (Kepecs et al., 2008), and the lateral intraparietal (LIP) cortex in rhesus macaques (Kiani & Shadlen, 2009).



Another study showed that pulvinar neurons reduce their activity when the monkey decides to opt out, suggesting its role in confidence judgment (Komura, Nikkuni, Hirashima, Uetake, & Miyamoto, 2013).

## ***2.6 Architecture of confidence forming networks***

Interestingly the neural correlates of confidence reflected the behavior of confidence rating of the animals. In the study by Kepecs et al the rats were most confident for correct decisions in easy trials and least confident for incorrect decisions in easy trials. Similarly, activity in the orbitofrontal cortex was highest with correct decisions in easy trials compared to incorrect decisions in the same trials (Kepecs et al., 2008). It was shown that confidence in the decision arises as an emergent property in an integrate-and-fire attractor network model of decision making (Insabato, Pannunzi, Rolls, & Deco, 2010a). Insabato et al. have shown that confidence in the decision is formed in a second attractor network benefiting from the first decision network (**Figure 2.1**).

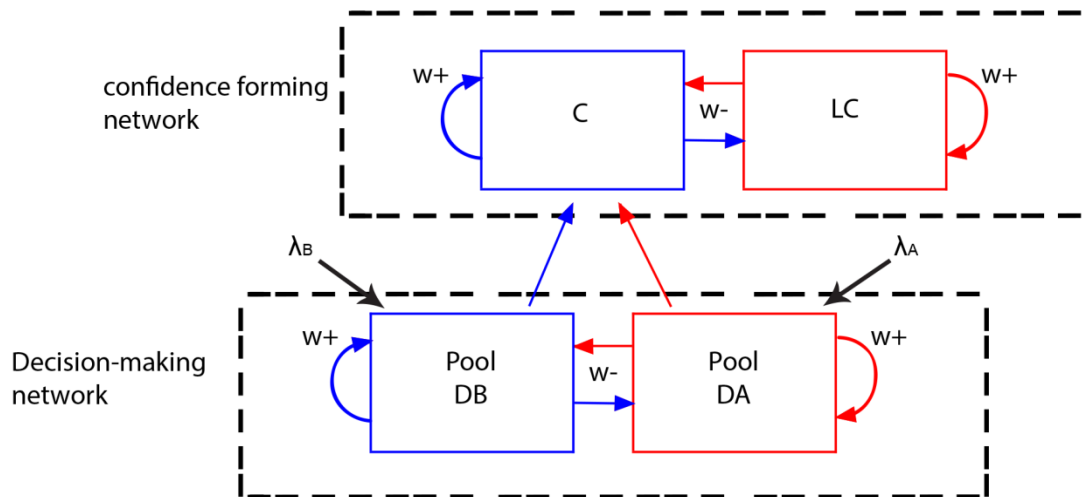


Figure 2.1. **The architecture of integrate-and-fire attractor confidence in the decision network.** The network starts with spontaneous activity. High firing in pool DA represents decision A and high firing in pool DB represents decision B. Pool DA receives sensory input  $\lambda_A$  and pool DB receives input  $\lambda_B$ . Sensory input biases the attractor networks, which have an internal feedback produced by recurrent excitatory connections ( $w_+$ ). Pools DA, DB compete through inhibitory interneurons ( $w_-$ ). Noise in the network is the result of neurons randomly spiking. Noise makes the decision probabilistic. The decision-making network that sends output to second network. The confidence forming network benefits from the output from the first decision network to form confidence in the decision. C is confidence forming pool LC is low confidence forming pool (Insabato et al., 2010).

Integrate-and-fire attractor simulations were able to fit both the behavioral and neural activity of confidence in decision in orbitofrontal recordings (Kepecs et al., 2008), LIP (Kiani & Shadlen, 2009). Rolls et al. tested predictions of the attractor network theory of decision-making in two fMRI investigations. They studied choice decision-making about the reward value and subjective pleasantness of thermal and olfactory stimuli (Rolls et al., 2010). They showed how the firing rates of the winning and losing attractors reflected the easiness of the decision; those of the neurons of the winning attractor increased approximately linearly with decision easiness while those of the neurons of the losing attractor decreased approximately linearly with decision easiness.

## ***2.7 Neural correlates of confidence in human fMRI***

To study the phenomenon of confidence in a perceptual decision is easier in humans than in animals, since humans can report their confidence in the decision. Fleming et al. 2012 asked subjects to perform near-threshold perceptual judgment tasks inside the fMRI scanner (Fleming & Dolan, 2012). In two-thirds of the trials, the subjects rated their confidence in their decision by moving a cursor on a scale. In one-third of the trials, the subjects were asked not to reflect on their confidence but move a cursor to any region of the scale. These follow-up trials provided control conditions for motor and perceptual decision requirements. The fMRI signal in the rostralateral prefrontal cortex (rIPFC), dorsal anterior cingulate, and right posterior parietal cortex increased in metacognitive trials compared to control trials, and the signal was stronger for high confidence judgments. Only the rIPFC signal predicted individual differences in metacognition across individuals. Transcranial magnetic stimulation over the dorsolateral prefrontal cortex (DLPFC) temporarily inactivated DLPFC and decreased metacognitive accuracy but not performance accuracy (Rounis, Maniscalco, Rothwell, Passingham, & Lau, 2010). Hebart et al. (2014) showed that activity in the ventral striatum reflected the degree of perceptual confidence, with activity in the ventrolateral prefrontal cortex reflecting the decision variable being connected to the ventral striatum (Hebart, Schriever, Donner, & Haynes, 2014). Heekeren et al (2015) investigated the possibility that the neural signal of confidence could be task-

independent. They tested a random dot motion task and color discrimination tasks and asked subjects to rate their confidence before reporting their decision. They used confidence rating as a parametric regressor to explain their fMRI signal. They found that the signal increased with subjective certainty in the right lingual, calcarine, and left angular gyrus, and decreased with increasing subjective certainty in the left lingual gyrus, right inferior parietal lobule, bilateral DMPFC/SMA, and left post-central gyrus (Heereman, Walter, & Heekeren, 2015). As such, the literature seems to agree on a role of the prefrontal regions in metacognitive processes such as confidence in the perceptual decision.

### ***2.8 Efforts to disentangle neural correlates of confidence in the decision from neural correlates of sensory evidence accumulation in humans***

One should note the presence of similarity between brain regions thought to be involved in the coding of the perceptual decision (see Chapter 1) and brain regions thought to code confidence in the decision. To disentangle the processes underlying confidence judgment and decision making Hilgenstock et al (2014) tested a grating orientation task in which subjects were required to indicate the orientation of tactile gratings and rate their level of confidence on a scale of 1 to 4 during the fMRI scan (Hilgenstock, Weiss, & Witte, 2014). To identify the neural correlates post-confidence and the decision itself they based their assumptions on the two-stage dynamic signal detection model (2DSD) (Pleskac

& Busemeyer, 2010). The model suggests that confidence in and metacognitive judgment about the decision only evolve post-decision by the ongoing accumulation of information (Hilgenstock et al., 2014). So, based on temporal evolution of the signal, it is possible to separate the neural correlates of confidence and decision. They found that DLPFC codes post-decision confidence. However, a study using EEG showed that, contrary to the Hilgenstock proposal, confidence emerges from the decision process itself and is computed continuously as the process unfolds and both confidence and the decision engage frontal and parietal cortices (Gherman & Philiastides, 2015). Therefore, it is still not clear if brain regions involved in sensory evidence accumulation as a core decision process are also involved in confidence in the perceptual decision.

### ***2.9 Methods in investigating confidence using fMRI:***

In this chapter, we will describe the theoretical background of the methods we used to disentangle the neural correlates of sensory evidence accumulation as a core decision process from the neural correlates of confidence in the decision. Integrate-and-fire models were able to fit behavioral and neural data of confidence in decision recorded from animals (Insabato., 2010). By convolving simulations of neuronal firing rate with hemodynamic response functions, it was possible to construct predictors of the BOLD signal behavior about confidence in the decision (Rolls et al., 2010). Integrate-and-fire attractor models propose

that confidence develops as a second layer over the decision forming nodes in an attractor network providing predictions of behavior and neural correlates of the perceptual decision and the confidence in the perceptual decision (Insabato., 2010). Critically, It was determined that the BOLD response was a monotonous function of task difficulty (Rolls et al., 2010). Based on IFA BOLD signal predictions, we proposed two criteria for a region that qualified as being involved in confidence in decision-making. Number one was the difference of signal between correct trials and error trials. Number two, was that the signal exhibit an interaction between correctness and task difficulty that mimics confidence-rating behavior. In addition we added a criterion that is not based on integrate-and-fire attractor model assumptions. This third criterion, not based on the IFA assumptions, is that the confidence rating should modulate the signal at the same level of accuracy and difficulty.

### **3. Spatial decision-making:**

A key evolutionary survival asset is the ability of organisms to navigate through space, relying mainly on visual and auditory information to decide between alternative spatial choices (Pearson, Watson, & Platt, 2014). Despite the importance of an understanding of how the brain uses auditory information to form spatial decisions, spatial decision-making literature mainly focused on the visual decision-making (Heekeren, 2008).

#### ***3.1 Anatomy of sound localization***

Studies of static sound source localization in animals have shown that the location of a sound source can be indicated by interaural time and/or intensity differences (ITD and IID respectively) (Phillips, Quinlan, & Dingle, 2012). Electrophysiology recordings studying interaural time difference have shown that the auditory information from left and right auditory afferents meets early in the auditory system, at the level of the superior olivary complex in the brainstem, and then projects to the medial geniculate nucleus of the thalamus via the inferior colliculus in the midbrain (Irvine, 1986). The auditory cortex is organized into four hierarchical levels: Heschl gyrus (core), belt, parabelt, and the projections of the parabelt regions, with information flowing from core to belt to parabelt (Kaas & Hackett, 2000). Efferent connections from the parabelt are arranged in two functional circuits. Relevant to the current study is the anterolateral parabelt, which sends projections to the inferior parietal lobule,

dorsolateral frontal cortex, frontal eye fields and the areas of the prefrontal cortex involved in spatial processing (Romanski et al., 1999).

### *3.2 Functional anatomy of sound localization from human neuroimaging studies*

In humans, fMRI studies showed that sound localization in the horizontal plane depended on the interaural time difference that elicited activity at the level of the midbrain (Thompson et al., 2006). In a study investigating auditory motion detection, it was shown that the lateral parietal cortex, lateral frontal cortex, anterior midline and anterior insular cortex have signals correlated with moving auditory stimuli (Lewis, Beauchamp, & DeYoe, 2000). Their analysis depended on a comparison of task activation to resting conditions and was thus not aimed at investigating the properties of sound motion detection. Warren et al (2002) investigated sound motion with fMRI by contrasting different aspects of the auditory motion itself against each other. Their results support the notion of a role of the posterior temporal-parietal regions in sound localization processing (Warren, Zielinski, Green, Rauschecker, & Griffiths, 2002). Maeder and associates investigated sound localization using interaural time difference and sound recognition tasks in fMRI (Maeder et al., 2001). They found that the following regions were more strongly activated by sound recognition than by sound localization: bilateral middle temporal, the posterior part of the inferior frontal gyrus on the left side, inferoposterior part of the precuneus bilaterally.



During the localization task, they found activity in the inferior parietal lobule on both sides, but predominantly on the right, in the premotor cortex on both sides, in the ventral prefrontal cortex on the right and in the anterior part of the cingulate gyrus. Evidence from functional magnetic resonance imaging, electrophysiology studies, and positron emission tomographic studies suggest that the posterior part of the superior temporal gyrus and inferior parietal lobule are involved in the localization of sound in space, and spatial orientation (Aron, Robbins, & Poldrack, 2004). Interestingly, it has been consistently shown with fMRI that the right inferior parietal lobule responds to both contralateral and ipsilateral stimuli, while the left inferior parietal lobule responds to contralateral stimuli (Griffiths, 1998; Maeder et al., 2001).

### ***3.3 Functional anatomy of visual-spatial processes***

In cognitive neuroscience, the visual system has been more extensively studied than other sensory modalities. Amassing proof suggests the presence of two pathways in the visual system, a ventral stream projecting from the striate cortex to inferior temporal regions which are involved in the identification of objects, and a dorsal stream that projects from the striate cortex to posterior parietal regions mediating sensorimotor transformations for visual guided choices (Goodale & Milner, 1992; Schneider, 1969). The dorsal stream was extended to include prefrontal regions with lesions affecting the dorsal stream lead to a specific deficit in spatial vision leading to considering the dorsal stream as the

‘where’ pathways (Macko et al., 1982). However, recent anatomical and functional evidence in primates indicates that the dorsal stream actually gives rise to three distinct, major pathways; a parietal prefrontal pathway primarily supporting spatial memory, a parietal premotor pathway involved in visually guided action, and a parietal medial temporal pathway supporting spatial navigation (Kravitz, 2011). Evidence from fMRI, MEG and lesion studies suggests that the posterior parietal cortex is an integral part of the circuit for visual spatial decisions (Andersen, Andersen, Hwang, & Hauschild, 2014; Bray, Arnold, Iaria, & MacQueen, 2013; Silver & Kastner, 2009; Vesia & Crawford, 2012), and suggests an asymmetry between the two hemispheres with the right hemisphere being consistently reported to be involved in spatial visual processing (Corbetta & Shulman, 2011; Heilman, 1980; Silver & Kastner, 2009; Woldorff et al., 1999).

### ***3.4 Lateralization of spatial processing as a multimodal property of the brain***

One can conclude from the previous two chapters that there is converging evidence pointing to the hemispheric specialization of spatial processing as a multimodal property of the brain (Fritz, Elhilali, David, & Shamma, 2007). Insights into lateralization of brain processes were gained using invasive techniques such as the Wada test (1960) and callosotomy (Gazzaniga, 2005). However, those invasive techniques are not suitable for testing healthy subjects. With the advent of fMRI, it was possible to investigate the lateralization of brain

functions in healthy human subjects and to replace the Wada test for establishing hemisphere dominance preoperatively (2016). However, the conclusions about hemispheric asymmetries drawn from neuroimaging studies have been criticized (Nagata, Uchimura, Hirakawa, & Kuratsu, 2001). Early studies were not based on direct statistical comparisons of the magnitude of activation in the two hemispheres, so their results were influenced by statistical thresholding (Corbetta & Shulman, 2011). Evaluating hemispheric lateralization on the basis of fMRI data is problematic (Jansen et al., 2006). For fMRI to be a useful marker of brain organization, the analysis approach has to be robust and reproducible (Nagata et al., 2001). One way to calculate hemisphere lateralization is by calculating a laterality index (LI). The estimation of LI is often based on the extent of the activated brain region, i.e., the number of active voxels, or the magnitude of the fMRI signal change. Comparing which approach yielded the most robust and reproducible effect found that neither LIs based on active voxel counts at one single fixed statistical threshold nor LIs based on unthresholded signal intensity were robust or reproducible. The best approach is to use an LI based on thresholded signal intensity (Jansen et al., 2006).

### ***3.5 Hemispatial neglect syndrome as a model for studying causal contribution of lesions in spatial decision-making deficits***

The hemispatial neglect syndrome is defined as failure to report, respond, or orient to stimuli presented to the side opposite the damaged hemisphere that

cannot be solely attributed to primary motor or sensory deficits (Heilman & Valenstein, 1972). It is considered a frequent and debilitating outcome of lesions affecting both hemispheres (Kerkhoff, 2001). It affects up to two-thirds of patients with acute right hemisphere stroke (Parton, Malhotra, & Husain, 2004). Typically, neglect has been associated with lesions in the right posterior parietal cortex, particularly the inferior parietal lobe (IPL) or the temporoparietal junction (TPJ) (Vallar & Perani, 1986). However, other brain regions have been reported to lead to neglect. The right superior temporal gyrus (Karnath, 2001), the right frontal lobe (Husain & Kennard, 1996), subcortical lesions (involving the thalamus and basal ganglia) via indirect effects on connected cortical regions (Hillis, 2005; Hillis et al., 2002), and white matter pathways linking posterior cortical and frontal regions could be involved in individuals with neglect (Bartolomeo, Thiebaut De Schotten, & Doricchi, 2007). Despite the heterogeneity of lesions causing neglect, it has been consistently shown that neglect of the left side after a right hemisphere lesion is more frequent and severe than neglect of the right side after a left hemisphere lesion (Driver & Mattingley, 1998)

### ***3.6 Neglect and extinction***

Extinction is defined as an impairment of the ability to detect contralesional stimuli in the presence of a competing ipsilesional stimulus (Vossel et al., 2011). Extinction is often considered as part of neglect (Parton et al., 2004), however, it

is debatable whether neglect and extinction share similar neural mechanisms. It was shown that extinction can be distinguished from neglect behaviorally as well as at the neuroanatomical level (Vossel et al., 2011). It has been suggested that extinction results from a lesion to the temporoparietal junction (Karnath, Fruhmann Berger, Küker, & Rorden, 2004) or to subcortical regions (Vallar & Perani, 1986). An investigation into the degree of correlation between extinction and neglect in patients with right hemispheric lesions found that extinction and neglect occurred together in a subset of patients but were also observed independently (Vossel et al., 2011). Lesions within the right inferior parietal cortex were significantly associated with the severity of visual extinction, while lesions in frontoparietal regions correlated with the severity of visuospatial neglect (Vossel et al., 2011)

### ***3.7 Deficits in sound localization from the literature on neglect***

In contrast to lesions in the visual or the somatosensory system, lesions in the auditory cortices do not seem to cause specific contralesional deficits (Gutschalk, 2012). A study in patients with lesions in the right and left hemispheres performing a dichotic listening test with interaural time differences found a hemispheric asymmetry in auditory lateralization, but directional hearing was only impaired by lesions involving the right hemisphere (Bisiach, Cornacchia, Sterzi, & Vallar, 1984). Since the lesions spanned different brain regions it was not clear if the impairment was due to lesions involving the

primary auditory cortex or to those outside of it. A study of sound localization found that lesions in the primary auditory cortex had no effect on sound localization. However, a lesion in the right superior temporal gyrus located outside the primary auditory cortex was associated with disturbance of sound localization on both sides of space (Zatorre & Penhune, 2001). A more recent study on auditory localization compared the effect of lesions located in the primary auditory cortex to those located outside the auditory cortex in patients following a middle cerebral artery infarct. The authors found no effect of lesions in the primary auditory cortex itself, while lesions outside the primary auditory cortex were seen to have an effect, particularly when they involved the right hemisphere (Gutschalk, 2012). This converging evidence from literature on neglect and on neuroimaging suggests a role of the temporal and parietal regions in auditory spatial processing (Arnott, 2004, 2005; Barrett, 2010).

### ***3.8 Theories in neglect***

Several theories have been proposed to explain the phenomenon of neglect. Among these are the following: (1) Representational theories postulate a memory component resulting in a difficulty to mentally represent the contralesional space (Bisiach and Luzzatti, 1978, Bisiach et al., 1981, Bartolomeo et al., 1994). (2) Transformational theories hypothesize that neglect results as a failure to map multisensory inputs into motor commands (Karnath, 1997, Colby, 1998) (3) Attentional theories propose that neglect is due to a

deficit in the allocation of attentional resources of the brain (Kinsbourne, 1970). A striking phenomenon of neglect is that the neuropsychological deficit characterized by ipsilesional bias is stronger and more frequent after lesions affecting the right hemisphere (Driver & Mattingley, 1998). Two theories have been proposed to explain this asymmetry: (1) the orientation bias model hypothesizes that attention is shifted toward the contralateral side of space via inhibition of the ipsilateral hemisphere (Kinsbourne, 1970). Evidence supporting this model is provided mainly by transcranial magnetic stimulation studies inducing “virtual lesions” in parietal areas while measuring attentional performance (Hilgetag et al., 2001, Oliveri et al., 2001, Koch et al., 2008). (2) the right-hemisphere dominance model states that the left hemisphere represents the right side of space, whereas the right hemisphere represents both sides (Heilman, 1980). This asymmetry is predicted by recent anatomical evidence in humans showing that the superior longitudinal fasciculus, which connects frontal and parietal cortices, has a right-hemisphere dominance with a positive correlation between performance during detection of visual targets in left and right hemifield and the volume of white matter tracts in the right hemisphere (Thiebaut de Schotten et al., 2011).

### ***3.9 Causality and the study of lesions***

The brain is extremely complex. Most of what we know about it arose from techniques that differ in spatial and temporal resolutions. Functional MRI is usually assumed to establish a correlation between brain metabolic changes and behavioral output (Logothetis, 2008). Both critics and users of functional neuroimaging deny that it can establish causality. Causality means that a phenomenon A arises due to activity in region B. If region B were to be ablated, then phenomenon A would be extinct. However, functional neuroimaging can provide hints about causality, e.g., viewing a moving cloud of dots will lead to activity in the visual cortex. Nevertheless, supplementing functional neuroimaging studies with techniques that can manipulate neural activity is of great interest to neuroscience. In the study of causality it was traditionally fruitful to observe the effect of lesions on behavior. The, perhaps, first report was by Jean Cesar Legallios in 1812 who identified the role of the medulla in respiration. Charles Bell and Franqois Magendie demonstrated in 1822 that the spinal roots in dogs were anatomically and functionally distinct; sensory functions are ventral and motor functions are dorsal. Pierre Paul Broca in 1863 reported language impairments in two patients linked to the left inferior frontal gyrus of the brain. At about the same time that Broca and Wernicke were defining the importance of the left hemisphere in language production and comprehension, John Hughlings Jackson (1874, 1876) described what he termed “imperceptions,” in which patients suffered a “loss or defect of memory for



persons, objects, and places.” and associated this with damage to the right hemisphere.

### ***3.10 Issues in the study of lesions effect on cognitive tasks***

To understand effect of lesions, patients are usually grouped either by lesion or by behavior (Chao & Knight, 1998). The lesion approach gives valuable information regarding the role of regions of interest (ROI). However, it does not reveal much about the subregions in the ROI, and overlooks the role of regions outside the ROI. In the behavioral approach, patients are grouped by their behavior resulting in overlapping lesions based on the behavioral deficit (Dronkers, 1996). This approach provides information about brain regions that might contribute to cognitive processes. However, for continuous data a cut-off must be applied, possibly leading to a loss of information about performance.

### ***3.11 Voxel-based lesion-symptom mapping***

Voxel-based lesion-symptom mapping (VLSM) was introduced to investigate the relation between lesions and cognitive skills on a voxel-by-voxel scale (Bates et al., 2003). It can overcome the problems mentioned above in (Chapter 3.10). VLSM does not require patients to be grouped either according to lesion or behavior, as it benefits from continuous behavioral and lesion information (Bates et al., 2003). Important improvements have been made on the statistical tests used to implement VLSM (Rorden, Karnath, & Bonilha, 2007). In this manuscript, we applied voxel-based lesion-symptom mapping approach to investigate the causal contribution of cortical and subcortical lesions in the right hemisphere on auditory and visual spatial perceptual decision-making.

#### **4. The scope of the manuscript:**

The scope of this manuscript is to advance the knowledge of the neural correlates of sensory evidence accumulation in auditory and visual perceptual decision-making using functional magnetic resonance imaging and lesions study. Specifically, it investigates if the neural signature of sensory evidence accumulation is a modality-specific phenomenon. It also disentangles neural correlates of visual sensory evidence accumulation from neural correlates of decision-monitoring; confidence in the visual perceptual decision. Finally, it explores the effects of cortical and subcortical lesions in the right hemisphere on auditory and visual perceptual decision-making.

## **5. Empirical studies:**

In the previous chapters, we detailed the literature on perceptual decision-making, confidence in the decision, and auditory spatial processing. We concluded that one does not know if there is a brain region that accumulates sensory evidence regardless of sensory modality, nor does one know if the neural correlates of sensory evidence accumulation are also the neural correlates of decision-monitoring, confidence in the decision or error detection.

In the following chapters, we summarize our three studies in which we investigated auditory and visual perceptual decision-making in healthy participants and stroke patients. In the first study, we investigated the modality-specific signature of sensory evidence accumulation using model-based functional magnetic resonance imaging. In the second study, we explored neural correlates of perceptual decision and neural correlates of confidence in the decision. In the third study, we examined the causal role of cortical and subcortical lesions on visual and auditory perceptual decision-making.

## 5.1 Modality-specific neural signatures of perceptual evidence accumulation: a model-based fMRI approach

### **ABSTRACT**

Neural correlates of perceptual sensory evidence accumulation have been observed in sensory, frontal and parietal cortices, as well as in subcortical brain regions. However, it remains unclear if these neural correlates actually evidence of sensory information, salience, or action planning. In this study, we measured event-related fMRI in humans performing perceptual decisions based on noisy visual or auditory evidence and reported by a button response. The subjects saw or heard flashes or clicks on both the left and the right side and had to decide on which side there had been more events. Accumulation processes were fit to a quantitative model to estimate the perceptual evidence on a trial-by-trial basis. We found that BOLD signals in the occipital cortices correlated with accumulated visual evidence while signals in the superior temporal gyrus correlated with accumulated auditory evidence. BOLD signals in the frontal and parietal cortices were not correlated with spatially-specific perceptual evidence but instead with decision difficulty, i.e. regardless of the location in space, the BOLD signal increased in the harder trials in both the visual and auditory tasks. This suggests that sensory evidence accumulates in modality-specific sensory cortices. Thus, the well-known signatures of evidence accumulation observed in the frontal and parietal cortices may have been activity relayed from the sensory cortices, and may thus reflect secondary decision-making variables such as

salience, or action preparation.

## **INTRODUCTION**

For successful orientation in a multidimensional environment, the brain evolved and became able to receive and gradually accumulate sensory evidence to form perceptual decisions about the direction the animal should orient itself in space. Neuroimaging studies in humans investigating the neural correlates of sensory evidence accumulation have done so using mostly visual tasks (Filimon, 2013; Hebart et al., 2012; Heekeren, 2004, 2008; Philiastides & Sajda, 2007). Neuroimaging studies identified several brain regions as neural substrates of visual sensory evidence accumulation. These are e.g., the occipital cortex (Hebart et al., 2012; Philiastides & Sajda, 2007) or higher cortical regions such as dorsolateral prefrontal cortex (DLPFC) (Filimon, 2013; Heekeren, 2004), frontal eye fields, the inferior parietal lobule and insular cortex (Ho & Brown, 2009; Liu & Pleskac, 2011). In comparison, less is known about the neural correlates of auditory sensory evidence accumulation. It was shown that regions in the auditory sensory cortices contribute to object identification (Binder, Liebenthal, Possing, Medler, & Ward, 2004) and conscious perception of the auditory decisions (Kilian-hu et al., 2011). However, it remains unclear whether there is a brain region that accumulates spatial evidence regardless of the sensory modality.

Animal electrophysiology studies have shown that the neural correlates of evidence accumulation involve several brain nodes such as the posterior parietal cortex (PPC) (Roitman & Shadlen, 2002), the prefrontal cortex (PFC) (Hunt et al., 2012) such as frontal eye fields (FEF; (Kim & Shadlen, 1999; Purcell et al., 2010), PPC and PFC (Hanks et al., 2015). Recently, auditory tasks have been developed, in which stimuli are presented discretely over time and space allowing one to investigate signals of auditory evidence accumulation in epochs of time (Brunton., 2013). A drift diffusion based model was developed to fit behavioral data from the auditory accumulator task and showed that rats accumulate sensory evidence (Brunton., 2013). Despite recent developments in tasks and the importance of understanding the neural correlates of auditory sensory evidence accumulation, it is still not clear how auditory sensory evidence accumulates in the brain (Hanks & Summerfield, 2017).

Thus, the goal of this study was to identify brain regions that are involved in the modality-specific accumulation of sensory evidence, and brain regions that are sensory modality non-specific. Based on previously literature from previous neuroimaging studies in humans (Filimon, 2013; Hebart et al., 2012; Heekeren, 2004, 2008; Philiastides & Sajda, 2007), we hypothesized that frontal and parietal cortices would show correlations with modeled sensory evidence regardless of sensory modality. To explore this hypothesis, we used event-related model-based fMRI to test an auditory and a visual version of an accumulator task with two alternative choices, in which stimuli are presented

discretely over time and space allowing for use of a quantitative model to model accumulated evidence for each trial.

## **MATERIALS AND METHODS:**

### ***Participants***

Twenty-one right-handed healthy participants took part in the study. Four participants were excluded since they only finished one task and did not show up for the next session. Two participants were excluded because they showed systemic bias towards one choice. Fifteen of the participants finished all tasks (seven females, mean age  $23.25 \pm 3.72$  years) and were included in the final analysis. Participants had normal hearing, normal or corrected vision, no history of neurological or psychiatric disease. All participants gave written informed consent. All procedures were performed according to the declaration of Helsinki and were approved by the local Ethics Committee of the University Medical Center Göttingen. Participants were given monetary compensation for participating in our experiments.

### ***Task and Stimuli***

Participants were asked to perform an auditory and a visual version of an evidence accumulation task. In both versions, they were asked to form spatial decisions, i.e. whether more stimuli had been presented on the right or left side. In the auditory task, participants wore a headset and were asked to determine which ear had received more clicks. In the visual task, participants were asked to determine the side of the screen that had shown most flickers. The stimuli were



drawn from a Poisson distribution for both modalities and adjusted for the adaptation dynamics of the visual or the auditory system (Brunton., 2013). They were presented discretely over time and space, allowing the fitting of a dynamic model that captures the accumulation of sensory evidence towards a spatial decision. Changes in the color of the fixation cross indicated different stages of the task, in order to keep the visual input throughout different task stages as constant as possible. Each trial started with the presentation of a central red fixation cross. After a mandatory stable fixation period of one second the stimuli were presented for three seconds, followed by a variable delay of six to eight seconds inside the scanner. The color of the fixation cross changed to green indicating the beginning of the response period. Participants were asked to respond with their right hand using the index and middle fingers. Participants responded by pressing key '1' if they thought the trial had more stimuli on the left, or key '2' if they chose the right side. No feedback was given to the subjects. The following rest period inside the scanner varied between six and eight seconds. The duration of delay and rest times were randomized (6-8) seconds to prevent the participants from forming a response strategy, and to increase design efficiency in this event-related design (by reducing multicollinearity between predictors that follow closely in time). Participants were asked to use the entire information presented to them in each trial to form their choice. In the actual experiments, the participants were required to finish four runs inside the scanner of each modality; a total of 128 trials for each modality.

### ***Auditory stimuli***

Trains of 3ms clicks lasting three seconds were presented over headphones. Twenty clicks per second were presented randomly to each ear separately ( $\# \text{clicks right (CR)} + \# \text{clicks left (CL)} = 20$ ). There was a minimum inter-pulse interval of 33ms to minimize adaptation. The first, and last clicks were presented to both ears simultaneously to prevent bias towards the side of the first or the last click presented (Brunton et al., 2013). Easy trials differed by 40 clicks between the ears (CR-CL), while harder trials had a five-clicks difference. Stimuli were generated using MATLAB, version R2011b using custom scripts.

### ***Visual stimuli***

Trains of stereo flickers lasting three seconds were presented on the horizontal plane of the screen at an eccentricity of around 11 visual degrees. Each train had five flickers per second ( $\# \text{flickers right (FR)} + \# \text{flickers left (FL)} = \text{five per second}$ ). Each flicker lasted 16.7ms and had a visual angle of approximately two degrees. Consecutive flickers had a minimum inter-pulse interval of 120 ms to minimize adaptation (Brunton et al., 2013). The first and last flickers were presented bilaterally to prevent bias towards the side of the first or the last flicker presented. Easy trials differed by ten flickers between the sides (FR-FL), while harder trials had a two flickers difference. Stimuli were generated using MATLAB, version R2011b using custom scripts.

## *Data analysis*

### *Behavioral data analysis*

Repeated measures analysis of variance (rANOVA): To investigate the effect of modality, difficulty, and space on performance in the scanner we constructed an rANOVA with the following factors, each with two levels: modality (audio, visual), difficulty (absolute difference of stimuli presented to the right minus number of stimuli presented to the left resulting in two levels, i.e. hard, easy), and space (left and right). The percent correct decisions were calculated for each difference level for each participant across runs for each modality. Significant effects were followed up with post hoc t-tests. Moreover, the probability "press right" was plotted as a function of the number of stimuli presented to right minus number of stimuli presented to the left (**Figure 5.1.1A**).

### *Accumulator model:*

A recent nine-parameter model based on the drift-diffusion model was developed to study sensory evidence accumulation, and we will refer to it in the manuscript as the accumulator model (Brunton., 2013). In order to verify that participants accumulated the sensory evidence presented over the whole trial as auditory clicks or visual flickers, an accumulator model using the individual click times and the participants' choices in each trial was fitted (Brunton., 2013). Data was concatenated for all trials across all participants for the auditory task and the visual task separately. The accumulator model uses nine parameters to

transform the stimulus in each trial (input to the model are left and right stimulus times) into a probability distribution about the choice of the participant. For example, if for a given set of parameters, the model predicts that Trial 1 will result in a 75% chance of the participant choosing right, and the participant, in fact, did choose right, that trial would be assigned a likelihood of 0.75. In the case that the participant chose left, the trial would be assigned a likelihood of 0.25. We fit the model under the assumption that the trials are independent. Therefore, for a model with parameters  $\theta$  for all decisions  $D$ , the likelihood is given by:

$$P(D|\theta) = \prod_i P(d_i | t_{i,R}, t_{i,L}, \theta),$$

The product of the likelihood of the decision on trial  $i$ ,  $d_i$ , given the times of the right stimulus,  $t_{i,R}$ , times of the left stimulus  $t_{i,L}$ , and the set of nine parameters,  $\theta$ . A detailed description of the procedure for fitting the accumulator model can be found in the Modeling Methods section of the supplement to (Brunton et al., 2013). The model includes a ‘lapse’ parameter, which represents a fraction of trials in which subjects will ignore the stimulus and choose randomly. The presence of the lapse parameter also puts a lower bound on the likelihood of any individual trial, and thus no individual trial can dominate the results and the consequent fits of the model. Moreover, the model estimates a leakiness parameter referred to as lambda parameter. A lambda close to zero indicates that participants used the entire information presented to them at the trial to reach

their decision, meaning a perfect accumulator strategy.

The psychometric curves were generated by concatenating trial data across sessions for each participant and using Matlab's `nlinfit` to fit a four-parameter sigmoid as follows:

$$y(x) = y_0 + \frac{a}{1 + \exp\left(\frac{-(x-x_0)}{b}\right)}$$

For these fits,  $x$  is the click difference in each trial ( $\#Right$  stimulus  $- \#Left$  stimulus),  $y$  is 'P (Chose Right)', and the four parameters to be fit are:  $x_0$ , the inflection point of the sigmoid;  $b$ , the slope of the sigmoid;  $y_0$ , the minimum 'P(Chose Right)'; and  $a + y_0$  is the maximum 'P(Chose Right)'.

### ***Functional Magnetic Resonance Imaging (fMRI)***

#### ***General experimental setup inside the scanner***

Participants were placed in the MR scanner (3T, Siemens TIM Trio, Siemens Healthcare, Erlangen, Germany) in a supine position. In order to prevent the head from moving, it was stabilized inside the Siemens 12 channel head coil by means of cushions. Headphones were used to protect the ears from scanner noise. Auditory stimuli were played binaurally through insert earphones (Sensimetrics corporation, Malden, MA). For the visual task, the subjects wore additional in-ear foam plugs for further noise protection instead of the earphones. Visual stimuli were delivered using MR-compatible, liquid crystal display (LCD) goggles (Resonance Technology, Northridge, CA). The spatial

resolution was  $800 \times 600$  pixels, covering a visual field of  $32 \times 24$  degrees, at a refresh rate of 60 Hz. Eye position was monitored with an MR compatible 60 Hz eye tracking system (Arrington Research, Scottsdale, AZ). The participants responded using an MR-compatible, fiber optic, four-button response pad (Current Designs, Philadelphia, PA, USA). Trigger pulses from the MR Scanner were used to synchronize functional image acquisition and experimental tasks. The participants were invited to do either the visual or the auditory task on the measurement day. The order of days the participants performed the visual or the auditory task was counterbalanced.

### ***MRI data acquisition***

All images were acquired using a 3Tesla Magnetom TIM Trio scanner (Siemens Healthcare, Erlangen, Germany) with a 12-channel phased-array head coil. First, a high-resolution T1-weighted anatomical scan (three-dimensional (3D) turbo fast, low angle shot, echo time (TE): 3.26 ms, repetition time (TR): 2.250 ms, inversion time: 900 ms, flip angle  $9^\circ$ , isotropic resolution of  $1 \times 1 \times 1 \text{ mm}^3$ ) was obtained. All functional data were acquired using T2\*-weighted gradient-echo echo-planar imaging (EPI) (TE: 30 ms, TR: 1.800 ms, flip angle  $70^\circ$ , 34 slices of 3-mm thickness, 20% gap between slices, parallel imaging iPat2 with GRAPPA at an in-plane resolution of  $3 \times 3 \times 3 \text{ mm}^3$ ). Four dummy scans were added at the beginning of each run to allow for T1 equilibrium. A total of 425 whole brain volumes were acquired in each functional run. Participants performed two fMRI

sessions of 4 runs each.

### ***MRI data pre-processing and analysis***

BrainVoyager QX Software version 2.8 (Brain Innovation, Maastricht, The Netherlands), and the Neuroelf 0.9c toolbox for Matlab (retrieved from <http://neuroelf.net/>) were used for preprocessing and analysis of the functional data. Standard preprocessing steps included 3D motion correction, slice scan time correction and temporal filtering [linear trend removal and high pass filtering (2cycles/run)]. The functional data were co-registered to the anatomical reference scans, transformed into Talairach space and spatially smoothed with a Gaussian kernel (full width at half maximum  $6 \times 6 \times 6\text{mm}^3$ ). Further statistical analysis was performed using the general linear model (GLM) implemented in the BrainVoyager software. First level GLM was first estimated for each subject. For each run, stimulus presentation, delay period, and motor response were modeled based on the subjects' choice as right easy, right hard, and left easy, and left hard. For the final presentation of figures, GLM models prepared in BrainVoyager environment were analyzed in Neuroelf toolbox and Matlab. For the group results, a random effects analysis using the GLM was performed with 15 participants. For all statistical maps, multiple comparison corrections were performed at the cluster level. Maps were thresholded at an initial cluster-forming threshold with  $P < 0.005$ . The size of the resulting clusters was assessed for significance using AlphaSim simulations as implemented in Neuroelf's

cluster-level statistical threshold function. Reported clusters are significant at a level of  $P < 0.05$  unless stated otherwise.

### ***Voxel-wise repeated measure analysis of variance (rANOVA)***

A voxel-wise repeated measures analysis of variance (rANOVA) was performed in BrainVoyager QX Software version 2.8 (Brain Innovation, Maastricht, The Netherlands) at the whole brain level with the modality, difficulty, and space as the within-subject factors. In the case of statistical significance, the significant clusters were defined as regions of interest (ROIs), and post hoc t-tests were implemented at the ROI level for evaluating the specific contrasts. Maps were thresholded at an initial cluster-forming threshold with  $P < 0.005$ . The size of the resulting clusters was assessed for significance using AlphaSim simulations as implemented in NeuroElf's cluster-level statistical threshold function. Reported clusters are significant at a level of  $P < 0.05$ . For labeling the significant regions, the peak activation voxel from each cluster was entered into the Talairach client tool (<http://www.talairach.org/client.html>), a 6-mm range cube was defined around the peak voxel, and the cluster was labeled according to the region to which most of the defined voxels belong.

### ***Model-based analysis investigating regions accumulating sensory evidence***

In order to study which brain regions accumulated sensory evidence for each modality, a separate GLM was constructed with the following regressors: stimulus presentation, delay, response. The modeled estimates of sensory



evidence were used to build two predictors: (1) Signed evidence predictor: using the signed values of modeled evidence. (2) Absolute evidence predictor: using absolute values of the modeled evidence. Regions showing correlation with the signed evidence predictor were used as ROIs. Event-related averages were constructed from those ROIs. A region would qualify as an accumulator if the event-related averages were organized in a specific manner (i.e. an accumulator towards leftward decisions: left high evidence > left low evidence > right low evidence > right high evidence).

***Estimation of correlation level between beta estimates and modelled evidence:***

In order to systematically determine the level of correlation between beta estimates and accumulated sensory evidence as modeled from data inside the scanner, a scatter plot of mean beta values as a function of modeled evidence was plotted. Mean beta values from each participant were extracted from each ROI showing activity modulated by evidence. Beta values of each subject were demeaned by subtracting the mean value of all subjects. A correlation coefficient was determined between evidence values and mean beta values using built-in MATLAB functions.

***Contralateral selectivity index:***

Frontal eye field and inferior parietal lobule coordinates were determined based on mean coordinates from Krafft et al. (Krafft et al., 2013). Beta values were

extracted from assigned ROIs. A contralateral selectivity index was calculated as follows: CS index = (Contra-Ipsi)/max[abs(Contra), abs(Ipsi)] for each ROIs.

## **Results**

Participants were asked to perform an auditory and a visual version of an evidence accumulation task (Brunton et al., 2013). In both versions, participants were asked to decide whether more stimuli were presented to the left or right space. Two levels of difficulty were tested based on the absolute difference of the number of stimuli presented to the right minus number of stimuli presented to the left (**Figure 5.1.1A**).

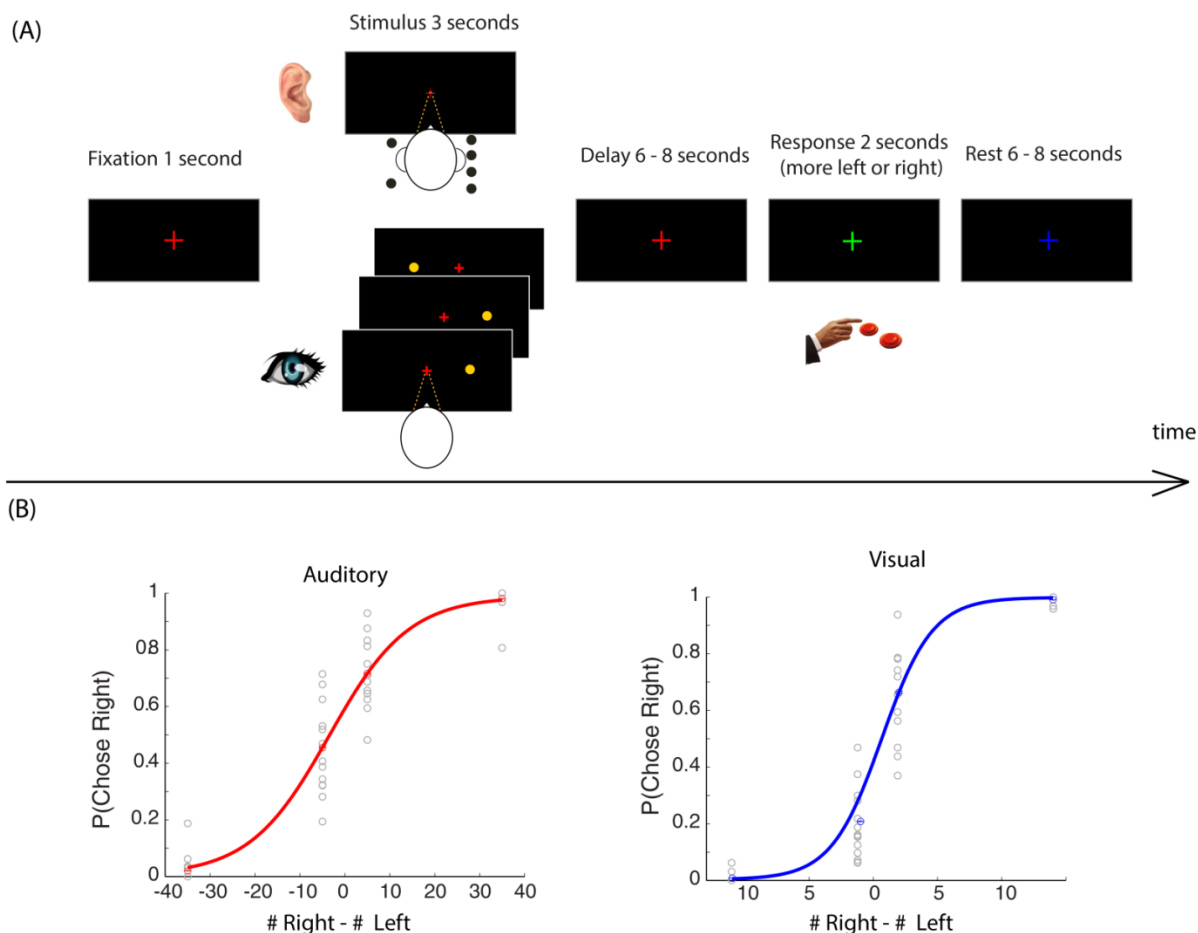


Figure 5.1.1. **Behavior of visual and auditory accumulator tasks.** (A) Task description: after a mandatory one second fixation, trains of lateralized clicks in the auditory task, and trains of lateralized flickers in the visual task were presented. Participants decided which side of space has more stimuli - right or left. Participants responded with a button press. Participants performed the tasks on separate days with the order of modality randomly balanced. (B) Probability of participants choosing right as function of total flickers right minus left. For easy trials  $\approx 100\%$  for both modalities, grey circles are individual participants data, color circles are the means with 95% binomial confidence intervals across accumulator trials from all subjects. The thick line is the psychometric curve generated by the accumulator model.

### ***Behavioral results***

The psychometric curves show that the participants performed both tasks inside the scanner with high accuracy. For easy trials in both tasks, the participants were able to detect the side with the most stimuli  $\approx 100\%$  (**Figure 5.1.1B**). We

were interested in the effect of modality, difficulty, and space. Therefore, we ran a *repeated measures* analysis of variance (rANOVA) on percent correct with modality, difficulty, and space as within-subject factors. We found a significant main effect of modality on percent correct ( $F(1, 14) = 5.01$ ,  $p = 0.04$ ) and a significant main effect of difficulty ( $F(1, 14) = 338.12$ ,  $p < 0.001$ ). There was no significant main effect of space ( $F(1, 14) = 0.323$ ,  $p = 0.57$ ). No significant two-way or three-way interaction between factors was found. Post hoc t-tests investigating the significant main effects revealed that mean percent correct in the visual task was significantly higher than the mean percent correct in the auditory task ( $t(14) = 2.24$ ,  $p = 0.04$ ). This was most likely due to the scanner noise. Importantly, mean percent correct was significantly higher for easy trials in both the visual and auditory modality as compared to harder trials (visual task ( $t(14) = 10.11$ ,  $p < 0.001$ ) and auditory task ( $t(14) = 14.42$ ,  $p < 0.001$ )).

### ***Model fitting results***

To investigate whether the participants used an accumulation strategy to reach their decision we fitted behavioral data to a nine-parameter accumulator model (Brunton et al., 2013). Due to the low number of data points per subject inside the scanner, we fitted a single model to combined data from all participants. A key feature of this high-dimensional model is that different parameter regimes reflect different strategies. Thus, rather than assuming that the subjects are accumulating evidence, we fitted this model to their choices to test whether they actually were using an accumulation strategy. One critical parameter is  $\lambda$ , which

is the reciprocal of the time-constant of the accumulation process. If  $\lambda$  is negative, it means that the process is "leaky" and early information is lost. If  $\lambda$  is positive, then the process is "unstable" and early evidence dominates the decision,  $\lambda = 0$  reflects a perfect integrator. Model fits show that the participants adopted a perfect integrator strategy (**Supplementary Table S5.1.1**).

### ***fMRI results***

We performed two types of fMRI analysis: (1) In the 'Non-model-based' analysis fMRI signals were submitted to a voxel-wise whole brain repeated measures ANOVA (rANOVA) with modality, difficulty, and space as within-subject factors. (2) In the 'Model-based analysis' sensory evidence estimates from the model were used to modulate the stimulus presentation period parametrically. In both analyses, GLMs were calculated using *random effects* (RFX) analysis. Maps were thresholded at an initial cluster-forming threshold with  $p < 0.005$  and corrected for multiple comparisons at the cluster level.

### ***Sensory cortices show modality-specific activity***

Voxel-wise whole brain rANOVA of the stimulus presentation period revealed a significant main effect of modality in the lentiform, precentral, and superior temporal gyri, the thalamus, the occipital gyrus, and the superior parietal lobule (**Figure 5.1.2A, Supplementary Table S5.1.2**). To explore effect of each modality, we extracted beta values of each modality from regions showing the main effect of modality. We performed post hoc t-tests for comparing auditory to

visual. Activity in superior temporal regions was significantly higher for auditory stimuli compared to visual stimuli ( $p < 0.001$ ), while occipital regions had significantly higher activity for visual stimuli compared to auditory stimuli ( $p < 0.001$ ). The activity in thalamus, precentral and lentiform gyri, and superior parietal lobule was significantly higher for the visual modality ( $p < 0.0001$ ).

### ***Frontal and parietal regions show multi-modal activity***

To investigate which brain regions showed activation in both auditory and visual modalities we conducted a conjunction analysis between the auditory stimulus presentation and resting, and visual stimulus presentation and resting. Brain regions with overlapping activity were: inferior frontal gyrus, medial frontal gyrus, insula, precentral gyrus, cingulate gyrus, inferior parietal lobule, superior temporal gyrus, and precuneus gyrus (**Figure 5.1.2C, Supplementary Table S5.1.3**). Post hoc t-tests comparing auditory to visual showed that there was no statistically significant difference between auditory and visual signals in the inferior frontal gyrus, medial frontal gyrus, insula, precentral gyrus, and cingulate gyrus. However, the posterior parietal and temporoparietal regions had a stronger signal for the visual modality.

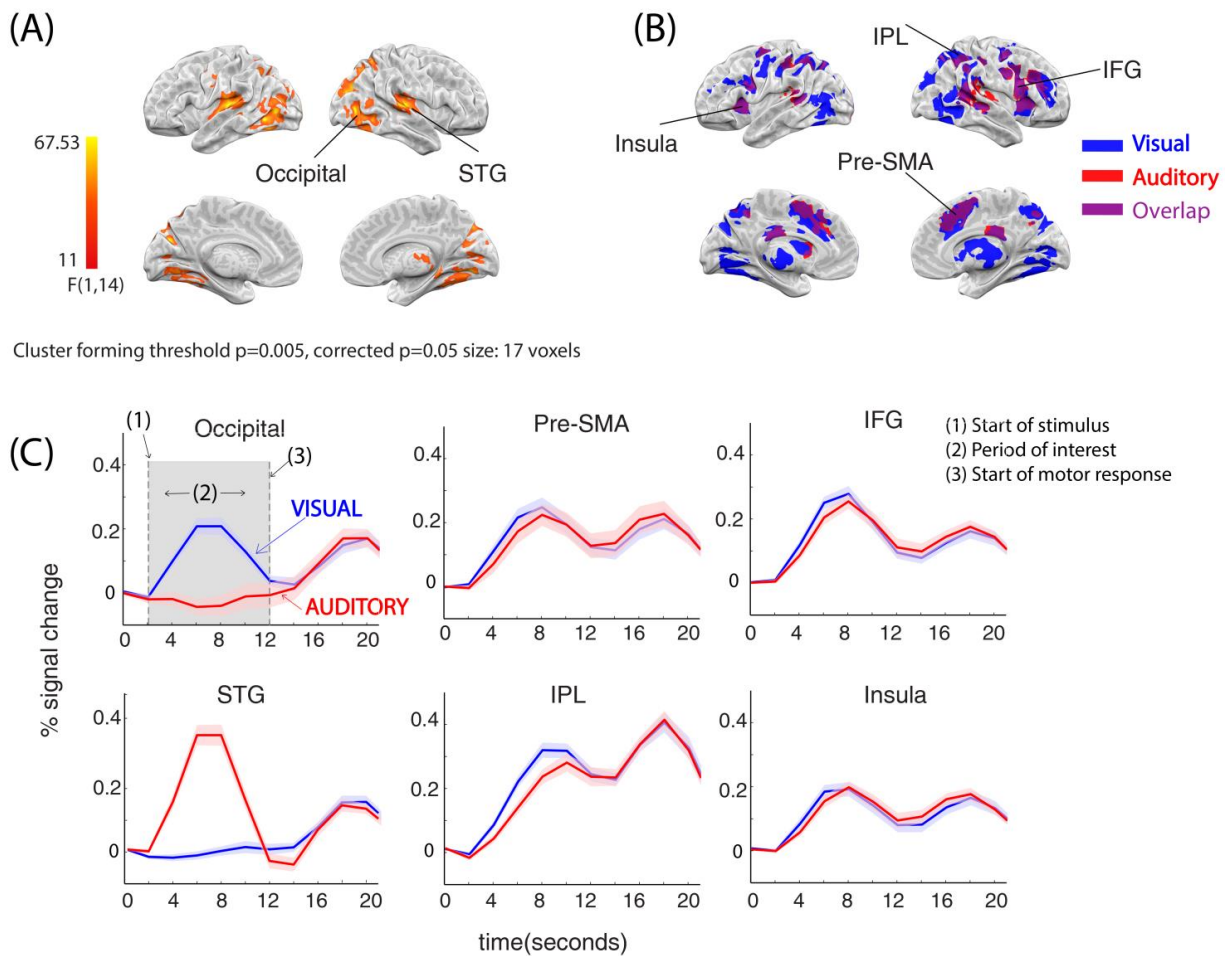


Figure 5.1.2. **Main effect of modality.** (A) Statistical map of brain regions showing main effect of modality ( $F(1,14) > 11.03$ ,  $p=0.005$ ) (B) Statistical map showing brain regions with overlapping signals of both modalities in purple, auditory stimulus > rest in red, and visual stimulus > rest in blue. Cluster forming threshold  $p=0.005$  corrected  $p=0.05$  size=17voxels. (C) Event-related averages visualize the effect of modality; sensory cortices show modality-specific effects while frontal and parietal regions show effects of both modalities.

### *Prefrontal and parietal activity is modulated by task difficulty in both modalities*

Based on the predictions of the BOLD signal behavior in relation to task difficulty, it has been proposed that brain regions involved in perceptual sensory evidence accumulation would have higher activity in easier trials, i.e. when the absolute difference between the number of left and right stimuli was larger (Filimon, 2013; Heekeren, 2004; Philiastides & Sajda, 2007; Rolls u. a., 2010). Therefore, we investigated the effect of task difficulty. In our task design, we used two levels of difficulty (easy vs. hard) for each modality based on the absolute difference of the number of stimuli presented to the right minus number of stimuli presented to the left. We found the main effect of difficulty in several brain regions: lentiform, claustrum, superior frontal gyrus, cingulate gyrus, cuneus gyrus, inferior parietal lobule, precentral gyrus, superior temporal gyrus, fusiform gyrus, and middle occipital gyrus (**Figure 5.1.3A, Table 5.1.1**). To investigate the role of modality, we extracted beta values from brain regions showing a main effect of difficulty and used follow-up t-tests comparing easy to hard trials in each modality. Post hoc t-tests showed that all regions exhibiting the main effect of difficulty had higher activity when the task was easier (**Table 5.1.1**). To determine whether other brain regions also had a stronger signal when the task was harder but did not statistical significance due to a conservative cluster-forming threshold we calculated a whole brain, voxels-wise t-test comparing easy to hard at cluster forming with  $p=0.05$  (**Supplementary Figure**



**5.1.1).** The following brain regions showed a stronger signal when the task was harder: left insula, right cingulate, right inferior frontal gyrus, right middle frontal gyrus, and right inferior parietal lobule. We formed ROIs from brain regions with stronger signal when the task was harder. Since it was possible that difficulty is handled differently for the different modalities, we explored the effect of difficulty separately for each modality in the aforementioned ROIs. For the visual task, all ROIs had a significantly stronger signal when the task was harder ( $p < 0.05$ ). For the auditory task, the signal was significantly stronger when the task was harder in the cingulate, inferior frontal and middle frontal gyri ( $p < 0.05$ ) (**Figure 5.1.3B**).

**Table 5.1.1. Brain regions showing main effect of task difficulty**

| Brain region | BA       | #Voxels | Post hoc<br>easy vs. hard |        | Post hoc<br>Visual<br>easy vs.<br>hard |       | Post hoc<br>Auditory<br>easy vs. hard |        | Tal<br>coordinates |     |    |
|--------------|----------|---------|---------------------------|--------|--|-------|---------------------------------------|--------|--------------------|-----|----|
|              |          |         | t(14)                     | P      | t(14)                                  | P     | t(14)                                 | P      | x                  | y   | z  |
| R Lentiform  | -        | 237     | 4.30                      | <0.001 | 3.93                                   | 0.002 | 5.03                                  | <0.001 | 25                 | -3  | 6  |
| L Claustrum  | -        | 407     | 5.11                      | <0.001 | 3.28                                   | 0.005 | 7.19                                  | <0.001 | -36                | -10 | 18 |
| L SFG        | BA10     | 134     | 6.70                      | <0.001 | 3.16                                   | 0.007 | 7.90                                  | <0.001 | -30                | 52  | 10 |
| L Cingulate  | BA<br>24 | 20      | 3.35                      | 0.004  | 1.18                                   | 0.25  | 4.02                                  | 0.001  | -2                 | -11 | 48 |
| L Cuneus     | BA31     | 44      | 5.95                      | <0.001 | 2.91                                   | 0.01  | 4.47                                  | <0.001 | -8                 | -67 | 30 |
| L IPL        | BA40     | 56      | 5.23                      | <0.001 | 2.84                                   | 0.01  | 5.13                                  | <0.001 | -46                | -55 | 49 |
| L Precentral | BA4      | 17      | 4.96                      | <0.001 | 1.34                                   | 0.19  | 5.58                                  | <0.001 | -19                | -26 | 56 |
| R STG        | BA22     | 39      | 4.16                      | 0.001  | 2.72                                   | 0.02  | 3.82                                  | 0.001  | 50                 | -3  | 3  |
| L Fusiform   | BA19     | 37      | 5.24                      | <0.001 | 3.75                                   | 0.002 | 3.69                                  | 0.002  | -31                | -86 | -7 |
| R MOC        | BA18     | 19      | 2.43                      | 0.02   | 2.51                                   | 0.03  | 1.88                                  | 0.08   | 49                 | -22 | 11 |
| R STG        | BA41     | 22      | 3.41                      | 0.004  | 0.60                                   | 0.55  | 3.61                                  | 0.003  | 34                 | -78 | 1  |

Left (L), right (R), superior temporal gyrus (STG), superior parietal lobule (SPL), inferior parietal lobule (IPL), middle occipital (MO).

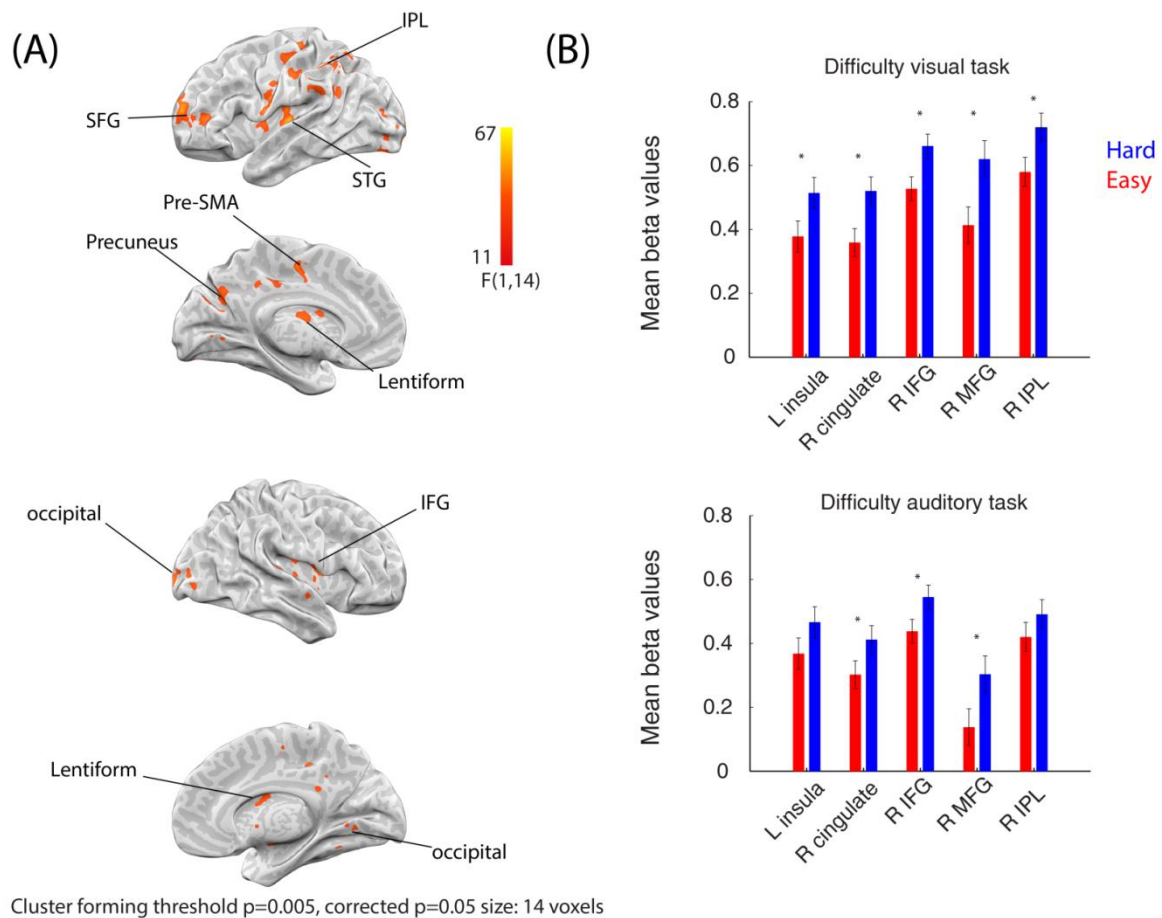


Figure 5.1.3. **Main effect of task difficulty.** (A) Statistical map of brain regions showing main effect of task difficulty ( $F(1,14) > 11.03$   $p=0.005$ ). post hoc t-tests revealed a significant difference between easy and hard for both modalities in regions showing main effect of modality  $p < 0.05$ . Post-hoc t-tests of regions with main effect of difficulty show higher in those regions when the task was easier (B) Bar plots of mean beta values from regions showing higher activity for hard compared to easy trials of cluster forming threshold  $p=0.05$ . To visualize regions where bar plots were extracted from refer to supplementary figure 5.1.1, inferior frontal gyrus (IFG), superior temporal gyrus (STG), superior frontal gyrus (SFG), inferior parietal lobule (IPL), middle frontal gyrus (MFG), right (R), left (L). Cingulate, IFG and MFG show higher signal for hard trials compared to easy trials.

*Spatially selective activity in sensory cortices and higher spatial selectivity in left parietal cortices*

In the current study, the perceptual evidence was spatially lateralized. We, therefore, investigated the brain regions showing activity modulated by space of the sensory evidence. We observed a main effect of space in the left inferior parietal lobule (**Figure 5.1.4A**). We extracted beta values from the brain regions showing a main effect of space and conducted post hoc t-tests to determine the role of modality. For both modalities, activity in left inferior parietal lobule was higher for rightward trials  $p=0.05$  auditory,  $p<0.001$  visual (**Supplementary TableS5.1.4**).

It is not considered advisable to base findings of hemispheric comparisons only on thresholded brain maps (Nagata et al., 2001). Thus, in order to investigate the degree of contralaterality in left and right frontal and parietal regions we calculated a contralaterality index  $(CS) = (Contra-Ipsi)/\max[\text{abs}(Contra), \text{abs}(Ipsi)]$  from orthogonal ROIs in frontal and parietal regions using mean coordinates (Krafft et al., 2013) and from the auditory and occipital cortices using mean coordinates as described by (Lewis et al., 2000). We found primary visual sensory and primary auditory sensory cortices to have a contralateral preference in both modalities. We found an asymmetrical preference in frontal and parietal regions. The left inferior parietal lobule had a rightward preference

in both modalities. The right inferior parietal lobule did not show a clear preference towards left or right space (**Figure 5.1.4C**).

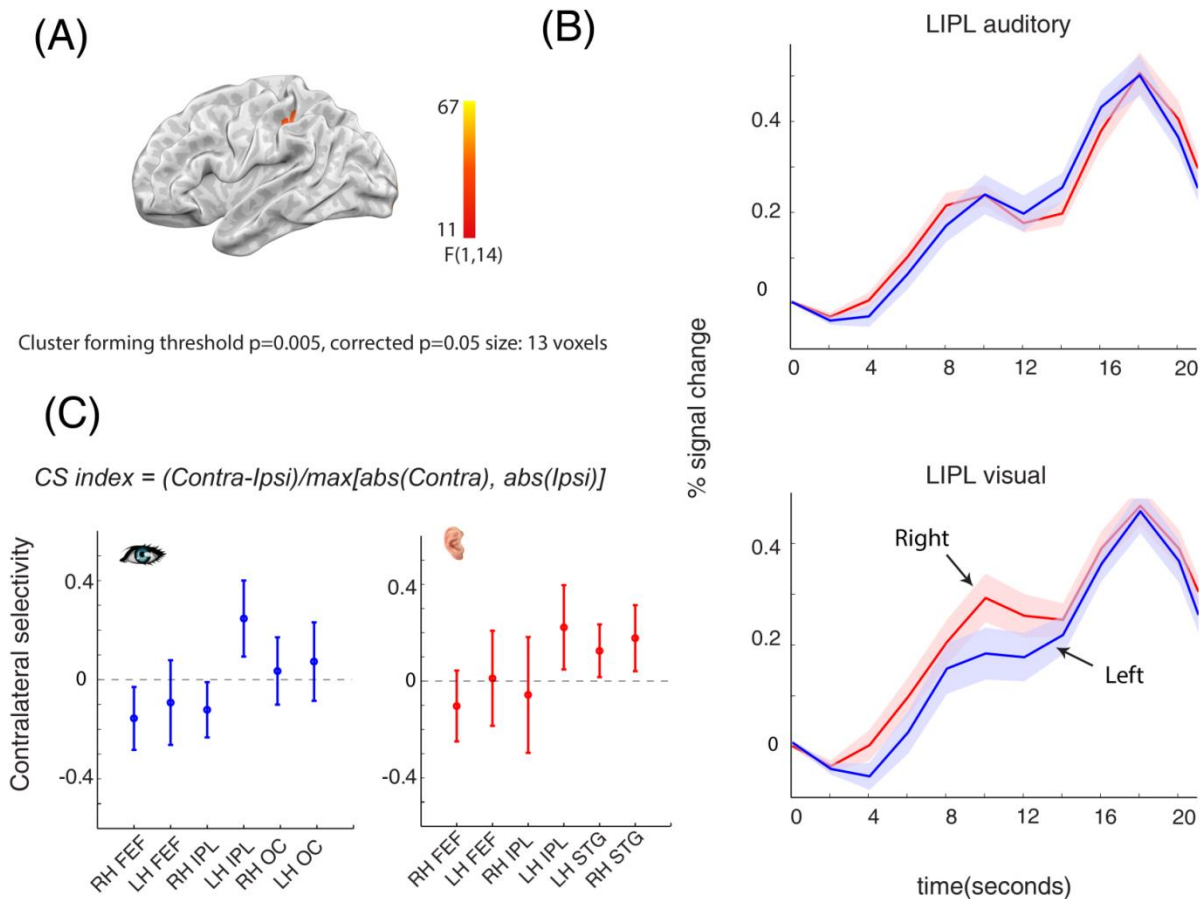


Figure 5.1.4. **Main effect of space** (A) Statistical map of brain regions showing a main effect of space. (B) Event-related averages (ERA) of right (red) and left (blue) trials for each modality from the left inferior parietal lobule (LIPL). (C) Contralaterality index from orthogonal ROIs ((Krafft, 2013) and (Lewis 2000) plots. Left (L), right (R), frontal eye fields (FEF), occipital (OC), superior temporal gyrus (STG).

*Sensory regions show an interaction between task modality, difficulty, and space*

In a search of multi-modal accumulator regions we hypothesized that such a multi-modal general accumulator would exhibit activity that is modulated by space and difficulty in a specific order, regardless of modality (for example for a region to qualify as accumulator towards left decisions its activity pattern will follow the order: left easy > left hard > right hard > right easy). We found no brain region exhibiting a two-way interaction between difficulty and space. To investigate if sensory evidence accumulated in a modality-specific manner we investigated brain regions exhibiting a three-way interaction between modality, difficulty, and space. We found the following region with this interaction: left cuneus region (**Table 5.1.2**). Visualizing time courses did not reveal an accumulator profile in the region identified by the three-way interaction.

**Table 5.1.2 Three-way interaction (difficulty, space, modality):**

| Brain region | BA    | #Voxels | Post hoc |        | Tal coordinates |     |    |
|--------------|-------|---------|----------|--------|-----------------|-----|----|
|              |       |         | t(14)    | P      | x               | y   | z  |
| L Cuneus     | BA 18 | 28      | -4.64    | <0.001 | -1              | -96 | 16 |

***Model-based analysis investigating brain regions accumulating sensory evidence:***

Our quantitative model allowed us to fit nine parameters using the precise timing of the sensory stimuli and the choices of the subjects. After fitting, we used the model to estimate the internal decision variable that the subjects computed in each trial. The model actually allowed us to calculate this variable at each moment of the trial (Hanks & Summerfield, 2017). However, the sluggish nature of the BOLD signal only enabled us to obtain one sample of neural activity per voxel/trial, so we compared the final amount of accumulated evidence with the BOLD signal at the end of the stimulus. We constructed two predictors using the model's estimates of accumulated evidence. The first predictor represents evidence pertaining to the spatial decision, and we refer to it as the signed evidence. The second predictor is based on the absolute level of uncertainty of the model (or ‘difficulty’).

***Regions with activity modulated by spatially specific sensory evidence:***

In order to study brain regions accumulating sensory evidence, we parametrically modeled the stimulus presentation period using values representing signed accumulated evidence as modeled by the accumulator model for each trial (see **Material and Methods**). For the visual task, we found the following regions to show the effect of signed, i.e. spatially specific evidence: middle temporal gyrus, postcentral gyrus, fusiform gyrus, cuneus gyrus and

precuneus gyrus (**Figure 5.1.5A**). We examined time courses and found that the occipital region exhibited an accumulator activity pattern (**Figure 5.1.5B**, **Table 5.1.3**).

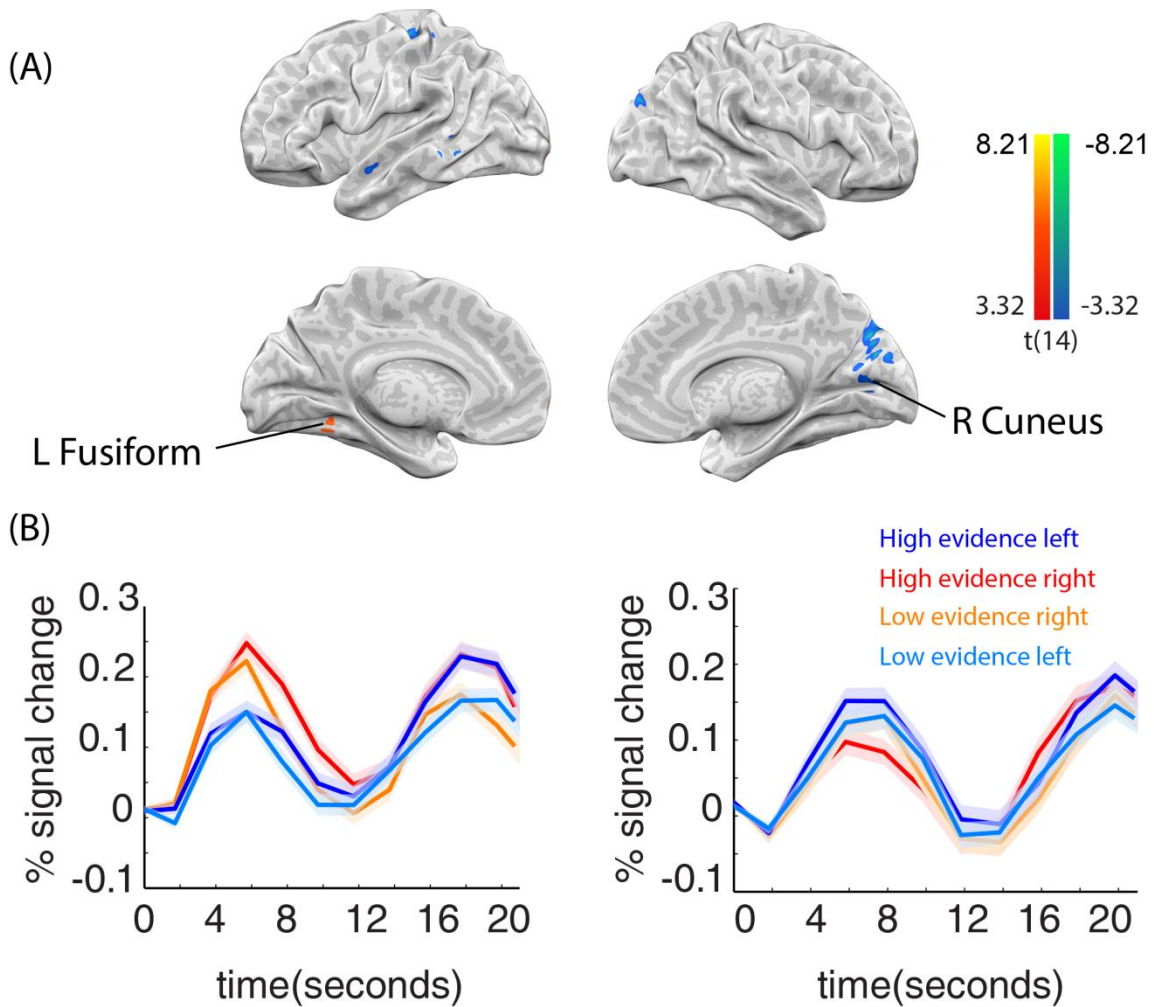


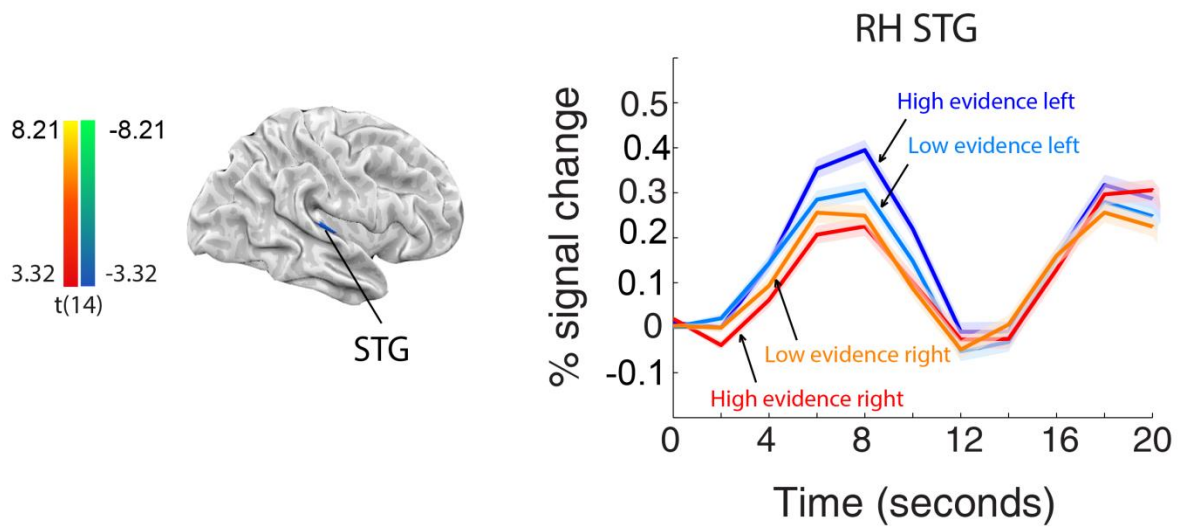
Figure 5.1.5. **Signal of visual sensory accumulation in the occipital cortex.** (A) Statistical map of brain regions showing signals modulated by signed accumulated sensory evidence. Cluster-forming threshold  $p=0.005$ , corrected  $p=0.05$  voxels = 11. (B) Event-related averages show signals in cuneus and fusiform being modulated by quality: side and quantity: level of sensory evidence.



**Table 5.1.3 Visual accumulator regions**

| ROIs signed visual evidence predictor       | BA | #Voxels | Tal coordinates |     |     | Correlation |        |
|---|----|---------|-----------------|-----|-----|-------------|--------|
|   |    |         | x               | y   | z   | r           | p      |
| L MT  | 20 | 11      | -54             | -4  | -14 | 0.3         | 0.02   |
| L Postcentral                               | 3  | 16      | -21             | -25 | 55  | -0.45       | <0.001 |
| L MT  | 21 | 11      | -63             | -49 | -2  | -0.41       | 0.001  |
| L Fusiform                                  | 19 | 20      | -33             | -55 | -11 | 0.53        | <0.001 |
| R Cuneus                                    | 23 | 16      | 15              | -73 | 10  | -0.31       | 0.01   |
| R Precuneus                                 | 7  | 67      | 18              | -76 | 34  | -0.26       | 0.04   |
| <b>ROIs main effect of visual stimulus</b>  |    |         |                 |     |     |             |        |
| L Fusiform                                  | 19 | 88      | -39             | -67 | -14 | 0.28        | 0.02   |
| L IPL                                       | 40 | 178     | -39             | -40 | 40  | 0.28        | 0.03   |
| L MO  | 19 | 118     | -51             | -73 | 7   | 0.28        | 0.03   |
| L Fusiform                                  | 19 | 63      | -27             | -70 | -14 | 0.40        | 0.001  |
| R MO  | 19 | 96      | 45              | -73 | 4   | -0.30       | 0.02   |
| L Lingual                                   | 18 | 74      | -15             | -64 | -8  | 0.33        | 0.008  |
| L MO  | 19 | 82      | -39             | -64 | 10  | 0.28        | 0.02   |
| R MO  | 19 | 96      | 39              | -70 | 10  | -0.28       | 0.03   |
| R SPL                                       | 7  | 11      | 21              | -64 | 64  | 0.30        | 0.02   |
| L IO  | 18 | 35      | -33             | -76 | -2  | 0.36        | 0.004  |
| R Precentral                                | 6  | 21      | 42              | -4  | 58  | 0.30        | 0.02   |
| L MO  | 19 | 27      | -51             | -76 | -5  | 0.29        | 0.02   |
| <b>ROIs auditory accumulator</b>            |    |         |                 |     |     |             |        |
| R STG                                       | 41 | 17      | 51              | -22 | 10  | 0.26        | 0.04   |
| <b>ROIs main effect of auditory stimuli</b> |    |         |                 |     |     |             |        |
| L IPL                                       | 40 | 116     | -42             | -34 | 40  | 0.29        | 0.03   |
| L insula                                    | 13 | 229     | -48             | -37 | 19  | -0.25       | 0.04   |
| L IPL                                       | 40 | 53      | -30             | -31 | 40  | 0.42        | 0.007  |

In the auditory task, we found that the superior temporal gyrus exhibited signals modulated by signed auditory evidence (**Figure 5.1.6A**). We examined the time courses for an accumulator activity profile (a region accumulating for rightward decisions: right high evidence > right low evidence > left low evidence > left high evidence). We found that the superior temporal gyrus had an activity pattern that fitted the accumulator profile (**Figure 5.1.6B**). We explored the level of correlation of beta activity in regions with accumulator profiles and modeled sensory evidence, and found a correlation for the superior temporal gyrus ( $r = -0.48, p < 0.001$ ) for auditory evidence and occipital regions ( $r = .53, p < 0.001$ ) for visual evidence (**Table 5.1.4**). To make sure we didn't miss other regions with accumulator activity we investigated level of correlation between beta values and level of evidence in ROIs based of stimulus presentation as shown in (**Table 5.1.3**) and (**Table 5.1.4**). Moreover to investigate possibility of a region accumulating evidence for both modalities, we investigated level of correlation using ROIs identified from the other modality (**Table 5.1.3, 5.1.4**). However, only superior temporal gyrus and occipital regions showed time courses with accumulator profile and significant correlation in a modality-specific manner.



Cluster-forming threshold  $p=0.005$ , corrected  $p=0.05$  voxels = 11.

Figure 5.1.6. **Signal of auditory sensory evidence accumulation in the superior temporal gyrus (STG).** (A) Statistical map of brain regions showing modulation by signed accumulated visual sensory evidence. (B) Event-related averages show signals in STG being modulated by quality and quantity of sensory evidence (quality and quantity).

**Table 5.1.4 Auditory accumulator regions**

| ROIs signed auditory evidence predictor     | BA | #Voxels | Tal coordinates |     |     | Correlation |        |
|---|----|---------|-----------------|-----|-----|-------------|--------|
|   |    |         | x               | y   | z   | r           | p      |
| R STG                                       | 41 | 17      | 51              | -22 | 10  | -0.48       | <0.001 |
| <b>ROIs main effect of auditory stimuli</b> |    |         |                 |     |     |             |        |
| R Cingulate                                 | 23 | 183     | 6               | -22 | 28  | 0.26        | 0.04   |
| L Insula                                    | 13 | 106     | -39             | -16 | -2  | 0.37        | 0.003  |
| R Transverse temporal                       | 41 | 118     | 39              | -31 | 10  | 0.33        | 0.009  |
| L STG                                       | 41 | 63      | -35             | -24 | 10  | 0.48        | <0.001 |
| L IPL                                       | 40 | 87      | -30             | -31 | 40  | 0.30        | 0.02   |
| R Posterior Cingulate                       | 31 | 37      | 9               | -34 | 19  | 0.35        | 0.006  |
| <b>ROIs visual accumulator</b>              |    |         |                 |     |     |             |        |
| L MT  | 21 | 11      | -63             | -49 | -2  | -0.26       | 0.03   |
| <b>ROIs main effect of visual stimuli</b>   |    |         |                 |     |     |             |        |
| L Cingulate                                 | 23 | 63      | 9               | -25 | 25  | 0.29        | 0.03   |
| L IPL                                       | 40 | 100     | -42             | -28 | 37  | 0.31        | 0.02   |
| L Thalamus                                  | -  | 42      | -21             | -22 | 10  | 0.32        | 0.01   |
| R Thalamus                                  | -  | 46      | 15              | -22 | 13  | 0.28        | 0.03   |
| R Posterior Cingulate                       | 31 | 15      | 15              | -34 | 28  | 0.29        | 0.02   |
| L Cerebellar lingual                        | -  | 54      | 0               | -43 | -11 | -0.26       | 0.04   |

***Regions with activity modulated by spatially non-specific sensory evidence:***

We investigated brain regions exhibiting activity that is modulated by the absolute values of the modeled evidence; values related to the level of sensory evidence regardless of its directionality; i.e. regions that would be modulated by difficulty regardless of space. We found, similar to the ANOVA analysis of the main effect of difficulty, that activity in the middle frontal gyrus, inferior frontal, and cingulate gyri, and the inferior parietal lobule to be negatively correlated with the level of evidence regardless of modality; a stronger signal when evidence was low in both modalities; regardless of direction of evidence (**Figure 5.1.7A, B, C**).

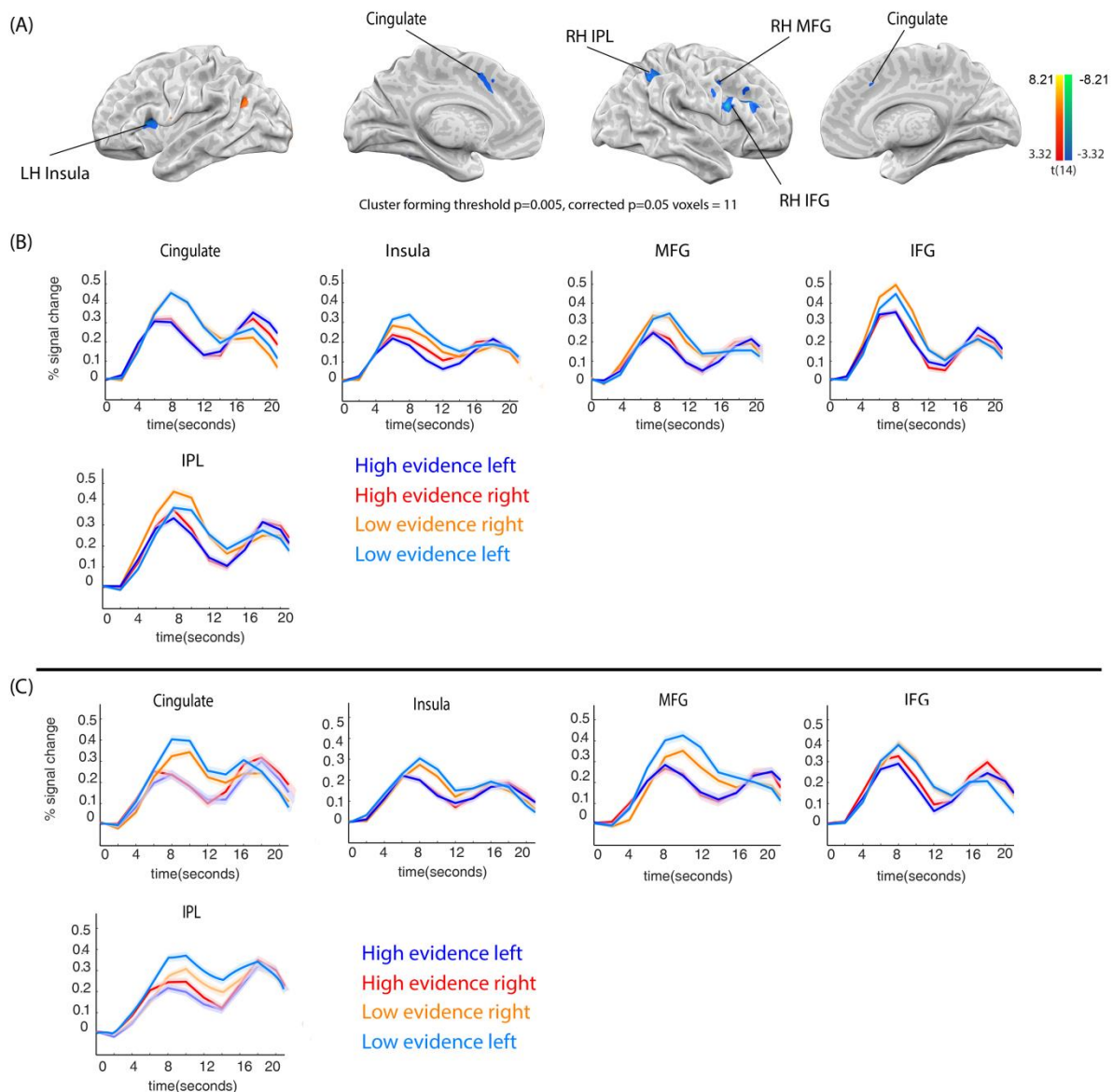


**Figure 5.1.7. Frontal and parietal cortices show spatial non-specific modulation by level of sensory evidence regardless of modality.** (A) Statistical map of brain regions showing modulation by level of sensory evidence (blue regions mean stronger signals for trials with low sensory evidence while red regions have stronger signals when the level of evidence is high). Cluster forming threshold  $p=0.005$ , corrected  $p=0.05$  voxels = 11. (B) Event-related averages showing modulation of signal by level of visual sensory evidence without spatial preference. (C) Event-related averages showing modulation of signal by level of auditory sensory evidence without spatial preference. Time courses were extracted from right hemisphere. Middle frontal gyrus (MFG), inferior frontal gyrus (IFG), inferior parietal lobule (IPL).

### ***Similarities and differences between ANOVA results and the model base findings:***

In this study, we investigated accumulator regions using two complementary analysis approaches; one that is based on ANOVA and another that is based on parametric modulation of GLM predictors using modeled sensory evidence. Both the ANOVA analysis and the model-based analysis approaches showed that the frontal and parietal regions had higher activity when the task was harder (ANOVA approach), and likewise when the evidence was low (model-based approach) for both modalities in a spatially non-specific manner. However, the parametric modulation by sensory evidence estimates was able to localize coordinates of voxels with time courses suggestive of a sensory evidence accumulation profile, which was not possible by only using the ANOVA based analysis.

## **DISCUSSION**

The goal of the study was to identify brain regions involved in the accumulation of sensory evidence in either sensory modality-specific or sensory modality non-specific manner.

### ***Perceptual evidence accumulation in sensory cortices***

We found that accumulation of sensory evidence in a given modality correlates with activity in the respective modality-specific sensory cortices. This finding is in line with previous visual imaging studies showing that regions in the occipital cortex are involved in the representation of sensory evidence and correlate with

the decision and perceptual report (Heeger, 2012; Philiastides & Sajda, 2007). It was shown that occipital regions contain signals of visual sensory evidence accumulation once disentangled from motor preparation (Hebart et al., 2012). On the other hand, previous auditory studies did not use auditory tasks that allow one to study sensory evidence accumulation in a discrete manner (Hanks & Summerfield, 2017). Thus, it was not possible to directly test for sensory evidence accumulation. In our study, we investigated an auditory accumulator task and showed that regions in the auditory cortex correlate with accumulated auditory sensory evidence.

### *Supramodal and space-independent accumulation signals in the frontoparietal cortices*

In our data, activity in the prefrontal and parietal cortices correlated with stimulus presentation regardless of modality, and we concluded that those regions had a multi-modal role. However, activity in the frontal and parietal cortices was not modulated by the spatially-specific accumulated sensory but was modulated by the level of sensory evidence irrespective of space. Therefore, it is suggestive that activity in the frontal and parietal cortices reflects secondary decision-making processes such as handling task difficulty (Heekeren, 2008). Such a finding is consistent with previous reports from the literature proposing a role of the frontal, parietal cortices as a saliency map (Corbetta, Kincade, Lewis, Snyder, & Sapiro, 2005). However, whether this effect is a bottom up (sensory →



frontoparietal) or top-down (frontoparietal → sensory) activity is not clear due to the temporal resolution of the fMRI (Ptak, 2012). EEG-fMRI showed that the frontal, parietal, anterior cingulate, and insula regions have a top-down role in visual decision-making tasks (Philiastides & Sajda, 2007). Using dynamic causal modeling it was shown that the signal from parietal regions optimizes the through reallocation of attentional resources (Feldman & Friston, 2010b).

***Regions correlating with accumulated evidence versus decision difficulty comparison with previous studies***

In earlier reports on fMRI studies in humans, various brain regions were shown to accumulate sensory evidence (Mulder, van Maanen, & Forstmann, 2014). One of the first studies that applied assumptions from the accumulator models to identify brain accumulator regions using a faces vs. house discrimination task reported stronger BOLD signals in the DLPFC with easier decisions (Heekeren, 2004). Per se, the choice difficulty is closely related to how rapidly the evidence reaches a threshold, i.e. the drift rate parameter. It was shown that effects of difficulty appeared in the DLPFC and insula, while the lateral occipital cortex is the region of evidence accumulation (Philiastides & Sajda, 2007). However, other studies proposed that BOLD is negatively correlated with the drift rate and therefore with evidence accumulation. Thus, one would expect a weaker BOLD signal for higher drift rates (Ho & Brown, 2009). Such studies showed that the frontal eye field (FEF), and intraparietal sulcus (IPs) exhibited higher activity

when the task was harder (Ho & Brown, 2009; Liu & Pleskac, 2011). However, if we consider other studies that suggest that accumulation signals can be detected in difficult trials, it is also possible to view pre-SMA, inferior frontal gyrus, and right inferior parietal lobule activity as an accumulator signal. Nevertheless, we propose that, for our spatial accumulator tasks, regions considered as accumulators were the ones that exhibited modulation by level of evidence and direction of the evidence (i.e. an area accumulating evidence towards left decisions would be regarded as an accumulator region if it has the following signal profile: left high evidence > left low evidence > right low evidence > right high evidence). Only regions exhibiting such signal were sensory cortices in a modality-specific manner.

Electrophysiological studies have shown that regions equivalent to the human IPL and FEF are involved in evidence accumulation (Hunt et al., 2012; Kim & Shadlen, 1999; Roitman & Shadlen, 2002). It is interesting that the IPL and FEF are also considered to be part of the saccade control network and attention (Li & Krishnamurthy, 2015). Thus, a buildup of activity in such regions could also reflect preparation of a motor response (Bennur and Gold, 2011). A recent electrophysiological study in monkeys showed a dissociation between correlation and causation in decision variables in the lateral intraparietal sulcus (LIP) activity, suggesting a role of LIP in secondary processes rather than one in perceptual decisions (Katz et al., 2016). Traditionally, monkey studies used speeded tasks, which make it difficult to disentangle motor preparation from

sensory evidence accumulation. We employed delayed tasks. Previous fMRI decision-making studies using delayed tasks came to a different conclusion than studies employing non-delayed tasks. Pederson et al. addressed this discrepancy by using delayed vs. non-delayed tasks in fMRI comparing easy and difficult trials (Pedersen, 2015). They made the following prediction based on firing patterns of LIP neurons in monkeys, which both accumulate evidence and maintain decisions. They proposed that if a region exists in humans that behaved similarly to the firing pattern of the LIP in monkeys, it would have the following signal: first, it would be more active for difficult than for easy decisions in a self-paced condition. Second, it would be more active during easy than during difficult decisions in a forced delay condition (Pedersen, 2015). They found no region with an activation pattern consistent with these predictions, thus suggesting a different decision-response mechanism in humans than the one observed in LIP neurons of monkeys. However, they did find that evidence accumulation is probably implemented in frontal regions and/or insula while potential choice maintenance regions span the frontal, temporal and occipital cortices (Pedersen, 2015).

***Regions showing supra-modal decision signal comparison with previous studies***

Previous literature investigating neural mechanisms of decision-making regardless of sensory modality; i.e. showing a supramodal signal investigated

combined tasks where effect of auditory stimuli on visual decision-making or vice versa could be explored (Rohe & Noppeney, 2015). In their study they relied on a spatial ventriloquist paradigm, where synchronous audiovisual originating from four possible locations were presented to the participants. Participants had to report the auditory or the visual stimuli location and ignore the other. They demonstrated a hierarchy of multisensory processes in the human brain. At the bottom of the hierarchy, signal is segregated in auditory and visual areas, location is represented on the basis that the two signals are generated by independent sources. At the next stage, at the level of posterior intraparietal sulcus, signal shows forced fusion where location is estimated under the assumption that the two signals are from a common source. While they show that only at the top of the hierarchy, in anterior intraparietal sulcus, the uncertainty about the causal structure of the world is taken into account and sensory signals are combined. The major difference between our study and the Noppeney study is that our study uses a clear accumulator task for each the auditory and visual modalities. Therefore, our experimental design investigates core decision-making strategies in each modality while their study is more focused on mechanisms of sensory integration. Our results agree on the possibility that regions in inferior parietal lobule exhibit a supramodal signal that deals with uncertainty due increased sensory noise resulting in harder trials. We argue that since sensory evidence accumulation towards a decision is highly correlated to the sensory processing that it is reasonable that accumulator signal

is carried in modality-specific sensory cortices and decision signal is relayed to higher cortical regions in a supramodal manner.

### *Limitations of the study*

Despite the fact that fMRI is superior to single unit recording by its ability to view activity on a whole-brain scale, it has limitations in terms of temporal resolution and lack of fine-grained neural tuning on a voxel-based level (Logothetis, 2008). The low temporal resolution prevented us from measuring the dynamic buildup of the accumulation signal on a click-by-click basis or flicker-by-flicker basis. Our detected signal represents the summated evidence over the stimulus presentation period, and was not possible to study effect of each click or flicker on the accumulation process. Therefore, it is valid to assume that signal in proposed accumulator regions could be related to processing of spatial stimuli and not an accumulation signal. Also, frontal and parietal regions might carry an accumulator signal towards spatial choice but the spatial tuning of fMRI in the range of 3x3x3 mm voxel size could have obscured the signal. Moreover, scanner noise led to decrease in performance in the auditory task in comparison to the visual task particularly in the difficult trials. Nevertheless, performance in the easy trials was almost 100% in both modalities. Model fits showed a higher lapse rate in the auditory task explained by higher background noise, probably due to the scanner, which was impossible to eliminate. We had to fit all trials from all participants to one model, as it was

not possible to fit each participant data from inside the scanner due to the limited number of data points that can be acquired per session.

## ***Conclusions***

In this study, we provide answers to the question of how different types of sensory information are accumulated: is a region involved in the accumulation of visual evidence expected to also accumulate auditory evidence?

We showed that sensory evidence accumulated in modality-specific sensory cortices. Thus, the well-known neural correlates of evidence accumulation in frontal and parietal cortices do not reflect evidence accumulation, but rather task difficulty. Therefore, our data show that evidence accumulates in a modality-specific manner, and suggest a possible role of the frontal and parietal cortices in secondary decision-making processes.

## **ACKNOWLEDGEMENTS**

This work was supported by the Hermann and Lilly Schilling Foundation, German Research Foundation (DFG) grants WI 4046/1-1 (M.W.). Prof. Dr. Thomas Crozier proof read and edited this manuscript.

## **Contributions**

Ahmad M. Nazzal (A.N.), Melanie Wilke (M.W.), and Jeffrey C Erlich (J.E) designed the study. A.N, M.W, Carsten Schmidt-Samoa (C.S.), and (J.E) interpreted the results. A.N. wrote the paper. J.E. provided scripts for auditory stimuli preparation. A.N modified scripts and prepared stimuli for auditory and visual tasks. A.N. and C.S. programmed scripts for running the task outside the scanner. A.N. modified scripts to use inside the scanner. A.N. planned, performed, and supervised behavioral and imaging data collection. Marie Dewenter (M.D.) contributed to data collection. A.N. prepared scripts, performed the analysis. J.E. fitted behavioral data to the model. A.N prepared scripts and implemented model fitting results for fMRI analysis. M.W., C.S., and J.E. provided corrections to the paper. A.N prepared the figures.

Supplementary Table 5.1.1 Model parameters for most relevant parameters to study decision-making strategy based on model fits for each modality

| Modality | $\lambda$ | $\sigma(a)$ | $\sigma(s)$ | $B$     | Lapse rate |
|----------|-----------|-------------|-------------|---------|------------|
| Auditory | -0.26505  | 27.446      | 64.062      | 14.25   | 0.032939   |
| Visual   | 0.2612    | 2.5280      | 0.0141      | 11.7675 | 0.0144     |

$\sigma_a$  A diffusion constant, parameterizing noise in  $a$ , the decision variable.

$\sigma_s$  parameterizes sensory noise when adding the evidence

$\lambda$  parameterizes consistent drift in the memory  $a$ . In the ‘leaky’ or forgetful case ( $\lambda < 0$ ) drift is towards  $a = 0$ , and late stimuli pulses impact the decision more than earlier pulses. In the ‘unstable’ or impulsive case ( $\lambda > 0$ ), drift is away from  $a = 0$ , and early stimuli pulses impact the decision more than later pulses. The memory’s time constant  $\tau = 1/\lambda$ .

$B$  The height of the ‘sticky’ decision bounds and parameterizes the amount of evidence necessary to commit to a decision.

*Lapse rate* The fraction of trials in which a random response is made

For details on model fitting procedure and model parameters (Brunton, 2013).

Supplementary Table 5.1.2 Modality effect

| Brain region | BA   | #Voxels | Post hoc t(14)<br>Audio vs. Visual |        | Tal coordinates |     |    |
|--------------|------|---------|------------------------------------|--------|-----------------|-----|----|
|              |      |         | t-value                            | P      | x               | y   | z  |
| L lentiform  | -    | 44      | -5.57                              | <0.001 | 18              | 11  | -5 |
| R precentral | BA6  | 17      | -5.81                              | <0.001 | 36              | -1  | 37 |
| L precentral | BA6  | 31      | -5.19                              | <0.001 | -48             | -13 | 34 |
| R STG        | BA13 | 533     | 9.03                               | <0.001 | 36              | -22 | 10 |
| L STG        | BA13 | 581     | 8.67                               | <0.001 | -39             | -22 | 7  |
| R Thalamus   | -    | 32      | -6.74                              | <0.001 | 18              | -28 | 4  |
| L Thalamus   | -    | 22      | -5.27                              | <0.001 | -18             | -22 | 7  |
| R Occipital  | BA19 | 1436    | -9.45                              | <0.001 | 42              | -73 | 4  |
| L Occipital  | BA19 | 1107    | -8.72                              | <0.001 | -39             | -61 | -8 |
| L SPL        | BA7  | 146     | -5.38                              | <0.001 | -24             | -58 | 46 |

Left (L), right (R), superior temporal gyrus (STG), superior parietal lobule (SPL).



Supplementary Table 5.1.3 Conjunction between auditory stimulus and visual stimulus

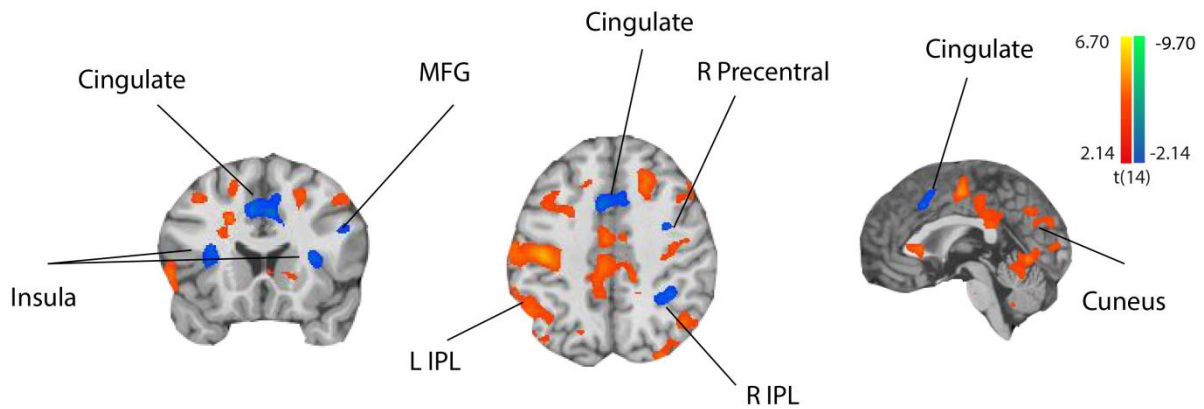
| Brain region     | BA   | #Voxels | Post hoc t(14)<br>Audio vs. Visual |       | Tal coordinates |     |    |
|------------------|------|---------|------------------------------------|-------|-----------------|-----|----|
|                  |      |         | t-value                            | P     | x               | y   | z  |
| R IFG            | BA13 | 1047    | -1.73                              | 0.11  | 38              | 12  | 24 |
| L Medial frontal | BA32 | 323     | -1.32                              | 0.21  | 0               | 14  | 45 |
| L Insula         | BA13 | 200     | -0.53                              | 0.60  | -32             | 16  | 10 |
| R Precentral     | BA6  | 104     | -1.67                              | 0.12  | -26             | -8  | 53 |
| R Cingulate      | BA23 | 144     | -0.30                              | 0.77  | 2               | -26 | 25 |
| R IPL            | BA40 | 322     | -2.83                              | 0.01  | -38             | -42 | 41 |
| L IPL            | BA40 | 261     | -2.93                              | 0.01  | -37             | -43 | 43 |
| L STG            | BA13 | 47      | 2.90                               | 0.01  | -51             | -41 | 13 |
| R STG            | BA22 | 193     | 2.62                               | 0.02  | 54              | -41 | 14 |
| L Precuneus      | BA7  | 51      | -3.64                              | 0.002 | -15             | -62 | 46 |
| R Precuneus      | BA7  | 37      | -2.38                              | 0.03  | 14              | -64 | 44 |

Left (L), right (R), superior temporal gyrus (STG), superior parietal lobule (SPL), inferior parietal lobule (IPL).

Supplementary Table 5.1.4 Main effect of space

| Brain region | BA   | #Voxels | Post hoc      |        | Post hoc                 |        | Post hoc                   |      | Tal coordinates |     |    |
|--------------|------|---------|---------------|--------|--------------------------|--------|----------------------------|------|-----------------|-----|----|
|              |      |         | Right vs.Left |        | Visual<br>Right vs. Left |        | Auditory<br>Right vs. Left |      |                 |     |    |
|              |      |         | t(14)         | P      | t(14)                    | P      | t(14)                      | P    | x               | y   | z  |
| L IPL        | BA40 | 24      | 4.77          | <0.001 | 5.04                     | <0.001 | 2.20                       | 0.05 | -35             | -33 | 44 |

Left (L), right (R), superior temporal gyrus (STG), superior parietal lobule (SPL), inferior parietal lobule (IPL), middle occipital (MO).



Cluster-forming threshold  $p=0.05$ , corrected for  $p=0.05$  voxels = 50

Supplementary Figure 5.1.1. Brain regions showing effect of difficulty (easy > hard). Cluster-forming threshold  $p=0.05$ , corrected for  $p=0.05$  voxels = 50. Middle frontal gyrus (MFG), inferior parietal lobule (IPL).

## 5.2 Dissociated neural signature of visual sensory evidence accumulation and decision-monitoring.

### *Abstract*

Monitoring of decisions accuracy through estimation of confidence in the decision or error detection optimizes the decision-making process. Behaviorally, it is established that confidence in a decision increases for correct decisions and decreases for error decisions as the level of available sensory evidence is higher (i.e. easy trials). However, it is still not clear whether sensory evidence accumulation and confidence in the decision engage the same brain regions. Here, we used a model-based, event-related fMRI approach to study neural correlates of visual sensory evidence accumulation and confidence in the visual decision. The participants performed a visual accumulator task, responding with a button press. We devised criteria based on assumptions from integrate-and-fire attractor models to identify the neural correlates of decision-monitoring, i.e. confidence in the decision and error detection. We hypothesized that activity in the frontal and parietal cortices will correlate with sensory evidence accumulation and/or confidence in the decision. We found that signals of sensory evidence accumulation could be disentangled from the neural signature of decision-monitoring; signals in the occipital region represented visual sensory evidence accumulation, while signals in frontal and midbrain regions were suggestive of decision-monitoring. The data suggest that the right middle frontal gyrus correlates with subjective reports of confidence in the decision. Our

finding is in line with previous neuroimaging studies which demonstrated a role of the frontal cortex in decision-monitoring.

### **Introduction:**

Monitoring decision accuracy by estimating confidence in the decision or error detection optimizes the decision-making process (Schwartenbeck, 2015). The subjective ability to estimate the level of accuracy of a decision is referred to as confidence in the decision (Mamassian, 2016). As such, it is possible to view confidence in the decision or error detection as a judgment on a judgment. Therefore, confidence in a decision belongs to the domain of metacognition (Metcalf & Shimamura, 1994). Confidence in decision increases for correct decisions and decreases for erroneous decisions as the task become easier (Pierce & Jastrow, 1884; Vickers & Packer, 1982). Signal detection theory (SDT) assumes that both perceptual choices and perceptual confidence are based on a continuous decision variable (DV) (Green & Swets, 1966; Macmillan & Creelman, 2005). One can measure estimates of decision-monitoring either by using the correlation between percent correct and confidence rating (Sandberg, 2010) or by depending on calculating metacognitive accuracy using signal detection (Fleming, 2014). In any case, it is hard to disentangle neural correlates of core decision processes such as sensory evidence accumulation from secondary decision processes that might influence the decision, such as confidence in the decision (Gold & Shadlen, 2007). It was recently shown that

confidence is part of the decision process and not a separate, post-decision process (Gherman & Philiastides, 2015). The neural signature of sensory evidence accumulation in humans involves several brain regions. Using functional magnetic resonance imaging (fMRI) it was shown that the dorsolateral prefrontal cortex (DLPFC) (Heekeren, 2004), the occipital cortex (Philiastides & Sajda, 2007), insular cortex, frontal eye fields, and inferior parietal lobule (Ho & Brown, 2009; Liu & Pleskac, 2011) exhibit signals suggestive of sensory evidence accumulation. On the other hand, neural correlates of confidence in the decision were consistently identified in prefrontal regions in human neuroimaging studies (Fleming, 2014; Hebscher & Gilboa, 2015; Heereman et al., 2015). Moreover, several studies have shown the involvement of anterior cingulate, and prefrontal regions in error detection ((Gehring & Fencsik, 2001; Kennerley, Walton, Behrens, Buckley, & Rushworth, 2006). However, it remains unclear whether activity related to sensory evidence accumulation and confidence in the decision is encoded in same brain regions, or if it rather engages different brain regions.

Therefore, the aim of this study was to investigate the neural correlates of visual sensory evidence accumulation, and to investigate the neural correlates of decision-monitoring using fMRI. We intended to determine if the same brain regions which show neural correlates of sensory evidence accumulation also code confidence in the decision. For this propose, we used model-based, event-related fMRI to study the neural correlates of sensory evidence accumulation

and propose criteria to localize the neural correlates of confidence in the decision based on integrate-and-fire attractor models (Insabato., 2010; Rolls., 2010). We employed visual flickers accumulator task where we present trains of flickers to the right or the left side of screen and ask subjects to decide which side had more flickers presented to it after a delay using a button press. We maximized number of error trials in the easiest condition by using a difference that results in around 75% accuracy rate. Therefore, for a region to qualify as involved in confidence in the decision we propose that it must fulfill the following criteria based on expectations from integrate-and-fire attractor models (Wang, 2002): (1) there is a difference between correct and error trials, (2) there is an interaction between correctness and difficulty mimicking confidence behavior. Based on earlier neuroimaging studies in the literature we hypothesize that activity in the frontal and/or parietal cortex will correlate with sensory evidence accumulation and/or confidence in the decision ( Fleming & Dolan, 2012; Fleming & Dolan, 2014; Heereman et al., 2015).

## **Materials and Methods**

### ***Participants***

Fifteen right-handed, healthy participants took part in the study. They had normal hearing, normal or corrected vision, and no history of neurological or psychiatric disease. All participants gave written informed consent. Twelve participants (seven females) were included in the final analysis (mean age 26.5

yrs;  $SD \pm 5.1$  yrs). Three participants were excluded due to poor eye fixation. All procedures were performed according to the declaration of Helsinki and were approved by the local Ethics Committee of the University Medical Center Göttingen. Participants received monetary compensation for participating in our experiments.

### ***Task and Stimuli***

The participants were asked to perform a visual version of an evidence accumulation task. They were asked to form decisions about space, i.e. whether more stimuli had been presented to the right or left side of a screen. The stimuli were presented discretely over time and space, allowing for the fitting of a dynamic model that captures the accumulation of sensory evidence towards a spatial decision. Changes in fixation cross color were used for different stages of the task in order to keep the visual input throughout different task stages as constant as possible. Each trial started with the presentation of a central red fixation cross. After a mandatory, stable fixation period lasting one second, the stimuli were presented for three seconds, followed by a variable delay of six to eight seconds. The beginning of the response period was indicated by a change of the fixation cross color to green. The participants were asked to respond with their right hand using the index and middle fingers. Participants responded by pressing key '1' if they thought the trial had more stimuli on the left, or key '2' if they chose the right side. Afterwards, the fixation cross color changed to

yellow indicating confidence rating period. The participants had to rate their confidence on a scale of one to four with one as the lowest confidence and four as highest confidence. The following rest period varied between six and eight seconds. No feedback was given to the subjects. The duration of delay and rest times was random to prevent participants from forming a response strategy, and to increase design efficiency in this event-related design (by reducing multicollinearity between predictors that follow closely in time). The participants were asked to use the entire information presented to them in each trial to form their choice. Each participant completed four runs for a total of 196 trials as training before being asked to perform the task inside the scanner. The participants were required to finish four runs of each modality inside the scanner; each run consisted of 30 trials.

### *Visual stimuli*

Trains of stereo flickers lasting three seconds were presented on the horizontal plane of the screen at an eccentricity of approximately 11 visual degrees. The flicker frequency was 5 Hz ( $\#flickers\ right\ (FR) + \#flickers\ left\ (FL) = five\ per\ second$ ). Each flicker lasted 16.7ms and size of two visual degrees. Consecutive flickers had a minimum inter-pulse interval of 120 ms to minimize adaptation (Brunton et al., 2013). The first and last flickers were presented bilaterally to prevent bias towards the side of the first or the last flicker presented. Inside the scanner, easy trials differed by three flickers between the sides (FR-FL), while



hard trials had a one-flicker difference. Stimuli were generated using MATLAB, version R2011b using custom scripts. To maximize the number of error trials easy trials had only 3 flickers difference while hard trials had only 1 flicker difference.

### ***General experimental setup inside the scanner***

The participants were placed in the MR scanner (3T, Siemens TIM Trio, Siemens Healthcare, Erlangen, Germany) in a supine position. In order to prevent the participant's head from moving, it was stabilized inside the Siemens 12 channel head coil by means of cushions. Headphones were used to protect the ears from scanner noise, and in-ear foam plugs were used for further noise protection. Visual stimuli were delivered using MR-compatible liquid crystal display (LCD) goggles (Resonance Technology, Northridge, CA). The spatial resolution was  $800 \times 600$  pixels, covering a visual field of  $32 \times 24$  degrees, at a refresh rate of 60 Hz. Eye position was monitored with an MR compatible 60 Hz eye tracking system (Arrington Research, Scottsdale, AZ). The participants responded using an MR-compatible fiber optic four-button response pad (Current Designs, Philadelphia, PA, USA). Trigger pulses from the MR scanner were used to synchronize functional image acquisition and experimental tasks.

### *Accumulator model*

A recent nine-parameter model based on the drift-diffusion model was developed to study sensory evidence accumulation, and we will refer to it in the manuscript as the accumulator model (Brunton et al 2013). In order to verify that participants accumulated the sensory evidence presented over the whole trial, an accumulator model using the individual flicker times and the participants' choices in each trial was fitted (Brunton et al., 2013). The accumulator model uses nine parameters to transform the stimuli in each trial (input to the model are left and right stimulus times) into a probability distribution about the choice of the participant. For example, if for a given set of parameters, the model predicts that Trial 1 will result in a 75% chance of the participant choosing right, and the participant, in fact, did choose right, that trial would be assigned a likelihood of 0.75. In the case that the participant chose left, the trial would be assigned a likelihood of 0.25. We fit the model under the assumption that the trials are independent. Therefore, for a model with parameters  $\theta$  for all decisions  $D$ , the likelihood is given by:

$$P(D|\theta) = \prod_i P(d_i | t_{i,R}, t_{i,L}, \theta),$$

The product of the likelihood of the decision on trial  $i$ ,  $d_i$ , given the times of the right stimulus,  $t_{i,R}$ , times of the left stimulus  $t_{i,L}$ , and the set of nine parameters,  $\theta$ . A detailed description of the procedure for fitting the accumulator model can

be found in the Modeling Methods section of the supplement to Brunton et al. (2013). The model includes a ‘lapse’ parameter, which represents a fraction of trials in which subjects will ignore the stimulus and choose randomly. The presence of the lapse parameter also puts a lower bound on the likelihood of any individual trial, and thus no individual trial can dominate the results and the consequent fits of the model. Different parameter value regimes of this model can implement many different strategies, such as responses based on the first or last few stimuli, or to a burst of stimuli, and many others.

The psychometric curves were generated by concatenating trial data across sessions for each participant and using Matlab’s `nlinfit` to fit a four-parameter sigmoid as follows:

$$y(x) = y_0 + \frac{a}{1 + \exp\left(\frac{-(x-x_0)}{b}\right)}$$

For these fits,  $x$  is the stimulus difference on each trial ( $\#Right$  stimulus  $-\#Left$  stimulus),  $y$  is ‘P (Chose Right)’, and the four parameters to be fit are:  $x_0$ , the inflection point of the sigmoid;  $b$ , the slope of the sigmoid;  $y_0$ , the minimum ‘P(Chose Right)’; and  $a + y_0$  is the maximum ‘P(Chose Right)’.

### ***Behavioral analysis***

The difficulty was assigned based on the absolute difference of flickers presented on the right minus the number of flickers presented on the left side. Two levels of difficulty were used; a three-flicker difference represented an easy

trial, and a one-flicker difference represented a hard trial. Probability correct and mean level of confidence were estimated for each difficulty and flickers difference bins (#FR-#FL=-3,-1, 1, 3). Mean confidence ratings were plotted as a function of stimulus difference **Figure (1C)**. Scatter plots were used to plot the accuracy level of each participant as a function of mean confidence, and the level of correlation was estimated using Pearson correlation in MATLAB **Figure (1D)**. Moreover, data was categorized for correct or incorrect (error). Mean confidence levels were then calculated for each difficulty for correct and error trials **Figure (1D)**.

### ***2-by-2 Repeated Measures ANOVA***

Percent correct and mean confidence were calculated for each difficulty. To determine whether confidence rating was modulated by difficulty and accuracy, we performed a 2-by-2 repeated measures ANOVA on mean confidence with accuracy and difficulty as within-subject factors.

### ***MRI acquisition***

All images were acquired using a 3Tesla Magnetom TIM Trio scanner (Siemens Healthcare, Erlangen, Germany) with a 12-channel phased-array head coil. First, a high-resolution T1-weighted anatomical scan (three-dimensional (3D) turbo fast low angle shot, echo time (TE): 3.26 ms, repetition time (TR): 2.250 ms, inversion time: 900 ms, flip angle 9°, isotropic resolution of 1 x 1 x 1 mm<sup>3</sup>) was obtained. All functional data were acquired using T2\*-weighted gradient-echo

echo-planar imaging (EPI) (TE: 30 ms, TR: 1.800 ms, flip angle 70°, 34 slices of 3-mm thickness, no gap between slices at an in-plane resolution of 3 x 3 x 3mm<sup>3</sup>). Four dummy scans were added at the beginning of each run to allow for T1 equilibrium. A total of 425 whole brain volumes were acquired in each functional run. Participants performed one fMRI session of four runs each.

### ***MRI data preprocessing and analysis***

BrainVoyager QX Software version 2.8 (Brain Innovation, Maastricht, The Netherlands), and the Neuroelf 0.9c toolbox for Matlab (retrieved from <http://neuroelf.net/>) were used for preprocessing and analysis of the functional data. Standard preprocessing steps included 3D motion correction, slice scan time correction and temporal filtering [linear trend removal and high pass filtering (2cycles/run)]. The functional data were co-registered to the anatomical reference scans, transformed into Talairach space and spatially smoothed with a Gaussian kernel (full width at half maximum 6 x 6 x 6mm<sup>3</sup>). Further statistical analysis was performed using the general linear model (GLM) implemented in the BrainVoyager software. For the final presentation of figures, GLM models prepared in BrainVoyager environment were analyzed in Neuroelf toolbox and Matlab. For the group results, a random effects analysis using the GLM was performed with 12 participants. For all statistical maps, multiple comparison corrections were performed at the cluster level. Maps were thresholded at an initial cluster-forming threshold with  $P < 0.005$ . The size of the resulting clusters

was assessed for significance using AlphaSim simulations as implemented in NeuroElf's cluster-level statistical threshold function. Reported clusters are significant at a level of  $P < 0.05$ . First level GLM was first estimated for each subject. For each run, trial periods were modeled as regressors (stimulus, delay, motor response, rest). Stimulus presentation period was modeled as following: correct easy, correct hard, error easy, error hard. Contrasts of interest were correct > error for accuracy map. A separate GLM was calculated to study confidence effect at the same level of accuracy and difficulty. Trials were categorized into confident trials (when subjects rated confidence as 3, 4) and not confident (when subject rated confidence as 1, 2); first level GLM: confident correct easy, not confident correct easy, stimulus, delay, motor response, and rest. We expected the difference between confident and not confident to be largest in easy correct trials. This GLM was not used to calculate a statistical map but was used to extract beta values from ROIs satisfying the first two criteria to investigate whether any had activity modulated by confidence at the same level of accuracy and difficulty.

### ***Accumulator map***

To investigate brain regions with activity modulated by sensory evidence, likelihood estimates from model fits representing accumulated sensory evidence on a trial-by-trial basis were used to construct parametric predictors of the stimulus presentation period. Two such predictors were constructed: First, to

investigate brain regions with a spatially specific sensory evidence accumulation signal (we will refer to it as the spatially specific sensory evidence accumulator map) and second, absolute likelihood values were used to construct a predictor to investigate brain regions modulated by the level of sensory evidence in a non-spatially specific manner (we will refer to it as the non-spatially specific sensory evidence accumulator map).

### ***Decision monitoring regions***

In order to explore brain regions with activity correlating with decision-monitoring we implemented the following criteria: (1) Difference in signal between correct and error trials, (2) An interaction between correctness and difficulty mimicking confidence behavior and (3) Signal has to show modulation by confidence rating of the subjects at the same level of accuracy and difficulty. Two GLMs were constructed to investigate the aforementioned criteria: (1) First, a GLM was constructed to study brain regions showing activity modulated by the level of accuracy with the main contrast Correct vs. Error (we will refer to as accuracy map), (2) A second GLM was constructed to study brain regions showing the effect of confidence at the same level of accuracy and difficulty.

### **ROI analysis**

Seventeen separate, healthy, right handed participants were tested using the same visual accumulator task inside the scanner (seven females, mean age  $23.25 \pm 3.72$  years). We fitted their data to the nine-parameter accumulator model. We

built the same GLM as described under Methods for investigating the spatially specific and non-spatially specific accumulator regions. We localized brain regions showing spatially specific signal of visual sensory evidence accumulation and a non-spatially specific signal of visual sensory evidence accumulation. We formed ROIs of a sphere around the peak voxel of resulting significant regions. We used those ROIs to determine whether brain regions showing modulation of localizer group would also show modulation in the current group.

## **Results**

In order to investigate sensory evidence accumulation and confidence in the decision, we tested a visual accumulator task. We presented spatially segregated trains of flickers. Participants had to decide if there were more flickers presented to the left or the right side by pressing a button (**Figure 5.2.1A**). Afterward, participants were required to report how confident they were that their decision was correct using a scale from 1 to 4 (with 1 indicating least confident and 4 indicating most confident). We used two levels of difficulty based on the difference between number of right and left flickers: easy trials had a three-flicker difference, while hard trials had a one-flickers difference.

### ***Behavioral results***

We showed that the participants benefited from the difference between the number of right and left flickers when forming their decisions. When the



difference was larger for the right side, participants chose more flickers on the right and were most accurate for easy trials (large difference) (**Figure 5.2.1B**). Moreover, the participants were most confident in easy trials on both left and right side (**Figure 5.2.1C**). We also investigated the relationship between probability correct and confidence rating. We found a significant linear relationship between probability correct and confidence rating; when subjects were more accurate in their decision, they also reported higher levels of confidence  $R= 0.72$   $p<0.001$  (**Figure 5.2.1D**).

*Confidence is greater for correct trials compared to error trials at the same level of sensory evidence:*

In the literature, it is proposed that confidence is greater for easy correct trials than for easy error trials (Kepecs et al., 2008). In order to investigate the relation between confidence rating, difficulty, and accuracy we arranged trials into correct and error trials. Moreover, we categorized trials into two levels; easy trials, i.e. trials with  $|\#FR-\#FL|=3$  and hard trials  $|\#FR-\#FL|=1$ . We computed the mean confidence for correct easy trials, correct hard trials, error easy trials, error hard trials for each of our subjects. To study the effect of accuracy and difficulty on confidence rating, we conducted a repeated measure ANOVA with two factors: accuracy (correct, error) and difficulty (easy, hard) as the within-subject factor. This showed a significant main effect of accuracy  $F(1, 11) = 55.60$   $p<0.001$  and no main effect of difficulty  $F(1, 11) = 3.74$   $p=0.079$ .

Importantly, ANOVA revealed a significant interaction between accuracy and difficulty  $F(1, 11) = 20.60$   $p=0.001$ . Participants were most confident in easy correct trials and least confident in correct error trials (**Figure 5.2.1E**) Post hoc t-tests within the same level of sensory evidence showed that the subjects had higher confidence ratings in correct easy trials compared to incorrect easy trials.  $t(11) = 6.97$   $p<0.001$  (**Figure 5.2.1F**).

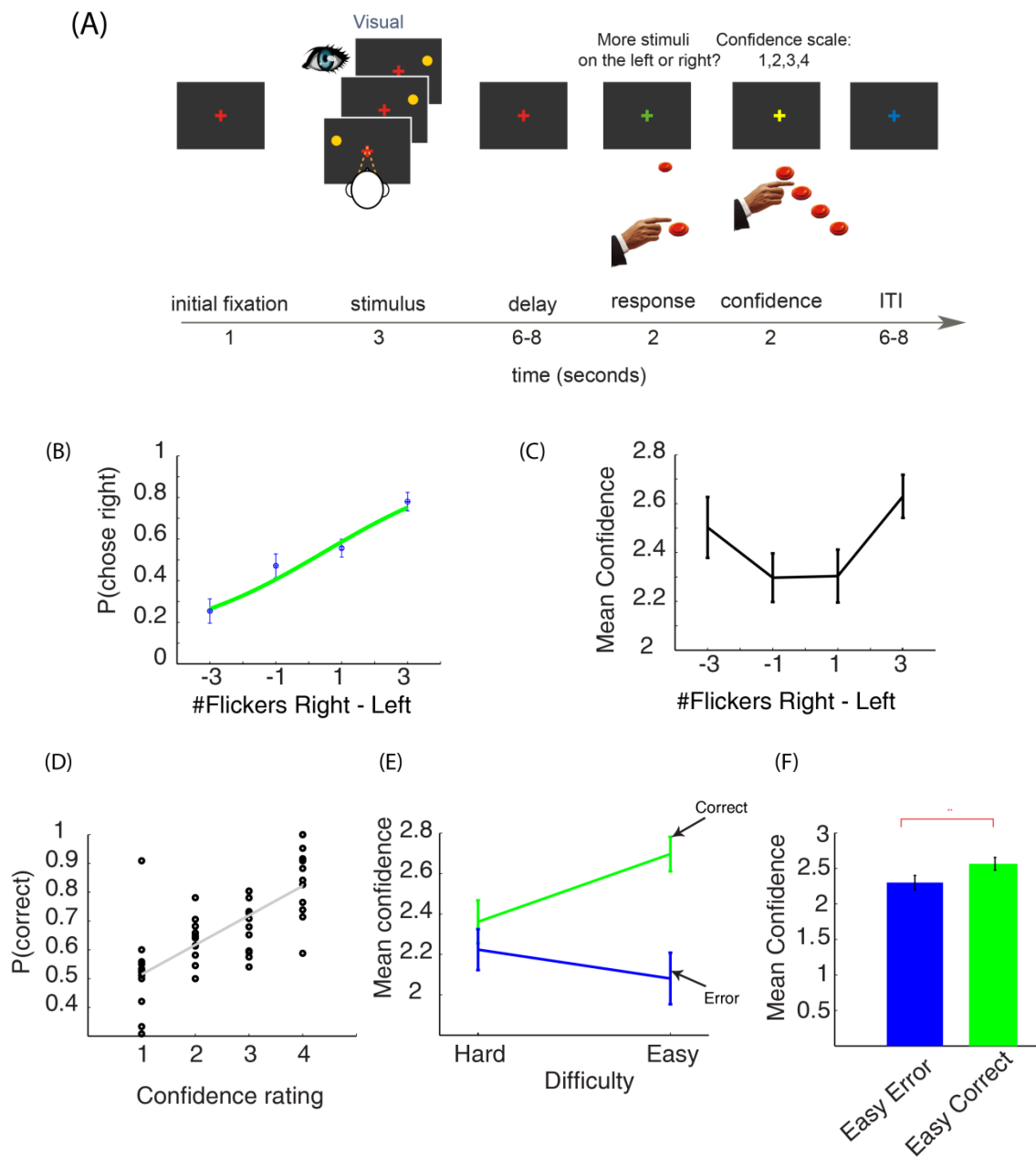


Figure 5.2.1. **Visual perceptual task performance.** (A) Description of the trial: after an obligatory fixation period, streams of flickers were presented to the right and left visual fields and the subjects were asked to form a decision about which side had more flickers and to evaluate their level of confidence in the decision using a scale of 1 to 4; response was by button press. (B) Probability of choosing right as function of total right minus left flickers, For easy trials, performance is  $\approx 75\%$  correct, colored circles are the means with  $\pm 95\%$  binomial confidence intervals across accumulator trials from all subjects. The thick line is the psychometric curve generated by the accumulator model. (C) Mean confidence as function of flicker difference; confidence was highest for easy trials. (D) Linear relationship between probability correct and confidence  $R=0.72$   $p<0.001$ , dots are individual subject accuracy at each confidence level, grey line is linear fit. (E) Mean confidence is higher for correct trials compared to error trials  $t(11) = 7.46$   $p<0.001$ , and a significant interaction between probability correct and difficulty ( $F(1,11)=20.60$   $p=0.001$ ). (F) Mean confidence is higher for correct trials compared to error trials at the same difficulty level; easy trials  $t(11)= 6.97$   $p<0.001$ .

### *Model fitting results*

To investigate whether the participants used an accumulation strategy to reach their decision we fitted behavioral data to a nine-parameter accumulator model (Brunton et al., 2013). Due to the low number of data points per subject inside the scanner, we combined data from all participants and fitted a single model. In this model, different parameters reflect different decision-making strategies. Thus, it is possible to investigate if the subjects were accumulating sensory evidence rather than just assuming that they used an accumulator strategy in forming their decision. One critical parameter is  $\lambda$ , which is the reciprocal of the time-constant of the accumulation process. If  $\lambda$  is negative, it means that the process is "leaky" and early information is lost. If  $\lambda$  is positive, then the process is "unstable" and early evidence dominates the decision,  $\lambda = 0$  reflects a perfect integrator. Model fits show that participants adopted a perfect integrator strategy (**Supplementary Table S5.2.1**). Using output of model as probability of model choosing right and plotting it as function of flickers difference shows that model nicely fits the behavioral data (**Figure 5.2.1B**).

### **fMRI Results**

The gradual accumulation of sensory evidence is a core decision-making process (Erich, 2015). However, it is hard to disentangle the neural correlates of the various decision-making processes, such as decision-monitoring, confidence in decision or error detection, from sensory evidence accumulation (Gold &

Shadlen, 2007; Shadlen & Kiani, 2013). Thus, it is not clear whether activity related to evidence accumulation and confidence in the decision are encoded in the same brain regions, or rather engage different brain regions. To investigate the brain regions with activity modulated by the sensory evidence we used likelihood estimates from model fits representing accumulated sensory evidence on a trial-by-trial basis to build parametric predictors of the stimulus presentation period (Methods). All maps were formed using a cluster-forming threshold  $p=0.005$  corrected for multiple comparisons at the cluster level at  $p=0.05$  for significant clusters.

## **Accumulator regions**

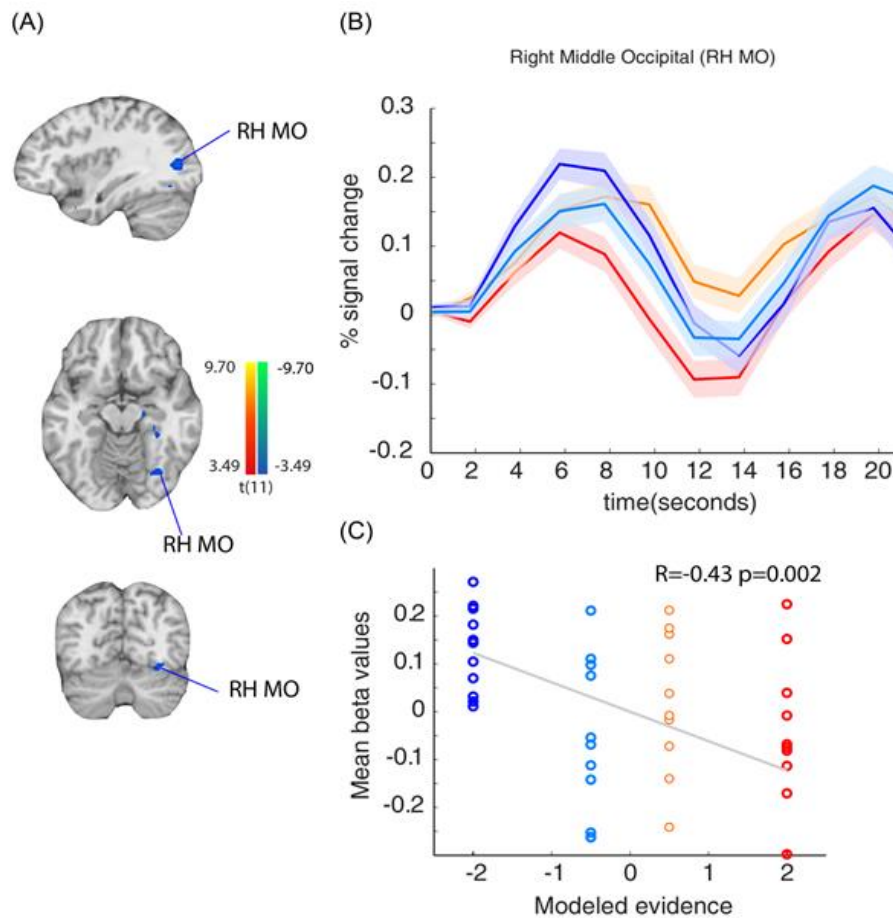
### ***Spatially specific sensory evidence accumulator map***

The perceptual decision formed in our task is about spatially segregated streams of flickers. In order to investigate brain regions with activity correlated to accumulated evidence favoring right or left choices, we used likelihood estimates of the decision as modeled by a quantitative model to build a parametric predictor of accumulator regions. The following brain regions showed modulation by spatially specific accumulated sensory evidence: precentral gyrus, parahippocampal gyrus and middle occipital gyrus (**Table 5.2.1**). A region is considered to accumulate sensory evidence for leftward decision if it shows the following signal profile: left strong evidence > left weak evidence > right weak evidence > right strong evidence. On the other hand, a

region accumulates sensory evidence for rightward decision if it shows the following signal profile: right strong evidence > right weak evidence > left weak evidence > left strong evidence. Investigating time courses from previous regions we found that the signal in the right middle occipital cortex followed the proposed accumulator profile towards rightward decisions (left strong > left weak > right weak > right strong) (**Figure 5.2.2A, B**). Also, the left precentral gyrus accumulates evidence for leftward decisions (**Figure 5.2.3A, B**). We also extracted beta activity from the aforementioned regions and correlated it to modeled sensory. Scatter plots show a significant linear correlation between the signal in occipital regions and spatially specific evidence  $R=-0.43$ ,  $p=0.002$  (**Figure 5.2.2C**) and for precentral region  $R=-0.36$   $p=0.03$  (**Figure 5.2.3C**).

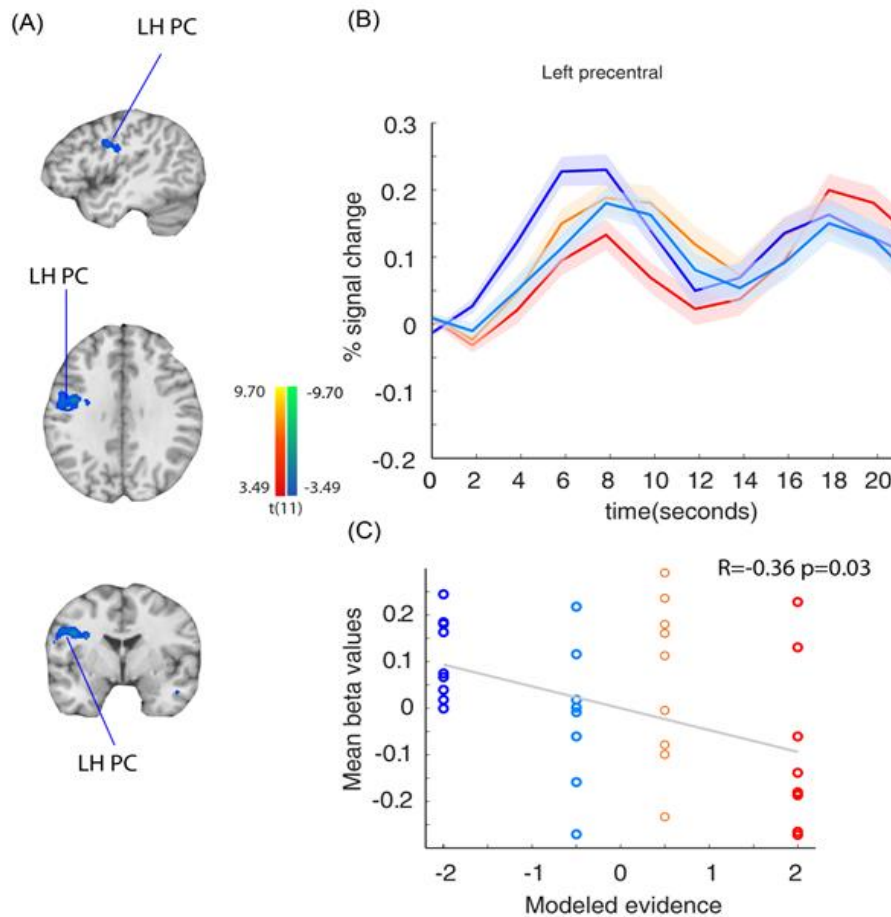
**Table 5.2.1 Spatially specific accumulator regions**

| Regions name             | BA | # voxels | Talairach |     |    | Correlation |        |
|--------------------------|----|----------|-----------|-----|----|-------------|--------|
|                          |    |          | x         | y   | z  | r           | p      |
| LH Precentral            | 6  | 90       | -39       | -4  | 31 | -0.36       | 0.03   |
| RH Parahippocampal gyrus | 19 | 43       | 21        | -19 | -5 | -0.54       | 0.0006 |
| RH Middle occipital      | 19 | 29       | 33        | -73 | 10 | -0.43       | 0.002  |



Cluster thresholded at  $p=0.005$  corrected at  $p=0.05$  voxels= 29

Figure 5.2.2. **Spatially specific accumulator regions** (A) Statistical map showing right hemisphere middle occipital (RH MO) with spatially specific accumulator activity. (B) Event-related averages from MO showing this signal suggest that it is accumulating sensory evidence for leftward decisions. The signal is strongest in trials with strongest evidence towards the left, and is weakest in trials with strongest evidence towards the right. When the evidence does not clearly favor one side, the signal did not clearly favor one choice. Blue is strong evidence towards left, light blue is weak evidence towards the left, orange is weak evidence towards the right, red is strong evidence towards the right (C) Scatter plot of beta values extracted from a 6mm sphere around the peak voxel from MO as a function of modeled evidence shows a significant linear correlation towards the contralateral side  $R=0.43$ ,  $p=0.002$ .



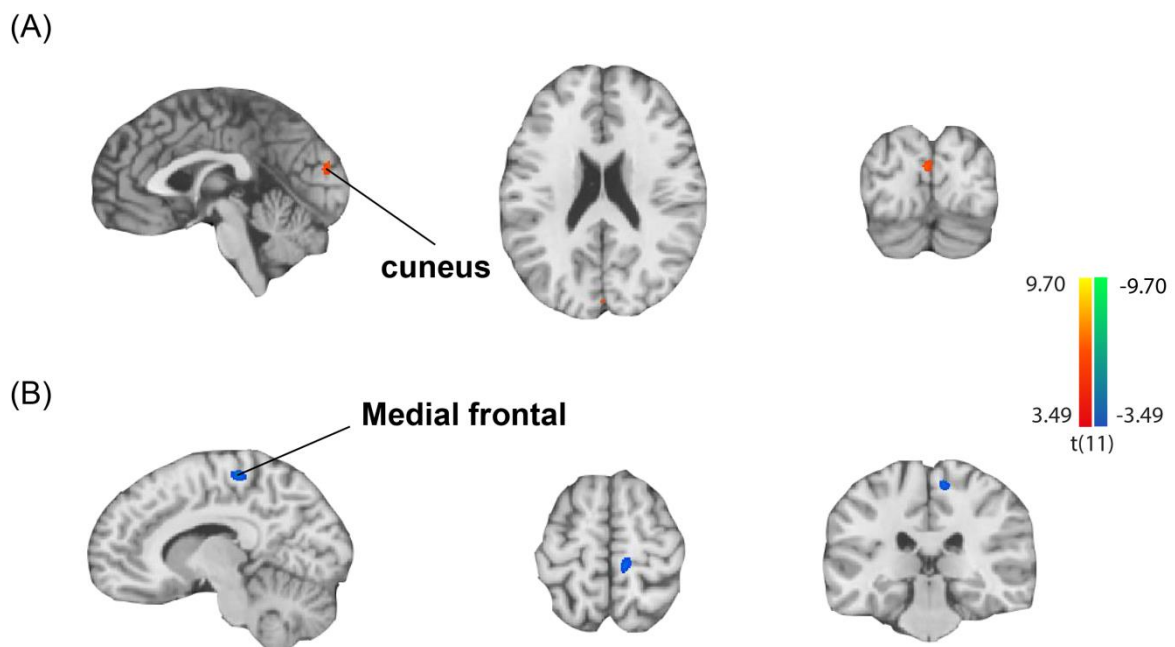
Cluster thresholded at  $p=0.005$  corrected at  $p=0.05$  voxels= 29.

Figure 5.2.3. **Spatially specific accumulator regions** (A) Statistical map showing left hemisphere precentral (LH PC) region with spatially specific accumulator activity. (B) Event-related averages from PC showing that signal suggest it is accumulating sensory evidence for leftward decisions. Signal is highest for trials with highest evidence towards left and signal is lowest for trials with strongest evidence towards the right. When the evidence does not clearly favor one side, the signal was also did not clear favor one choice. Blue is strong evidence towards left, light blue is weak evidence towards the left, orange is weak evidence towards the right, red is strong evidence towards the right. (C) Scatter plot of beta values extracted from a 6mm sphere around the peak voxel from PC as a function of modeled evidence shows a significant linear correlation towards the contralateral side  $R=0.36$ ,  $p=0.03$ .



### *Non-Spatially specific sensory evidence accumulator map*

In order to investigate brain regions with a signal that is modulated by sensory evidence but in a non-spatially specific manner (i.e. difficulty), we used absolute values of likelihood estimates of the decision to build a parametrically modulated predictor for the stimulus presentation period. The following brain regions showed a signal that was positively modulated by non-spatially specific accumulated sensory evidence: Cuneus gyrus - strong signal when evidence was strong (i.e. easy trials) (**Figure 5.2.4A**). The following brain regions showed a signal that was stronger when the absolute level of evidence was low (i.e. hard trials): medial frontal gyrus (**Figure 5.2.4B, Table 5.2.2**).



Cluster thresholded at  $p=0.005$  corrected at  $p=0.05$  voxels= 11.

Figure 5.2.4. **Non-spatially specific accumulator regions.** (A) Cuneus showed increase in signal strength when the absolute level of evidence was high. (B) Medial frontal region (BA6) show increase in signal strength when the absolute level of evidence was low.

**Table 5.2.2 Non-spatially specific accumulator regions (i.e. difficulty)**

| Regions name      | BA | # Voxels | Talairach |     |    | Strong evidence (easy) > weak evidence (hard)<br>t-test |      |
|-------------------|----|----------|-----------|-----|----|---|------|
|                   |    |          | x         | y   | z  | t(11)   | p    |
| LH Medial frontal | 6  | 11       | 9         | -28 | 58 | -0.92   | 0.38 |
| LH Cuneus         | 18 | 13       | -3        | -85 | 19 | 2.35  | 0.04 |

***ROI based spatially specific sensory evidence accumulation signal***

We constructed regions of interest (ROIs) based on the coordinates of peak activity of regions showing modulation by signed accumulated visual sensory evidence from a localizer group. We tested the same visual task in the localizer group with a wider evidence range (easy had ten flickers difference and hard had two flickers difference). ROIs showing a spatially specific sensory evidence accumulation signal from the localizer group were: left and right middle occipital, and right lingual. We extracted beta values from those regions and tested the correlation of the signal to modeled sensory evidence of participants in this group. We found that the right middle occipital ( $r= 0.37$ ,  $p=0.008$ ), and right lingual ( $r= 0.30$ ,  $p= 0.03$ ) were significantly modulated by sensory evidence in the current sample of participants as well.

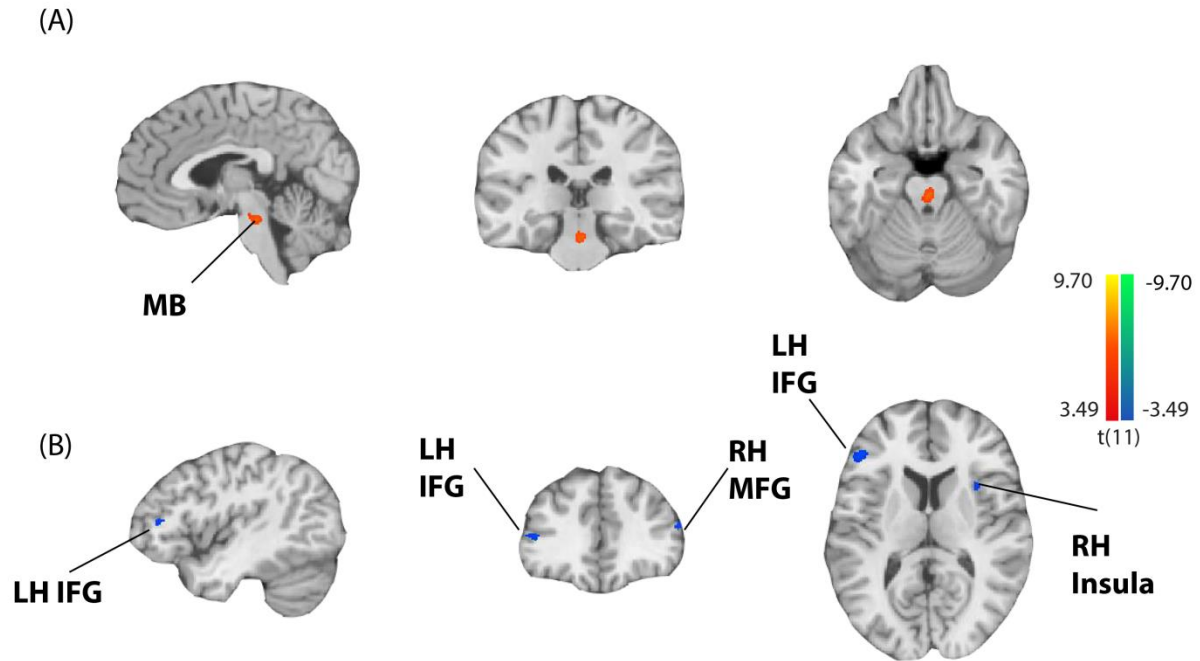
### ***ROI based spatially non-specific sensory evidence accumulation signal***

From the localizer group, ROIs of non-spatially specific sensory evidence accumulation were: right middle frontal gyrus, left lentiform, bilateral precentral, right post-central gyrus, left insula, right inferior occipital lobule, right angular gyrus, right middle occipital. We extracted beta values and comparing strong evidence > weak evidence using t-tests for each ROI. None of the regions localized by the localizer group showed the effect of non-spatially specific sensory evidence in the current group. Probably ROIs chosen didn't overlap with voxels from current study showing effect of spatially non-specific sensory evidence accumulation signal.

### **Decision-monitoring regions**

To explore brain regions with signal suggestive of decision-monitoring activity, we proposed triangulate criteria. The testing strategy was to identify ROIs based on one criterion and perform ROI analyses on the identified ROIs to see whether they met the other criteria. To investigate candidate regions that satisfied the first criterion, i.e. the presence of a difference between correct and error trials, we contrasted correct and error trials. A trial was graded "correct" if it had a 3 flickers difference or 1 flicker difference to the right, and the subjects chose right response, and "error", if the subjects chose left response. We found that the only brain region that showed a stronger signal for correct trials was the

midbrain (**Figure 5.2.5A, Table 5.2.3**). Moreover, brain regions that showed a stronger signal for error trials were the inferior and middle frontal gyrus, insula, cingulate (**Figure 5.2.5B, Table 5.2.3**).



Cluster thresholded at  $p=0.005$  corrected for  $p=0.05$  voxels= 8

Figure 5.2.5. **Accuracy map contrast (Correct>Error)**. (A) Statistical map showing midbrain (MB) with higher signal for correct trials. (B) Statistical map showing middle frontal gyrus (MFG), inferior frontal gyrus (IFG), and insula with higher signal for error trials, left hemisphere (LH), right hemisphere (RH). Map cluster thresholded at  $p=0.005$  corrected for  $p=0.05$  voxels= 8.

**Table 5.2.3 Decision monitoring regions**

| Region                    | BA | # Voxels | Talairach |     |     | Correct vs. error t-test |        |
|---------------------------|----|----------|-----------|-----|-----|--------------------------|--------|
|                           |    |          | x         | y   | z   | t(11)                    | p      |
| LH Inferior frontal gyrus | 46 | 9        | -42       | 35  | 13  | -4.4269                  | 0.0013 |
| RH Middle frontal gyrus   | 46 | 9        | 54        | 32  | 22  | -6.7036                  | 0.0001 |
| RH Insula                 | 13 | 8        | 33        | 26  | 7   | -6.0548                  | 0.0001 |
| RH Cingulate              | 6  | 8        | 15        | -1  | 49  | -5.4147                  | 0.0003 |
| Midbrain                  | -  | 14       | 3         | -25 | -17 | 4.9955                   | 0.0005 |

We treated inferior frontal gyrus, middle frontal gyrus, cingulate, insula, and midbrain as regions of interests (ROIs). For demonstration purposes we examined the time courses of brain regions showing the effect of accuracy and found that the signal from inferior, middle frontal gyrus, cingulate, and insula were stronger for error trials during stimulus presentation period, while the midbrain had a stronger signal with correct trials (**Figure 5.2.6A**). Therefore, the aforementioned regions exhibited a difference between correct and error trials, thus satisfying the first criterion.

To explore which brain regions satisfies the second criterion, i.e. an interaction between correctness and difficulty mimicking the behavior of confidence modulation by task difficulty; we extracted beta values from ROIs of the following predictors: correct easy, correct hard, error hard, error easy. We found

significant positive linear correlations in the inferior frontal gyrus ( $R= 0.44$   $p= 0.002$ ), middle frontal gyrus ( $R= 0.36$   $p= 0.01$ ), cingulate ( $R= 0.51$   $p<0.001$ ) and insula ( $R= 0.39$   $p= 0.006$ ), which means that activity was highest for error easy trials and lowest for correct easy trials. On the other hand, there was a significant negative correlation in midbrain regions ( $R= -0.54$   $p <0.001$ ), meaning that activity was highest for correct easy trials and lowest for error easy trials (**Figure 5.2.6B**). As such, those regions also satisfy the second criterion and reflect the behavioral results for confidence rating.

To study which ROIs satisfied the third criterion, i.e. the presence of an activity difference between confident and not confident trials at the same level of difficulty and accuracy, we compared the extracted beta values from the ROIs of the following predictors: confident, correct easy trials, not confident correct easy trials. We studied this possibility in the correct easy trials since we expected the difference between confident and not confident trials to be largest when the evidence was stronger and subject was correct. We found that only the middle frontal gyrus exhibited a significant difference between confident and not confident trials at the same level of accuracy and difficulty  $t(11) = 2.37$   $p=0.03$  (**Figure 5.2.6C**).

Thus, only the right middle frontal gyrus region showed a signal suggestive of subjective estimates of decision accuracy. Activity in middle frontal gyrus was higher in error trials than in correct trials. Moreover, we found a positive linear

correlation between the signal in the middle frontal gyrus and task difficulty. The signal was strongest for error trials and weakest for correct trials at the same level of difficulty; easy trials suggestive of a role in error detection. Lastly, the signal in middle frontal gyrus was modulated by the confidence rating of the participants at the same level of difficulty (easy) and accuracy (correct) trials.

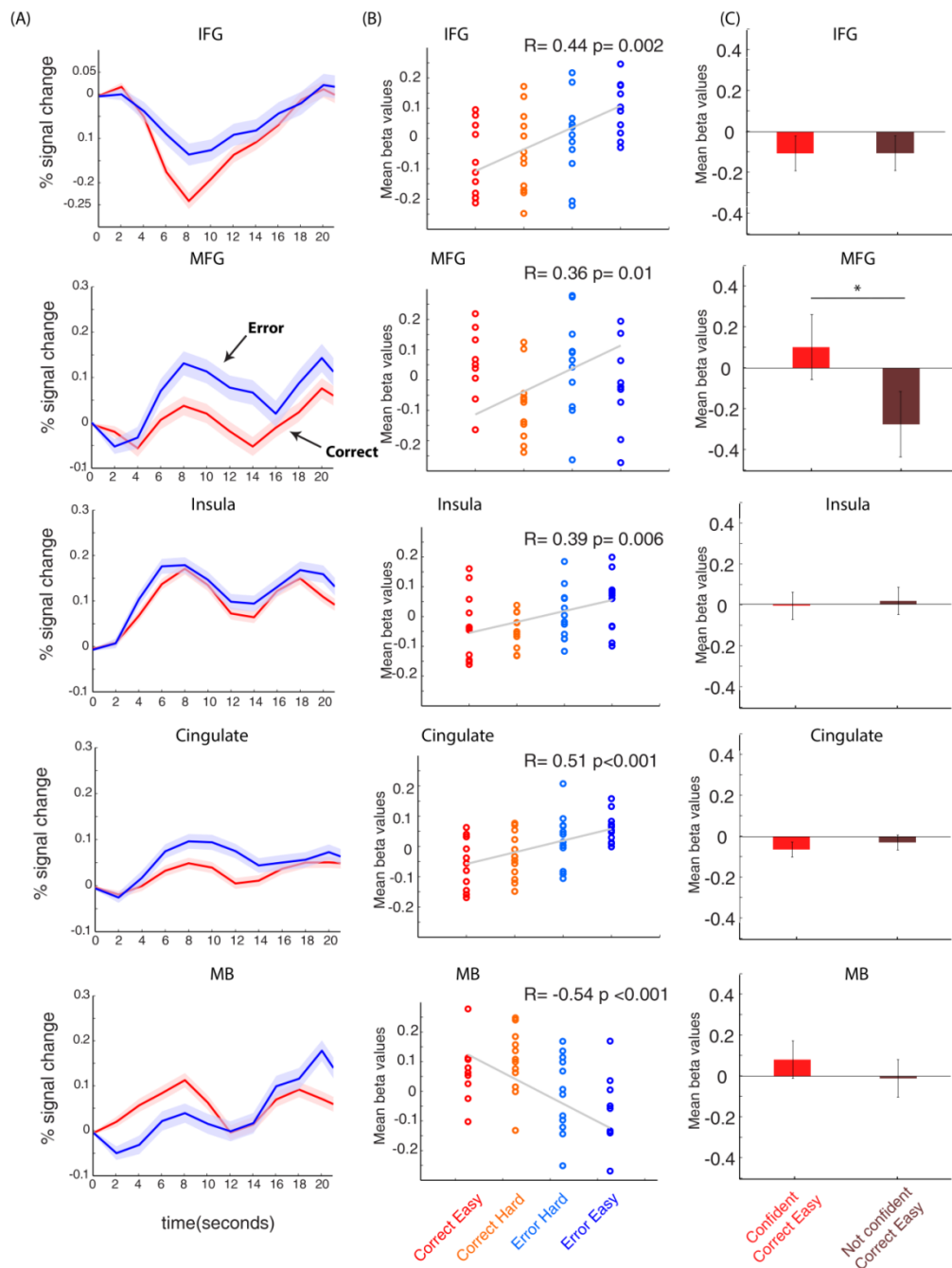


Figure 5.2.6. **Candidate regions of neural correlates of decision-monitoring.** (A) Event-related averages plots show a stronger signal for error trials in inferior frontal gyrus (IFG), middle frontal gyrus (MFG), cingulate, while there was a stronger signal for correct trials in the midbrain. (B) Scatter plots of beta values extracted from brain regions exhibiting an effect of accuracy show that the response in those regions was modulated by the difficulty level. The signal in MB is strongest for correct easy trials and weakest for error easy trials ( $t(11) = 3.1$ ,  $p = 0.009$ ), while the signal in IFG ( $t(11) = 2.49$ ,  $p = 0.03$ ), MFG ( $t(11) = 2.49$ ,  $p = 0.03$ ), and cingulate ( $t(11) = 2.49$ ,  $p = 0.03$ ) was strongest for error trials and weakest for correct easy trials. (C) Mean beta values for confident correct easy and not confident correct easy. Of the candidate regions with a signal suggestive of involvement in decision-monitoring, only the MFG showed a significant difference when the subjects were confident compared to not confident at the same level of difficulty and accuracy  $t(11) = 2.37$   $p = 0.03$ .



It is reasonable to propose that decision-monitoring signal should be explored in time periods later than the stimulus presentation period. Therefore, we also applied same methodology used earlier to the delay and motor period by contrasting correct vs error trials for each of those time periods. We found that medial frontal region in the delay and the motor period to show modulation accuracy (Supplementary figure 5.2.7). Moreover, posterior parietal region showed higher signal for error trials in the motor period only (Supplementary figure 5.2.7). However, signal in the delay and motor period is influenced by motor preparation and motor response. Thus, based on recent findings suggesting that confidence in the decision builds up as a second layer of the decision formation network (Insabato, Pannunzi, Rolls, & Deco, 2010b) and in parallel to the decision formation itself (Gherman & Philiastides, 2015) we favor investigating the stimulus presentation period itself for the decision-monitoring signals.

## **Discussion**

The aim of this study was to investigate if visual sensory evidence accumulation and confidence in the visual decision engages similar brain regions. We have presented data showing that visual sensory evidence engages occipital regions; middle occipital and lingual, in a spatially specific manner and frontal regions in a spatially non-specific manner. On the other hand, inferior frontal gyrus, middle

frontal gyrus, insula, cingulate, and midbrain showed signal suggestive of decision-monitoring; confidence in decision or error detection.

### *Neural correlates of visual sensory evidence accumulation*

We used model-based fMRI to investigate neural correlates of sensory evidence accumulation. We found that the occipital regions were modulated by spatially specific accumulated sensory evidence; activity in the right occipital cortex was as follows: (left high evidence > right low evidence > left low evidence > right high evidence). In our task, we used a slow event-related design, which allowed us to identify the sensory response from the motor response. Previous neuroimaging studies investigating sensory evidence accumulation have shown that once the perceptual component was dissociated from the motor component, as in our task design, the occipital cortices would show activity correlated with sensory evidence accumulation (Hebart, 2014; Philiastides & Sajda, 2007). Moreover, we found that the left precentral cortex accumulated evidence in a spatially specific manner towards leftward decisions (left high evidence > right low evidence > left low evidence > right high evidence). This is consistent with previous neuroimaging studies that proposed a role of prefrontal regions in sensory evidence accumulation (Heekeren, 2004, 2008; Liu & Pleskac, 2011; Philiastides, Aukstulewicz, Heekeren, & Blankenburg, 2011). However, since, in this task, the participants had to form a spatial decision, i.e. more flickers right or left, we assumed that the sensory evidence had to accumulate in a

spatially specific manner. Nevertheless, we investigated the possibility that sensory evidence would accumulate in a spatially non-specific manner. We found that medial frontal regions and the cuneus were modulated by the absolute level of sensory evidence, regardless of the spatial direction. Medial frontal activity was higher for low-level sensory evidence, while cuneus activity was higher for high-level sensory evidence. The absolute level of sensory evidence was highly correlated with decision difficulty; the stronger signal in the medial frontal gyrus was related to increasing task demands, such as effort or attention. This could be viewed in light of previous fMRI findings that suggest a role of the medial frontal gyrus in visual attention (Corbetta et al., 2005).

### ***The role of middle frontal gyrus in decision-monitoring***

Disentangling neural processes of decision-monitoring, i.e. confidence in the decision, from other decision-related processes, is challenging. We found that the right middle frontal gyrus was the only region in the brain that harbored activity fulfilling all three criteria for identifying a brain region of decision monitoring. Thus, we propose that activity in the middle frontal gyrus correlates with subjective estimates of decision-monitoring. Previous fMRI studies have shown that activity in the right rostralateral prefrontal (rLPFC) cortex is related to metacognitive aspects of decision-making (Fleming & Dolan, 2014). In their study, they showed that the rLPFC showed greater activity during self-report compared to a matched control condition. In addition, functional connectivity

between right rPFC and both contralateral PFC, and the visual cortex increased during metacognitive reports ( Fleming & Dolan, 2012).

### ***The role of anterior cingulate in error detection***

In our results, we found that activity in the anterior cingulate (ACC) region was higher for error trials than for correct trials. Studies investigating event-related brain potential (ERP) have reported error-related negative activity (ERN) that peaked 100 to 150 ms after electromyographic evidence of an error response that was localized to medial frontal regions (Ghering 1994, Falkenstein 1995). A seminal fMRI study investigating the role of the ACC in task performance, showed that activity in ACC was higher for error trials compared to correct trials in ACC (BA24/32) (Carter et al., 1998). Similarly, we showed that signal in ACC (BA24) is stronger for error trials compared to correct trials. We found that this activity was also modulated by task decision difficulty. This is in line with the increased activity in the ACC in trials with high response competition compared to low response competition.

### ***The role of the midbrain in confidence in the decision and decision optimization***

We found that midbrain activity satisfied the first two criteria: a difference in the signals between correct and error trials, and interaction between correctness and difficulty mimicking behavior of confidence. Signal strength was suggestive of generation of confidence in the decision (i.e. stronger in correct trials than in

error trials, strongest in easy correct and weakest in easy error trials). The midbrain includes the superior and inferior colliculi, tegmentum, substantia nigra, red nucleus and other nuclei and fasciculi. The basic function of the midbrain includes visual coordination (superior colliculi), auditory coordination (inferior colliculi), motor coordination (substantia nigra) and gait (red nucleus). Midbrain dopaminergic neurons are considered to be involved in reward (Schultz, 1998), working memory (Williams & Goldman-Rakic, 1995), and learning (Steinberg et al., 2013). Recent findings also showed that dopaminergic neurons are involved in certainty and precision of beliefs (Schwartenbeck, 2015). Schwartenbeck designed an event-related fMRI study, in which the subjects had to decide whether to accept the current offer or wait for a possibly higher offer, with the risk of losing everything. In this task, precision can be regarded as confidence that a more valuable offer would appear in the future. They found that midbrain activity might be associated with the expected precision of beliefs, which can also be understood as confidence of reaching the desired goal and not reflecting reward prediction error. Nevertheless, whether the strong BOLD signal in this region truly reflects dopaminergic neuronal activity is still under debate (Düzel et al., 2009). However, the physiology of dopaminergic neurotransmission is more consistent with a role in mediating precision, since the expected precision needs to be widely broadcasted because it plays a crucial role in hierarchical inference (Feldman & Friston, 2010a). These features are anatomically and neurophysiologically consistent with the encoding

of precision by neuromodulators (Friston et al., 2012), and with dopaminergic activity, in particular. It is important to note that our task does not require reward learning. Therefore, there was nothing that would call upon reward prediction error (Schultz, Dayan, & Montague, 1997). Such a view of the role of midbrain dopaminergic activity in precision fits with formulations in terms of signal-to-noise (Williams & Goldman-Rakic, 1995), uncertainty, and precision (Fiorillo, Tobler, & Schultz, 2003), and the crucial role that dopamine plays in selecting among alternative actions (Frank, 2005). Establishing a link between confidence and dopaminergic activity provides insights into the psychopathology of confidence in decision-making which has been discussed in the context of a number of disorders including psychosis (Adams, Stephan, Brown, Frith, & Friston, 2013) and Parkinson's disease (Frank, 2005; Friston et al., 2012).

### ***Disentangling decision correlates from post-decision confidence***

In this study, we aimed at disentangling the neural correlates of sensory evidence accumulation as a core decision process from the neural correlates of confidence in the decision. To disentangle the processes underlying confidence judgment and decision making Hilgenstock and colleagues (Hilgenstock et al., 2014) used a grating orientation task, in which the subjects were required to indicate the orientation of tactile gratings and rate their level of confidence on a scale of 1 to 4 while they were being scanned with fMRI. To identify the neural

correlates of post-confidence and the decision itself, they based their assumptions on the two-stage dynamic signal detection model (2DSD) (Pleskac & Busemeyer, 2010). This model suggests that confidence and metacognitive judgment about decisions only evolve post-decision with the ongoing accumulation of information (Hilgenstock et al., 2014). So, based on the temporal evolution of signal it is possible to separate the neural correlates from the confidence from the decision. They found that DLPFC strictly codes post-decision confidence. However, a study using EEG challenged their underlying assumption that confidence and decision are separated temporally. Gherman and Philiastides (Gherman & Philiastides, 2015) found that decision and confidence in the decision were generated simultaneously in the brain and they mapped neural correlates of the decision and confidence in the decision to frontal and parietal regions. Our criterion was based on predictions of integrate-and-fire attractor models (IFA) of the BOLD signal behavior. IFA proposed that confidence is an emerging property of the networks forming the decision (Insabato, 2010). IFA models were able to fit and explain behavioral data from animals and neural data from electrophysiology recordings in rats (Kepecs et al., 2008) and monkeys (Kiani & Shadlen, 2009). By convolving the firing rate with a hemodynamic response function, it was proposed that for a region to be involved in confidence, the BOLD signal had to be modulated by accuracy and difficulty levels (Rolls et al., 2010). We managed to disentangle the neural correlates of sensory evidence accumulation as a signal of regions involved in

the decision itself. We used the IFA criteria to show that the right middle frontal region was the only brain region that showed a signal of decision-monitoring.

***Relation of our findings to the literature:***

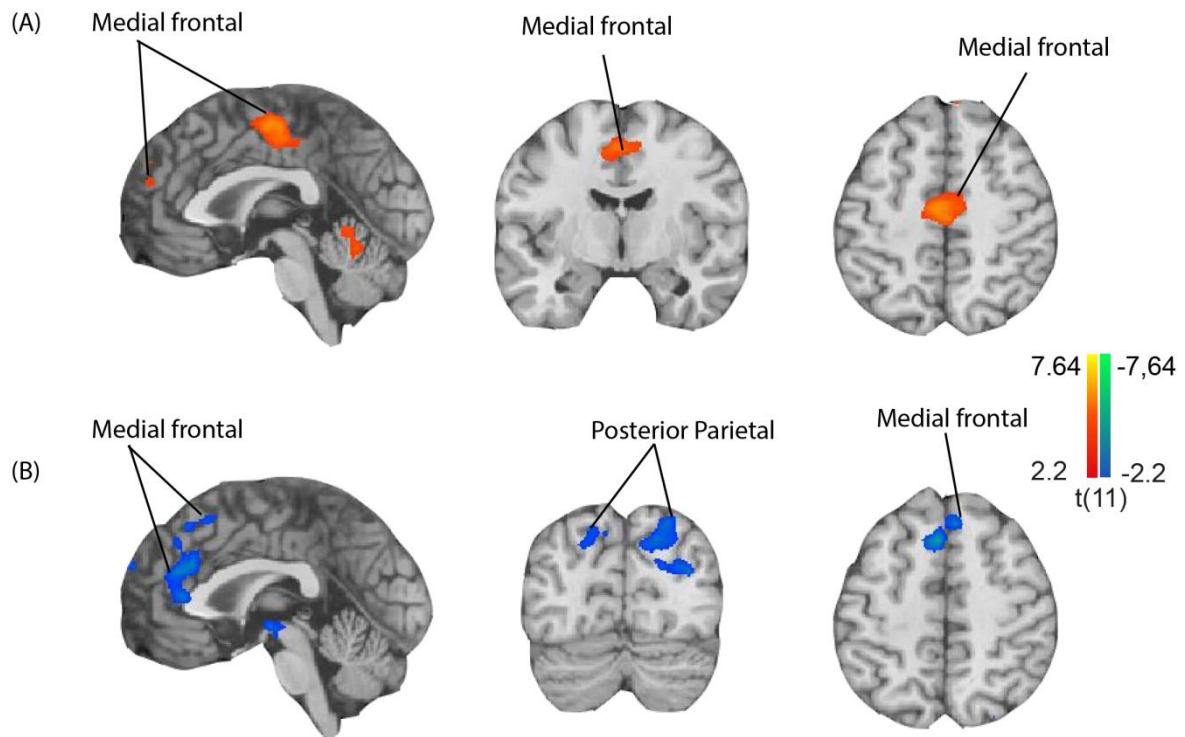
In this study we demonstrate that sensory evidence accumulation and decision-monitoring although behaviorally correlated could engage different brain regions. This is in line with previous findings in neuroimaging literature showing the visual evidence accumulate in occipital regions while confidence in the decision is better coded in posterior parietal cortices (Hebart, 2014). Moreover, we investigated the decision-monitoring signal in the same time period of sensory evidence accumulation based on recent findings that decision formation and confidence in the decision occurs simultaneously (Gherman & Philiastides, 2015). Also, in our study we show that signal in midbrain is suggestive of confidence coding while signal in cingulate and prefrontal regions is suggestive of error detection. Previous studies investigating metacognition didn't show whether metacognitive regions correlate with confidence in the decision or error detection (Fleming & Dolan, 2014).

**Limitations of the study**

In this study, we aimed at disentangling the neural process of sensory evidence accumulation from those of decision-monitoring. However, one major limitation of this study was the use of fMRI to investigate the neural correlates of sensory evidence accumulation (Hanks & Summerfield, 2017). fMRI has a low spatial



and temporal resolution (Logothetis, 2008), and we were therefore not able to benefit from the minute dynamics of sensory evidence buildup as modeled by the quantitative model that we applied. Moreover, it is conceivable that other brain regions outside of the occipital cortex, which have neural populations that are less spatially specific, to exhibit neural activity correlating with evidence accumulation. However, given the poor spatial resolution of fMRI, such detailed signal may have blurred. Moreover, our criteria were based on an assumption derived from predictions of the BOLD signal according to integrate-and-fire attractor models based on simulations of neural firing rates (Insabato, 2010). Such simulations have shown a linear relationship between the BOLD signal and neural firing rates (Rolls et al., 2010). However, the relation between neural activity and BOLD signal is still not fully understood.



Cluster thresholded at  $p=0.005$  corrected for  $p=.05$  voxels= 37

Supplementary Figure 5.2.1. **Accuracy map for delay and motor response periods** (A) Statistical map showing medial frontal regions with higher signal for correct trials in the delay period. (B) Statistical map showing medial frontal region and posterior parietal regions with higher signal for error trials during the motor response period.

## ***Conclusion:***

In this study we managed to disentangle the various brain regions involved in the build-up of the visual evidence accumulation signal from the regions involved in decision-monitoring.

## **ACKNOWLEDGEMENTS**

This work was supported by the Hermann and Lilly Schilling Foundation, German Research Foundation (DFG) grants WI 4046/1-1 (M.W.). Prof. Dr. Thomas Crozier proof read and edited this manuscript.

## **Contributions**

Ahmad M. Nazzal (A.N.) designed the study, interpreted the results, and wrote the paper. A.N. prepared stimuli. A.N. prepared scripts for running the task. A.N. planned, performed, and supervised behavioral and imaging data collection. Yian Liao (Y.L.) contributed to data collection. A.N. programmed analysis scripts and analyzed behavioral and fMRI data. Jeffrey C. Erlich (J.E.) fitted behavioral data to the model. A.N. implemented model-fitting results for fMRI analysis. Melanie Wilke (M.W.) and Carsten Schmidt-Samoa (C.S.) provided corrections to the paper. A.N. prepared the figures.

Supplementary Table 5.2.1. **Model parameters for the most relevant parameters in the study of decision-making strategy based on model fits.**

| Modality | $\lambda$ | $\sigma(a)$ | $\sigma(s)$ | $B$     | Lapse rate |
|----------|-----------|-------------|-------------|---------|------------|
| Visual   | 0.2612    | 2.5281      | 0.0135      | 24.8630 | 0.0144     |

$\sigma_a$  a diffusion constant, parameterizing noise in "a", the decision variable.

$\sigma_s$  parameterizes sensory noise when adding the evidence

$\lambda$  parameterizes consistent drift in the memory  $a$ . In the ‘leaky’ or forgetful case ( $\lambda < 0$ ), drift is towards  $a = 0$ , and late stimuli pulses have a greater impact on the decision than earlier pulses. In the ‘unstable’ or impulsive case ( $\lambda > 0$ ), drift is away from  $a = 0$ , and early stimuli pulses have a greater impact on the decision than later pulses. The memory's time constant  $\tau = 1/\lambda$ .

$B$  the height of the ‘sticky’ decision boundaries and parameterizes the amount of evidence necessary to commit to a decision.

*Lapse rate* the fraction of trials in which a random response is made

For details on model fitting procedure and model parameters (Brunton, 2013).

### 5.3 Voxel-based lesion-symptom mapping of the effect of cortical and subcortical lesions on auditory and visual perceptual decision-making.

#### **Abstract**

Neuropsychological studies revealed that hemispatial neglect patients have an ipsilesional choice bias in both auditory and visual tasks. However, most studies investigating hemispatial neglect use visual tasks, and the role of different cortical and subcortical lesions on auditory spatial perceptual decision-making is thus not entirely clear. In the fMRI study described above in this manuscript, we found that spatially specific sensory evidence accumulates in modality specific-sensory cortices, while neural signatures of secondary decision processes such as saliency, or confidence in the decision appear in frontal and parietal regions. We used the same auditory and visual tasks as in the previous fMRI studies to calculate the probability of a rightward choice as a function of the stimuli difference "right minus left". We estimated bias, i.e. probability that a participant would choose "rightward" when the difference between left and right was minimal. We also estimated the performance measure "slope". Based on the fMRI findings we formulated specific predictions of the effect of lesions on visual and auditory perceptual decision-making: (1) a lesion in accumulator areas such as the superior temporal gyrus or occipital regions will result in an ipsilesional choice bias in a modality-specific manner. (2) A lesion in the frontal or parietal cortex will lead to slope changes that suggest an effect of the lesion on task performance regardless of modality. To investigate causality we tested

patients with cortical and subcortical lesions in the right hemisphere. We used voxel-based lesion-symptom mapping to analyze the relationship between lesions and behavior on a voxel-by-voxel basis. We found data suggestive of a significant role of the parietal cortex resulting in a decrease of auditory task performance as shown by in slope change that conformed to our fMRI informed prediction.

## **Introduction**

Despite the importance of auditory cues in guiding spatial behavior, much of what is known about how the brain utilizes sensory information to form spatial decisions is based on the results of visual tasks (Gokhale, Lahoti, & Caplan, 2013). In the auditory domain, the brain's ability to form auditory spatial decisions relies on its capacity to detect an interaural time difference between the two ears (Thompson et al., 2006). Auditory information from the left and right auditory afferents meets early in the auditory system at the level of the superior olivary complex in the brainstem, and then projects to the medial geniculate nucleus of the thalamus via the inferior colliculus in the midbrain (Irvine, 1986; Heffner and Masterton, 1990). The auditory cortex is organized into four hierarchical levels: Heschel's gyrus (core), belt, parabelt, and the projections of the parabelt regions with information flowing from core to belt to parabelt (Kaas & Hackett, 2000). Efferent connections from the parabelt are arranged into two functional circuits. That relevant to the current study is the anterolateral parabelt which sends projections to the inferior parietal lobule,

dorsolateral frontal cortex, frontal eye fields and areas of the prefrontal cortex involved in spatial processing (Romanski et al., 1999). In humans, evidence from functional magnetic resonance imaging, electrophysiology, and positron emission tomography studies suggests that the posterior part of the superior temporal gyrus and the inferior parietal lobule are involved in the localization of sound in space and in spatial orienting (Arnott, 2004). Lesions in these structures would lead to auditory directional error and distorted spatial representation (Arnott, 2004, 2005; Barrett, 2010).

Functional magnetic resonance imaging (fMRI) is usually assumed to establish a correlation between metabolic changes in the brain and some behavioral output, but it is difficult to infer causality based on fMRI alone (Logothetis, 2008). Therefore, supplementing functional neuroimaging studies with causality-establishing methods such as studying the effect of lesions lead to a better understanding of disorders such as the hemispatial neglect syndrome (Corbetta et al., 2005; Heilman & Valenstein, 1972; Husain & Kennard, 1996; Jacobs, Brozzoli, & Farnè, 2012; Kinsbourne, 1970).

The hemispatial neglect syndrome is defined as failure to report, respond to, or orient to stimuli that presented to the side opposite the damaged hemisphere that cannot be solely explained by primary motor or sensory deficits (Heilman & Valenstein, 1972). Neglect of the left side after a lesion to the right hemisphere is more frequent and severe than right side neglect after a left hemispheric lesion

(Driver and Mattingley, 1998). Two main theories have been proposed to explain this pathophysiology. (1) The orientation bias model hypothesizes that attention is shifted toward the contralateral side via inhibition of the ipsilateral hemisphere (Kinsbourne, 1970). (2) The right-hemisphere dominance model states that the left hemisphere represents the right side of space, whereas the right hemisphere represents both sides (Heilman, 1980). Studies investigating the ability of neglect patients to localize perception of sound sources in the free field or lateralized via headphones found a prominent deficit of lateralization perception in patients with neglect (Bisiach et al., 1984). Deficits are typically, and more severely, observed in right-hemisphere lesions (Zatorre & Penhune, 2001).

In the fMRI study described in the previous chapter, we investigated the neural correlates of sensory evidence accumulation in auditory and visual tasks and the neural correlates of confidence in the decision. We found that sensory evidence accumulates in modality-specific brain regions; the signal in the superior temporal gyrus correlated with auditory sensory evidence accumulation, while the signal in occipital cortex correlated with visual sensory evidence accumulation. Moreover, we showed that the signal in the frontal and parietal regions did not correlate with sensory evidence accumulation, but rather correlated with decision difficulty; when the decision was harder to form the fMRI signal was stronger in those regions. However, the causal contribution of the previously identified brain regions to auditory perceptual decision-making is



not clear. Based on empirical findings from two previous fMRI studies we expected the following effect of lesions: (1) A lesion affecting accumulator regions in sensory cortices will lead to an ipsilesional choice bias in a modality-specific manner. (2) A lesion affecting the parietal or frontal cortex will decrease task performance regardless of modality (**Figure 5.3.1**).

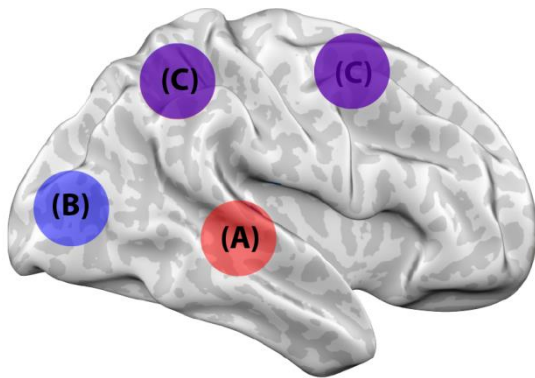


Figure 5.3.1. **Schematic illustration of fMRI-based predictions of the effect of lesions on auditory and visual perceptual decision-making.** (A) Lesions affecting the auditory accumulator in red will lead to auditory ipsilesional bias. (B) Lesions affecting the visual accumulator in blue will lead to visual ipsilesional bias. (C) Lesions affecting the parietal frontal cortex will lead to a performance decrease as demonstrated by slope changes.

To examine the fMRI-driven predictions, we tested patients with right hemispheric lesions affecting cortical and subcortical structures with the same auditory and visual tasks previously used. We estimated two behavioral measures based on the probability of participants to choose "right" as function of the stimuli difference" right minus left". First measure is rightward bias. Rightward bias is the probability of participants to make a rightward choice when the trials had the least difference between right and left. The second measure is slope. We use slope as a measure of task performance and estimate it from the 75% and 25% recognition points. We use voxel-based lesion-symptom mapping (VLSM) (Bates et al., 2003) to study the relationship between the

lesions and the behavioral estimates; bias and slope, for auditory stimuli in a voxel-by-voxel basis.

## **Materials and Methods**

### **Patients and age-matched healthy controls:**

A total of 25 participants were tested (18 patients, and seven healthy, age-matched volunteers as controls). We included nine patients in the final analysis. Seven patients had a right-sided cortical lesion (four males, mean age 58.7, SD 10.1 years). Two patients had a right subcortical lesion (one male, mean age 55, SD 5.67 years). Nine patients were excluded (four due a disease etiology other than stroke, e.g. tumor, trauma, dementia, sarcoidosis), five were excluded because they did not participate in all of the sessions. The patients were tested in the sub-acute or chronic stage after a stroke (> one month after the stroke). Control subjects were seven healthy, aged-matched volunteers (six males, mean age 62.6, SD 9.3 years). All participants gave their written informed consent. All procedures were performed according to the Declaration of Helsinki and were approved by the local Ethics Committee of the University Medical Center Göttingen. The participants received a monetary compensation for their participation in the experiments (**Table 5.3.1**).

**Table 5.3.1 Demographic data**

| Lesion                                | Age             | Sex | Handedness | Clinical symptoms | Time of testing after stroke in months |
|---------------------------------------|-----------------|-----|------------|-------------------|--|
| <i>Parietal</i>                       |                 |     |            |                   |  |
| AD                                    | 52              | M   | L          | H, A              | 17                                     |
| PJ                                    | 60              | M   | R          | H, A              | 18                                     |
| CG                                    | 63              | F   | L          | -                 | 1                                      |
| VH                                    | 48              | M   | R          | H                 | 17                                     |
| GB                                    | 63              | M   | R          | H                 | 21                                     |
| AE                                    | 53              | M   | R          | H, A              | 2                                      |
| SJ                                    | 53              | M   | R          | H, D              | 2                                      |
| Parietal<br>Mean $\pm$ SD<br>(yrs)    | 58.6 $\pm$ 10.1 |     |            |                   |  |
| <i>Subcortical</i>                    |                 |     |            |                   |  |
| CT                                    | 56              | F   | R          | H                 | 3                                      |
| JE                                    | 49              | M   | R          | H, A              | 2                                      |
| Subcortical<br>Mean $\pm$ SD<br>(yrs) | 52.5 $\pm$ 4.9  |     |            |                   |  |
| <i>Healthy controls n=7</i>           |                 |     |            |                   |  |
| Mean                                  | 62.6 $\pm$ 9.3  | 6 M | R          | -                 | -                                      |

*H= hemiparesis, A= hemianopia, D = hearing deficit. All patients had a stroke affecting the right brain hemisphere.*

## **Neglect test battery**

### ***Visual neglect test battery***

As screening tests for visual neglect, we used the following tests: line bisection, line cancelation and star cancelation (Fels & Geissner, 1996). The tests were not used to categorize patients.

### ***Auditory neglect test battery (dichotic test)***

For evaluating auditory neglect, we used the Uttenweiler test (Uttenweiler, 1980). This German dichotic test was originally developed for children, but we used it here since it is most appropriate for auditory testing neglect in the patient population (Gutschalk, 2012).

### ***Pure-tone audiometry***

Each of the patients was evaluated for a primary sensory hearing deficit using a pure tone auditory hearing-test mobile phone application (Masalski & Kręcicki, 2013). A Sennheiser HD pro 380 headset was used after calibration to 30-year-old healthy participant with no hearing deficit. The tone was presented at different frequencies. The tone with the frequencies 250, 500, 1000, 2000, 4000, 6000 and 8000 Hz was presented to each ear separately beginning with an amplitude of 40 dB. The amplitude was then reduced in 5 dB steps, and the participants had to indicate that they heard the tone after each reduction, either verbally or by raising their hand until they were no longer able to hear the tone. The results of the right and left ear were compared to a published database of hearing tests results. A difference of 10db between the left and right ear at frequencies of 1000 or 2000 Hz was considered to be a deficit.

### ***Experiment setup***

The participants sat in a small, closed quite room with their head position stabilized on a chin rest. They were instructed to fixate a central cross with their eyes. Eye position was monitored using the SMI RED system 120 Hz, and by the experimenter sitting in front of the patient. Matlab 2010Rb and Psychophysical Toolbox ([www.psychtoolbox.org](http://www.psychtoolbox.org)) was used to control stimulus delivery with a customized script. The clicks were presented using a headset (Sennheiser HD 380 pro headset). Monitor (Dell, Ultrasharp U2711b) with an

eye-screen distance of 57 cm. The spatial resolution was  $1920 \times 1200$  pixels, and the monitor had a refresh rate of 60 Hz. The participants responded to the task by pressing buttons on the mouse pad.

### *Task*

The participants were asked to determine whether the right or left side of the headset received more clicks during the auditory task. They were asked to determine whether the left or right side of the screen had had more flickers presented to it. Each run was started by the participant pressing a key on the keyboard. Fixation cross color changes indicated the different stages of the task. The task began with a red cross, and the participant was to answer when the cross turned green. The cross stayed red while the stimuli were being presented and also for a delay period of one to four seconds after the end of stimuli presentation. The participants used their right hand to respond by pressing either the left mouse button if more stimuli had been on the left, or the right mouse button if there had been more stimuli on the right. No feedback was given to the participants after completing the trial. There was a rest period of one to four seconds between response and beginning of the next trial. The duration of delay and rest times was random to prevent the participants from forming a response strategy. Each patient finished at least one run of 48 trials in total.

### ***Auditory stimuli***

Trains of 3ms clicks lasting one to four seconds were presented over headphones. Twenty clicks per second were presented randomly to each ear separately ( $\# \text{clicks right (CR)} + \# \text{clicks left (CL)} = 20$ ). There was a minimum inter-pulse interval of 33ms to minimize adaptation. The first, and last clicks were presented to both ears simultaneously to prevent bias towards the side of the first or the last click presented (Brunton et al., 2013). Stimuli were generated using MATLAB, version R2011b using custom scripts.

### ***Visual stimuli***

Trains of stereo flickers lasting one to four seconds were presented on the horizontal plane of the screen at an eccentricity of around 11 visual degrees. Each train had five flickers per second ( $\# \text{flickers right (FR)} + \# \text{flickers left (FL)} = \text{five per second}$ ). Each flicker lasted 16.7ms and had a visual angle of approximately two degrees. Consecutive flickers had a minimum inter-pulse interval of 120 ms to minimize adaptation (Brunton et al., 2013). Stimuli were generated using MATLAB, version R2011b using custom scripts.

## **Behavioral data analysis**

### **Cut-off estimation**

To investigate spatial bias we binned the data into seven bins based on the click differences ( $\# \text{right} - \# \text{left}$ ). The centers of the bins were as follow: -40, -20, -5, 0, 5, 20 and 40 for the auditory task and -10, -5, -2, 0, 2, 5, and 10 for the visual

task. We calculated the probability of rightward choice (ipsilesional choice, since all of our patients had a right-side lesion) for each bin. We calculated the probability of rightward choice for each bin. Bias was percent rightward choice at the central bin with 0 differences. We calculated the slope as:  $(y\text{-value of 75\% recognition point} - y\text{-value of 25\% recognition point}) / (x\text{-value of 75\% recognition point} - x\text{-value of 25\% recognition point})$ . We calculated the 2.5 and 97.5 percentiles for the healthy control group bias and slope values. We used percentiles as a cut-off point for estimating which patients had a bias and slope changes.

### **Auditory group analysis**

To investigate the role of cortical or subcortical lesions on choice bias in the auditory tasks, we calculated a 2-by-7 mixed ANOVA with cortical stroke vs. healthy as the between-subject factor, and probability rightward choice for click difference bins as the within-subject factor. The patient SJ was excluded from auditory group analysis due to a primary auditory sensory deficit. We binned the click differences ( $\# \text{clicks right} - \# \text{clicks left}$ ) into the following bin centers -40, -20, -5, 0, 5, 20, and 40 and calculated percent rightward choice for each bin. ANOVA was run for cortical lesions. The degrees of freedom were corrected for non-normally distributed data.

## **Lesion analysis**

### ***MRI data acquisition***

Scans were performed either in Göttingen or in Seesen. All images in Göttingen were acquired using a 3Tesla Magnetom TIM Trio scanner (Siemens Healthcare, Erlangen, Germany) with a 12 channel, phased-array head coil. High-resolution T1-weighted anatomical scans (three-dimensional (3D), turbo fast low angle shot, echo time (TE) 3.26 ms, repetition time (TR) 2.250 ms, inversion time 900 ms, flip angle 9°, isotropic resolution of 1 x 1 x 1 mm<sup>3</sup>) were obtained.

### **Probability map**

To visualize the lesions in the patients, we used the regions of interest tool for estimating probability maps in BrainVoyager QX Software version 2.8 (Brain Innovation, Maastricht, the Netherlands). The lesions in each patient were mapped into Talairach space using Neuroelf toolbox. The estimates of eight patient lesions were formulated as a volume of interest and used in the regions of interest analysis tool in BrainVoyager to estimate probability maps.

### ***Voxel-based lesion-symptom mapping***

We used voxel-based, lesion-symptom mapping to investigate the effect of lesions on auditory task behavioral measures in a voxel-by-voxel way. Patient SJ was excluded due to a primary auditory sensory deficit. Patient AE was not included in the voxel-based, lesion-symptom mapping because he had no scans of his lesion. We used MRICron for VLSM analysis (Rorden et al., 2007). The



lesions were manually mapped onto MNI templates in a slice-by-slice manner. A non-parametric design with four predictors was employed using the NPM plugin for MRICron. Predictors were: bias auditory, slope auditory. We used Brunner Munzel statistical rank tests, running 1000 permutations tests on continuous values of slope and bias. Since the software assumes higher values to indicate better performance, we inverted the magnitude of the bias values by multiplying with -1. The resulting statistical maps were overlaid on the same template used for drawing the lesions.

## Results

Nine patients and seven healthy, age-matched control persons were included in the final analysis (for details of patients and participants **Table 5.3.1**). Lateralized trains of flickers were presented to the left and right visual hemifield in the visual task. In the auditory task, lateralized clicks to the left and right headset were presented. Participants had to decide on which side there had been more stimuli (**Figure 5.3.2**).

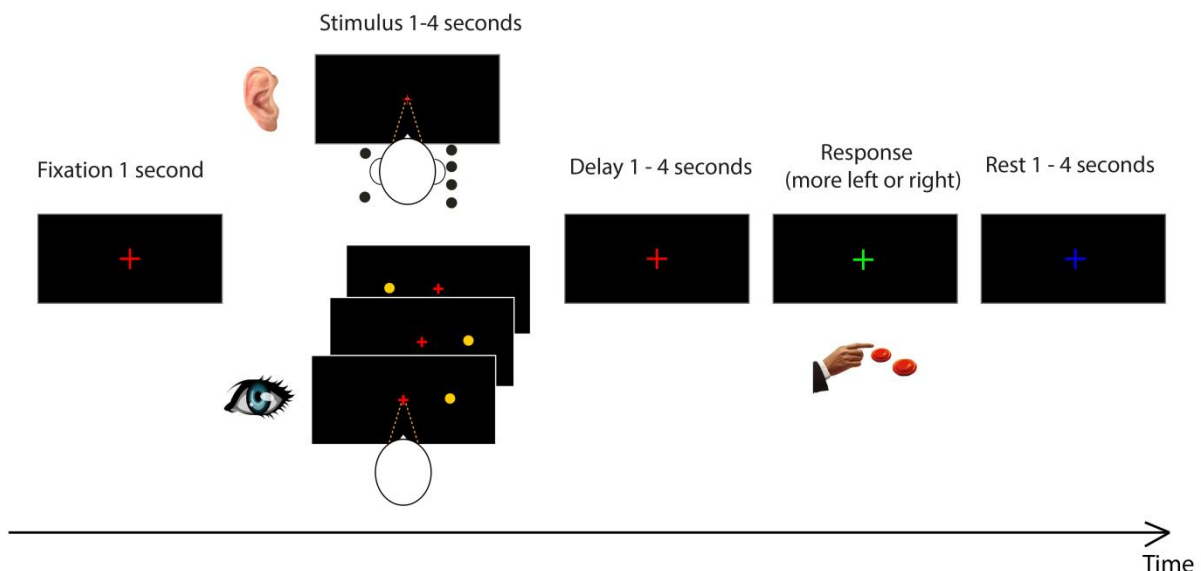


Figure 5.3.2. **Visual and auditory accumulator tasks.** Streams of spatially segregated stimuli were presented to the left or the right space (flickers for the visual task, and clicks for the auditory task). Patients were asked to make a decision on which side had had the most stimuli. After a delay time, the participants were asked to respond with the right hand by pressing a button. The durations of the delay and rest periods were randomized to prevent patients from developing response strategies.

We calculated the probability of participants choosing right as function of the stimuli difference "right minus left". We estimated bias (percent rightward choice in central bin with least difference between left and right) and slope (75%

discrimination – 25% discrimination point) for all participants (Table 5.3.2).

The lesions affected cortical and subcortical structures (Figure 5.3.3).

**Table 5.3.2 Behavioral measures results of individual patients**

| Lesion                       | Auditory task     |                   |                   | Visual task       |                   |                   | Dichotic            | Auditory            | Visual              | Star cancellation |
|------------------------------|-------------------|-------------------|-------------------|-------------------|-------------------|-------------------|---------------------|---------------------|---------------------|-------------------|
|                              | ML                | C                 | MR                | ML                | C                 | MR                | (R-L)/(R+L)         | Slope               | Slope               | (R-L)/(R+L)       |
| <i>Parietal</i>              |                   |                   |                   |                   |                   |                   |                     |                     |                     |                   |
| AD                           | 0.53              | <b>0.88</b>       | 0.66              | 0.14              | 0.53              | 0.87              | -0.09               | <b>0.003</b>        | 0.034               | 0                 |
| PJ                           | 0.05              | 0.66              | 0.89              | 0.30              | 0.72              | 0.83              | 1                   | <b>0.008</b>        | <b>0.005</b>        | 0.03              |
| CG                           | 0.17              | 0.55              | 0.66              | 0.07              | 0.66              | 1                 | 0                   | <b>0.003</b>        | 0.026               | 0                 |
| VH                           | 0.10              | <b>0.95</b>       | 1                 | 0                 | 0.58              | 1                 | 0.03                | <b>0.009</b>        | 0.036               | -0.07             |
| GB                           | 0.87              | <b>0.94</b>       | 1                 | 0.10              | <b>1</b>          | 1                 | 0.88                | <b>0.004</b>        | <b>0.010</b>        | -0.15             |
| AE                           | 0.17              | 0.55              | 0.66              | 0.33              | 0.75              | 0.75              | 0.15                | <b>0.004</b>        | 0.025               | 0.15              |
| SJ                           | 0.17              | <b>0.95</b>       | 1                 | 0                 | 0.67              | 1                 | 0.03                | <b>0.01</b>         | 0.046               | 0                 |
| <i>Parietal mean ± SD</i>    | 0.29<br>±<br>0.30 | 0.78<br>±<br>0.19 | 0.83<br>±<br>0.17 | 0.13<br>±<br>0.13 | 0.70<br>±<br>0.15 | 0.92<br>±<br>0.10 | 0.32<br>+/.<br>0.48 | 0.007<br>±<br>0.004 | 0.026<br>±<br>0.020 | 0<br>±<br>0.1     |
| <i>Subcortical</i>           |                   |                   |                   |                   |                   |                   |                     |                     |                     |                   |
| CT                           | 0                 | 0.54              | 1                 | 0                 | 0.44              | 0.75              | 0.05                | <b>0.01</b>         | 0.050               | 0                 |
| JE                           | 0                 | 0.30              | 1                 | 0                 | 0.60              | 1                 | 0                   | 0.015               | 0.036               | 0                 |
| <i>Subcortical Mean ± SD</i> | 0.02<br>±<br>0.03 | 0.32<br>±<br>0.21 | 0.92<br>±<br>0.13 | 0<br>±<br>0.11    | 0.52<br>±<br>0.17 | 0.88<br>±<br>0.17 | 0                   | 0.01<br>±<br>0.003  | 0.04<br>±<br>0.001  | 0                 |
| <i>Healthy controls n=7</i>  |                   |                   |                   |                   |                   |                   |                     |                     |                     |                   |
| Mean ± SD                    | 0<br>±<br>0.02    | 0.56<br>±<br>0.17 | 1<br>±<br>0       | 0<br>±<br>0       | 0.57<br>±<br>0.01 | 1<br>±<br>0       | 0                   | 0.014<br>±<br>0.001 | 0.015<br>±<br>0.001 | 0                 |

*Most left (ML), central (C), most right (MR). Right (R), Left (L).*

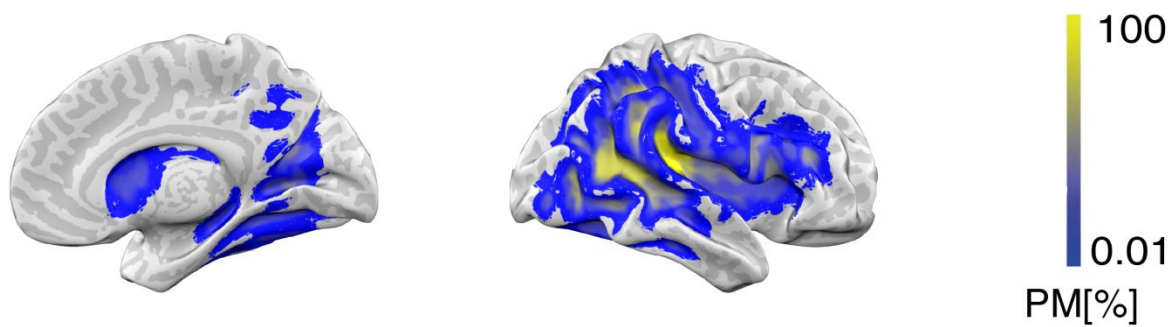


Figure 5.3.3. **Probability map (PM) of lesions.** The lesions were not localized to specific brain regions. The lesions affecting cortical and subcortical structures including accumulator and saliency regions identified by fMRI studies.

We applied three analytical approaches using cut-off estimates, auditory group analysis, and voxel-based lesion-symptom mapping (VLSM). We focused on the auditory task for the group analysis and for the VLSM. It was not possible to investigate the visual task in a group manner nor in patients with VLSM since only two patients had no primary visual sensory deficits. However, we obtained psychometric curves showing the probability of a rightward choice as a function of stimuli difference "right minus left" in all patients for the auditory and visual tasks. For the single patient analysis we excluded the following patients because of hemianopia: AD, AE, CG, PJ, and JE. We excluded patient SJ due to a history of left ear tinnitus and a difference of more than 10dB between the left and right ear in pure-tone audiometry.

### *Single subject cut-off estimates results*

Since each patient had a unique medical history and lesion anatomy we investigated behavior in a single patient manner. We focused on the following three patients in the single patient analysis approach: VH, GB, and CT. This gave a low number of patients who fulfilled the inclusion criteria and finished the visual and auditory tasks. To categorize the patients based on behavior, we estimated cut-off points by determining the 97.5 percentile based on bias and slope values from the healthy participants group. For the auditory task, the bias cut-off point was 0.87 while the slope cutoff point was 0.13 (**Figure 5.3.4A**). For the visual task, the bias cut-off was 0.76 and 0.13 (**Figure 5.3.4B**). Patients GB, VH, CT had a slope shallower than healthy controls in the auditory task, while patient GB had a slope below cut-off point for the visual task meaning that the performance of aforementioned patients was worse than that of healthy controls. Only patients with cortical lesions had a rightward bias (ipsilesional bias) beyond cut-off. Patients VH and GB had a bias in the auditory task beyond cut-off (**Figure 5.3.4C**), while patient GB exhibited a bias in the visual task (**Figure 5.3.4C, D**).

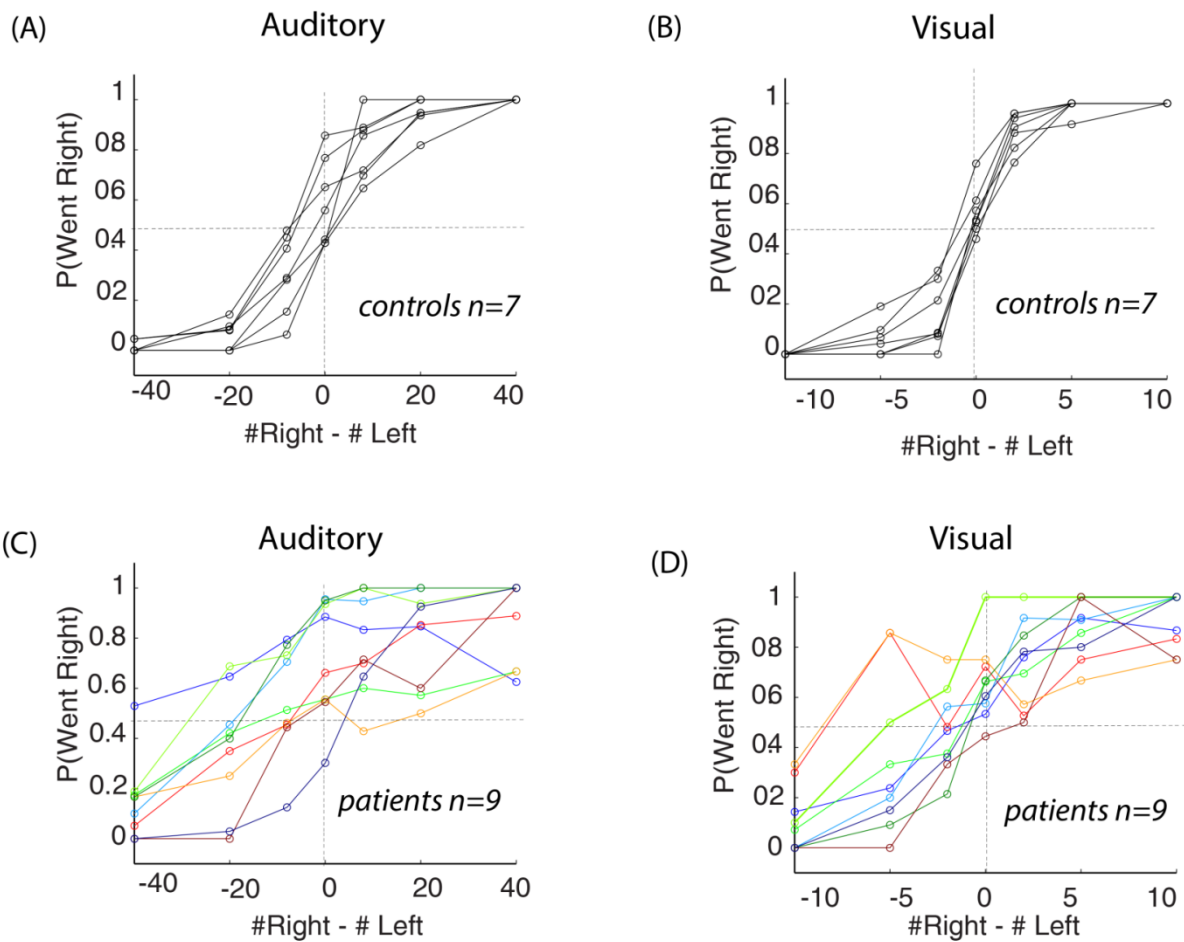


Figure 5.3.4. **Psychometric curves of the probability of choosing right as function of stimuli difference "right minus left" for auditory and visual tasks** (A) Probability of healthy, age-matched participants choosing right as a function of clicks difference in the auditory task; participants chose more to the right when more right clicks were presented. (B) Probability of healthy, age-matched participants choosing right as function of flickers difference in the visual task; participants chose more to the right when more right flickers were presented. Based on healthy, age-matched behavior we estimated rightward bias, i.e. probability of rightward choice in bin with the least difference of stimuli between right and left. Moreover, we estimated the slope of the curve as 75% detection - 25% detection. To evaluate pathological bias and slope we calculated the 97.5 and 2.5 percentiles for bias and slope. (C) Four patients with cortical lesions showed bias above cut-off in the auditory task. (D) One patient with a cortical lesion showed bias above cut-off for the visual task. Patients with cortical and subcortical lesions showed shallower slopes than healthy, aged matched controls in both modalities.

***Patient VH:***

VH was a 48-year-old male patient, who was diagnosed with a right-sided infarct, left spastic hemiparesis, depression, epilepsy, and left-sided hemineglect. His lesion was localized in the right frontal-temporo-parietal regions due to occlusion of the middle cerebral artery (**Figure 5.3.5A**). The patient had a history of metabolic syndrome. We tested the patient 17 months after the stroke incident.

The results of the paper and pencil tests for neglect were as follows: line bisection score was 9/9, line cancellation test (L 18/18, R 18/18), star cancellation score (L 26/27, R 20/27). This indicates that the patient did not exhibit left-sided visual spatial neglect. Left monaural score 100%, right monaural score 100%, dichotic testing score ((R-L)/(R+L)) 0.03, indicating no sign of auditory hemispatial neglect.

The ipsilesional bias in the auditory task was 0.95. The mean bias in the auditory task in the age-matched control group was  $0.56 \text{ Std} \pm 0.17$  (mean  $\pm$  SD). The patient's ipsilesional bias in the visual task was 0.57, while the mean bias in the visual task in the age-matched control group was  $0.51 \pm 0.01$ .

The slope for the patient in the auditory task was 0.009, while the mean slope for the auditory task in the age-matched control group was  $0.014 \pm 0.001$ . The patient had a slope in the visual task of 0.04 (mean slope for the visual task in the age-matched control group  $0.015 \pm 0.001$ ). Thus, VH exhibits bias and

performance decrease in the auditory, but not in the visual task. (Figure 5.3.5B, Table 5.3.2).

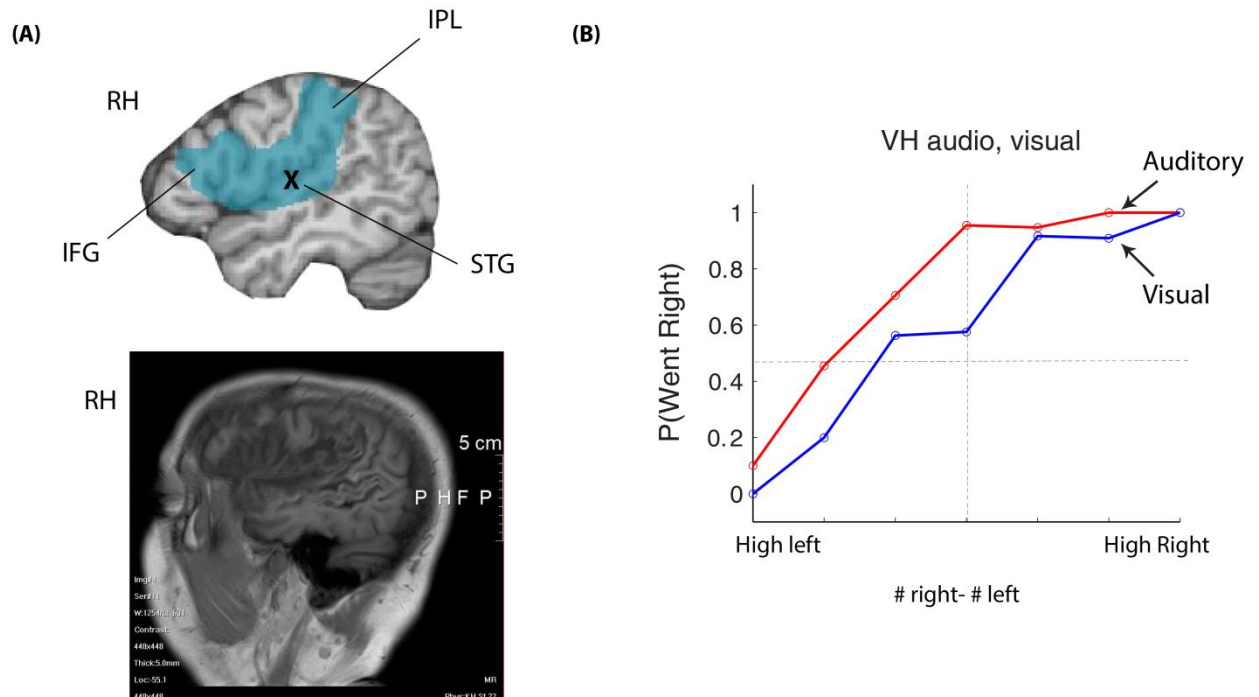


Figure 5.3.5. **Patient VH: lesion and behavior in auditory and visual tasks** (A) Depiction of lesion anatomy in patient VH. His lesion (in blue) involved the right hemisphere (RH), the inferior parietal lobule (IPL), superior temporal gyrus (STG), and inferior frontal gyrus (IFG). The lesion affected auditory accumulator regions (x) but not visual accumulator regions. (B) The psychometric curve of probability that the patient chooses right as function of stimuli difference (right-left). Number of trials = 96 for each modality. VH exhibited bias in the auditory task, but not in the visual task. His bias is consistent with the fMRI prediction of a role of sensory cortices in modality-specific sensory evidence accumulation. VH also had a lesion in frontal and parietal regions. His slope was lower than the cut-off value only in auditory modality. The decrease in the auditory task is in line with the fMRI prediction of a role of frontal and parietal cortices in task performance.



### ***Patient GB***

GB was a 63-year-old male patient, who was diagnosed with a right Art. media infarct on August 8, 2012, with left-sided hemiparesis, frontal lobe syndrome, symptomatic epilepsy, left sided hemineglect, anosognosia, and organic brain syndrome. The patient presented with a lesion extending from right frontal-temporal-parietal to occipital following the occlusion of the right middle cerebral artery (**Figure 5.3.6A**). We tested the patient 21 months after his stroke.

The results of the paper and pencil tests for neglect results were as follows: line bisection score was 9/9, line cancelation test (L 18; R 18), star cancelation score (L 27/27; R 25/27), indicating that there was no evidence of spatial neglect in the paper and pencil tests. The left and right monaural scores were 100%, and the dichotic testing score ((R-L)/(R+L)) was 1 meaning that the patient had a left-sided auditory hemispatial neglect.

GB had an ipsilesional bias in the auditory task of 0.94. The mean bias in the auditory task in the age-matched control group was  $0.56 \pm 0.17$ . The patient's ipsilesional bias in the visual task was 1 (mean bias in the visual task in the age-matched control group was  $0.51 \pm 0.01$ ). The patient's slope in the auditory task was 0.004, while the mean slope in the auditory task in the age-matched control group was  $0.014 \pm 0.001$ . The slope of the patient in the visual task was 0.01 with a corresponding value in the age-matched control group of  $0.015 \pm 0.001$ .

Thus, GB exhibited an ipsilesional choice bias as well as decreased performance in both modalities (**Figure 5.3.6B**).

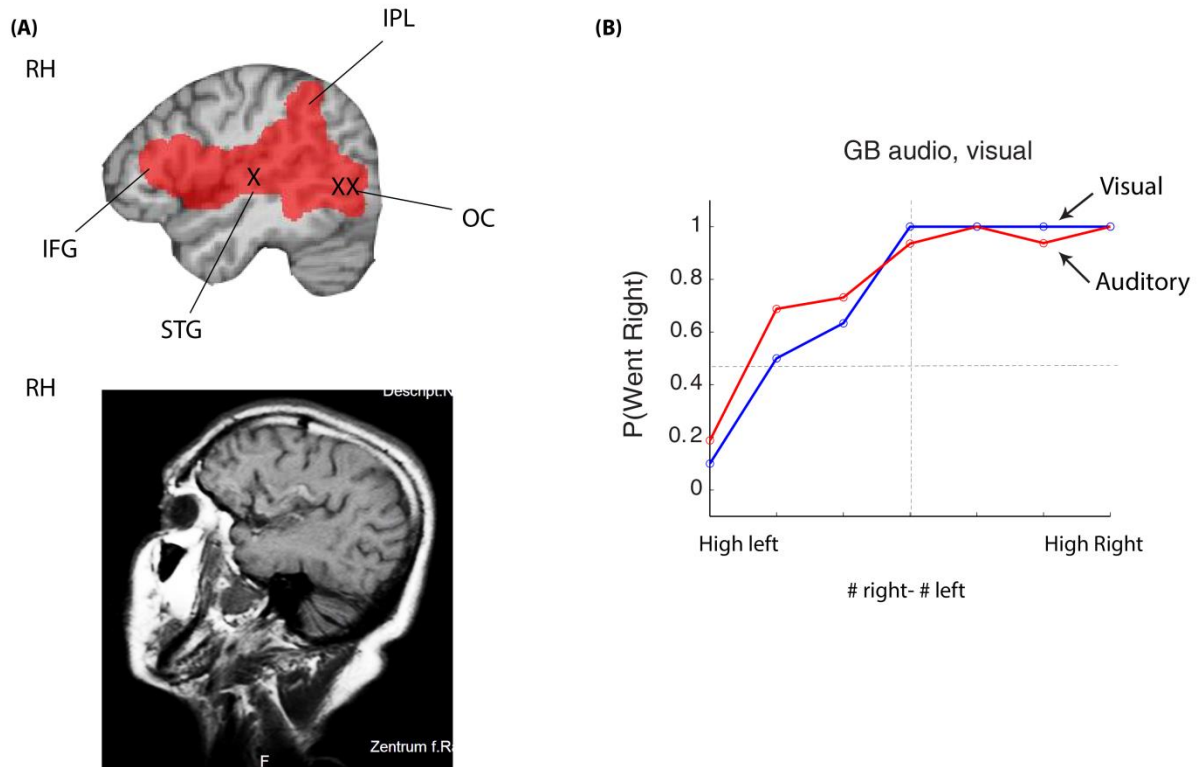


Figure 5.3.6. **Patient GB: lesion and behavior in auditory and visual tasks** (A) Depiction of lesion anatomy of patient GB. The lesion involved the right inferior parietal lobule (IPL), right inferior frontal gyrus (IFG), right superior temporal gyrus (STG), and right occipital gyrus (OC). The lesion affected auditory accumulator regions (x) and visual accumulator regions (xx) (B) The psychometric curve of the probability of the patient choosing "right" as function of stimuli difference (right-left). Number of trials = 144 for each modality. GB showed a pathological bias and slope in both modalities. His ipsilesional bias and performance decrease were consistent with the fMRI findings predicting ipsilesional choice bias after lesion affecting the accumulator regions in a modality-specific manner and a performance decrease after a lesion to the frontal and parietal regions.

***Patient CT:***

CT was a 56-year-old female patient, who was diagnosed with a right Art. media infarct due to occlusion of the right internal carotid artery on Dec. 12, 2015 resulting in a lesion in the right caudate nucleus (**Figure 5.3.7A** with left hemiparesis. We tested the patient February 5, 2016.

The results of the paper and pencil tests for neglect were as follows: line bisection score was 9/9, line cancelation test (L 18; R 18), star cancelation score (L 27/27; R 27/27), left and right monaural score was 100%, and the dichotic score  $((R-L)/(R+L))$  was 0, indicating that patient CT had no auditory or visual hemispatial neglect.

The patient's bias was 0.54 in the auditory task and 0.44 in the visual task; both were not above the cut-off point. The slope in the auditory test was 0.01 (below the cutoff point), but was above the cutoff point with a visual slope of 0.05. This patient with subcortical lesion did not exhibit spatial bias in either task, and no performance change in the visual task, but a slope change in the auditory task (**Figure 5.3.7B**).

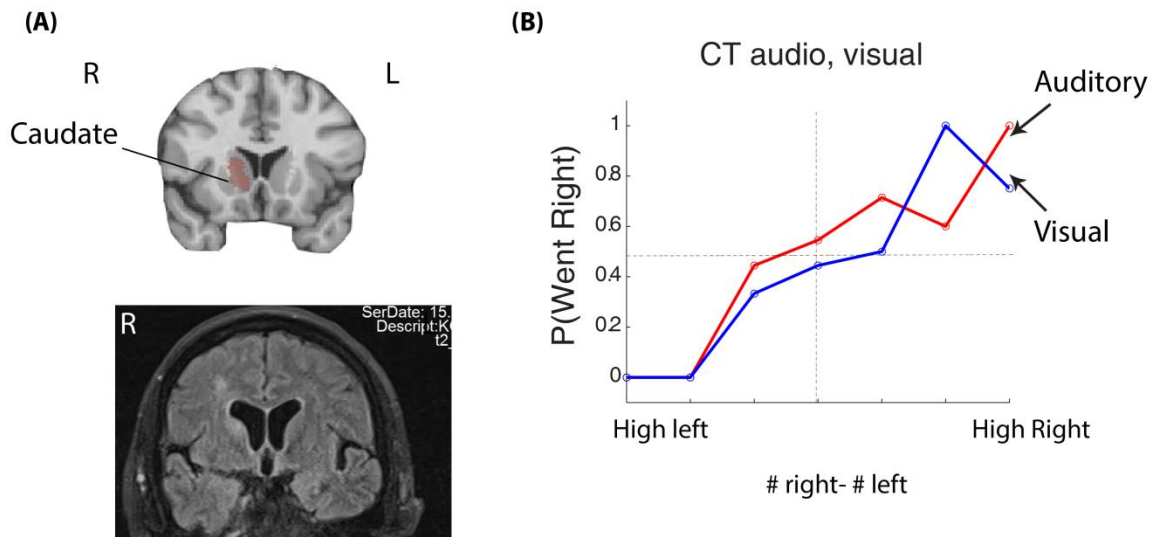


Figure 5.3.7. **Patient CT: lesion and behavior in auditory and visual tasks.** (A) Depiction of lesion anatomy of patient CT. Her lesion was confined to the right caudate nucleus (B) The psychometric curve of probability of the patient choosing "right" as a function of stimuli difference (right-left). Number of trials = 48 for each modality. Patient CT showed no bias in either tasks. She had an auditory slope lower than cutoff, but visual slope was not affected. From fMRI predictions one would not expect a lesion in the caudate to cause an ipsilesional choice bias in the auditory and visual tasks, or performance decrease. The slope change in the auditory task is more likely due to external noise.

### *Auditory group analysis*

To understand effect of cortical lesions on the ability of patients to benefit from sensory evidence, we investigated the probability of rightward ipsilesional choice as a function of bins of click differences between the right minus left. Clinicians usually evaluate visual or somatosensory signs of hemispatial neglect syndrome but do not usually evaluate auditory neglect (Gokhale et al., 2013). Moreover, it was not possible to run this analysis on the visual group because several patients presented with a primary visual sensory deficit. Therefore, we focused on the auditory task for group analysis. One patient SJ was excluded from the auditory group analysis because of a primary auditory sensory deficit. We binned the clicks difference (#clicks right - #clicks left) into the following bin centers -40, -20, -5, 0, 5, 20, and 40. We calculated the probability of a rightward choice for each bin. For the statistical comparison, we performed a 2x7 mixed ANOVA with stroke vs. healthy as the between-subject factor ('group') and percent rightward choice for click difference as the within-subject factor ('evidence'). The ANOVA showed a main effect of evidence [ $F(2.65, 29.20) = 89.73$   $p < 0.001$ ], meaning more frequent rightward choices when there were more clicks on the right. More importantly, there was a significant interaction between group and evidence [ $F(2.65, 29.20) = 17.93$   $p < 0.001$ ] meaning that patients with cortical lesions and healthy controls dealt with clicks difference in a different manner. As a follow up, we ran two-sample t-tests comparing patients to healthy controls with regard to percent rightward choice

for each bin. For all bins with more clicks towards the left, the patients showed a statistically significant rightward ipsilesional bias compared to age-matched healthy controls  $p < 0.05$  (**Figure 5.3.8**).

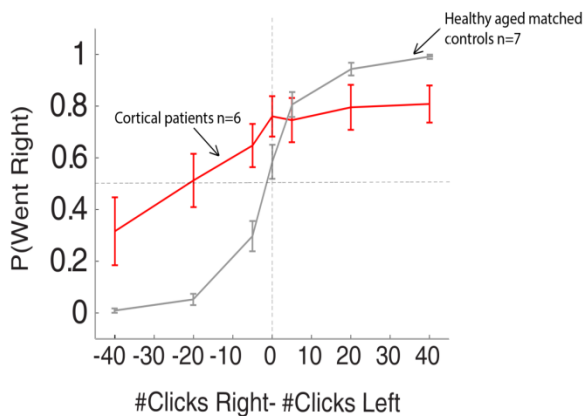


Figure 5.3.8. **Auditory group analysis.** Mean probability of choosing "right" as a function of clicks difference (right-left) showing patients with cortical lesions with an ipsilesional rightward bias for stimuli that had larger number of clicks on the left side compared to controls. Error bars are SEM across subjects. Patient SJ was excluded from analysis because of a primary auditory sensory deficit.

### ***Voxel-based lesion-symptom mapping (VLSM)***

It is challenging to establish a relationship between a lesion and cognitive processes. Lesion studies usually group patients either by lesion location or by behavior using cut-off estimates (Chao & Knight, 1998). However, such approaches have their drawbacks possibly resulting in a loss of information regarding behavior or lesion role (Bates et al., 2003). VLSM overcomes such obstacles by using continuous estimates of behavioral parameters, and benefits from all lesions data to investigate the relation of the lesion to behavior in a voxel-by-voxel manner (Bates et al., 2003; Rorden et al., 2007). Results from the permutation tests showed that lesions affecting voxels in the parietal cortex led to slope changes in the auditory modality (**Figure 5.3.9**). Moreover, it showed the effect of lesions in frontal temporal and parietal voxels leading to

ipsilesional choice bias in the auditory modality (**Figure 5.3.10**). We did not run the VLSM on the visual task due to an insufficient number of patients without primary visual sensory deficit.

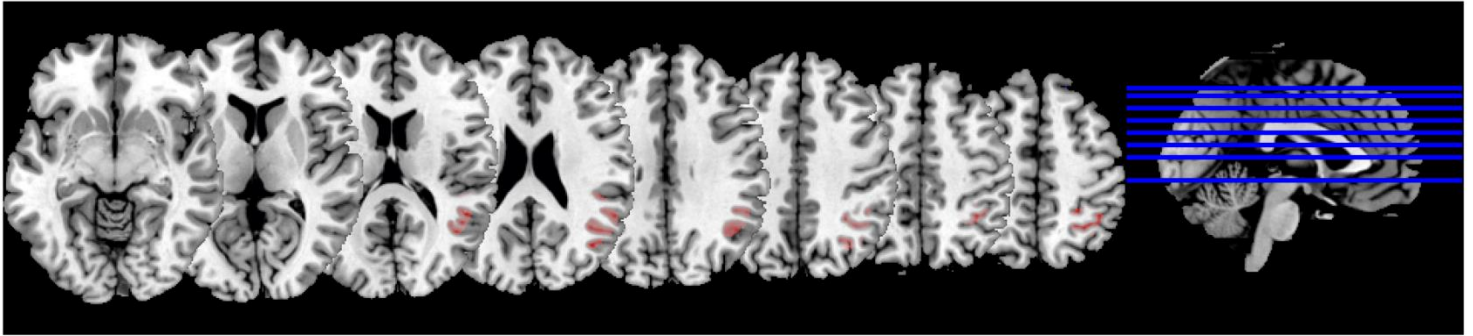


Figure 5.3.9. **Colorized depictions of results of permutation tests using Brunner Munzel (BM) rank statistics evaluating effect of patient lesion on slope of each patient on a voxel-by-voxel basis.** Lesion affecting voxels in right posterior parietal cortex lead to significant decrease in auditory task performance as evaluated by slope. We predicted a decrease in performance in the presence of a parietal or frontal lesion based on fMRI findings.

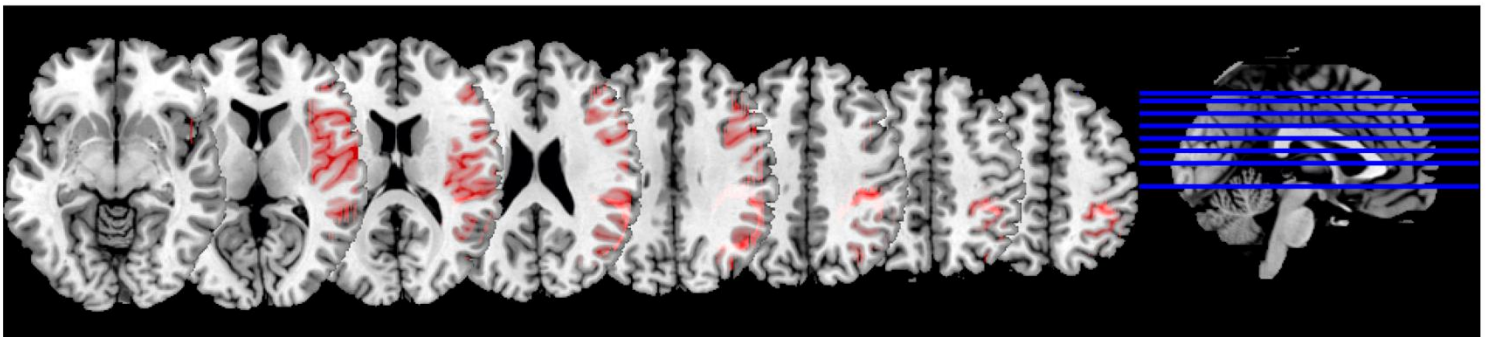


Figure 5.3.10. **Colorized depictions of results of permutation tests using Brunner Munzel (BM) rank statistics evaluating effect of patient lesion on bias of each patient on a voxel-by-voxel basis.** Lesions affecting voxels in right frontal, temporal, and parietal cortices right posterior parietal cortex led to a significant rightward choice bias in the auditory task. The VLSM results are consistent with fMRI predictions proposing a role of the superior temporal gyrus in auditory accumulation. However, fMRI did not predict a role of parietal and frontal regions in sensory evidence accumulation.

## **Summary of results**

In summary, results from the VLSM analysis suggest a causal role of the parietal cortex in auditory task performance as predicted by the fMRI results. However, due to the limited number of patients who were included in the final analysis, we approach our findings in this chapter carefully and avoid strong conclusions based on the patients' lesions.

## **Discussion**

In this study, we examined the causal contribution of right-sided cortical and subcortical lesions on auditory and visual perceptual decision-making accumulator tasks. We derived fMRI-based predictions of the effect of lesions in sensory cortices and parietal cortices on auditory and visual perceptual decision-making. We tested patients with lesions affecting cortical and subcortical structures in the right brain hemisphere. We investigated effect of lesions in single patients who managed to perform both the auditory and visual tasks and had no primary auditory or visual sensory deficits. We focused on the auditory task and performed auditory group analysis and voxel-based lesion-symptom mapping analysis. Lesions in frontal temporal and parietal voxels led to an ipsilesional choice bias in the auditory task, and lesion in parietal cortex lead to auditory task performance decrease.



### *Discussion of single patients results in relation to fMRI predictions*

In first fMRI study, we found that the neural correlates of sensory evidence accumulation are modality-specific. The superior temporal signal correlated with auditory sensory evidence accumulation, while the occipital cortex signal correlated with visual sensory evidence accumulation. Thus, we hypothesized that a lesion affecting these accumulator regions would result in a modality-specific deficit, ipsilesional bias. In patient VH the lesion affected the right temporal gyrus and parietal cortex but not the visual cortex. Thus, based on fMRI predictions one would predict a bias in the auditory task but none in the visual task. Indeed, Patient VH showed an ipsilesional choice bias in the auditory task but none in the visual task. Moreover, the lesion also extended to frontal and parietal regions. Thus, one would expect his lesion to effect task performance, shown by a shallower slope in both modalities. VH only showed a performance decrease in the auditory task. It could be that his lesion affected a subset of neurons that are tuned more to auditory tasks in the frontal and parietal regions. However, since his lesion was not localized in a specific node it is hard to conclude the patient's data that the frontal and parietal regions play no role in sensory evidence accumulation in the auditory task. But, nonetheless, the single dissociation between the visual and auditory ipsilesional bias remains interesting.

On the other hand, the lesion in patient GB affected the visual and auditory accumulator regions, the parietal cortex, and frontal regions. One might therefore expect an ipsilesional bias in both modalities. GB did exhibit ipsilesional bias in both the visual and auditory tasks. Moreover, his lesion involved the parietal and frontal regions. As predicted by fMRI, he showed a performance decrease in both modalities. Nonetheless, since his lesion involved several brain regions it is hard to infer any dissociation from his data.

And, finally, patient CT had a lesion localized in the right caudate, and, based on fMRI predictions, we would expect there to be no change in ipsilesional bias or slope. The patient exhibited no ipsilesional bias for both modalities, but a decrease in performance for the auditory task. Her slight slope decrease might have been ambient external noise.

***Discussion of voxel-based lesion-symptom mapping for the auditory task in relation to fMRI predictions***

Based on the fMRI results we expected the effect of the lesion in the parietal region to cause slope changes indicating a performance decrease in both modalities. However, due to the large number of patients with primary visual sensory deficit we were only able to perform VLSM for the auditory task behavioral measures. Consistent with the fMRI predictions of a role of the parietal cortex in performance, the VLSM results showed that patients with lesions in voxels in the parietal cortex had a slope decrease in the auditory

modality. However, contrary to fMRI, VLSM did not indicate a role of frontal regions. This could be a false negative, due to the small number of patients. Moreover, VLSM showed that a lesion involving the superior temporal gyrus would lead to an ipsilesional choice bias, consistent with the fMRI prediction that a lesion in the auditory accumulator region, i.e. the superior temporal gyrus, would cause an ipsilesional bias. On the other hand, VLSM showed that a lesion in parietal and frontal regions will also result in an ipsilesional bias, and that this was not predicted by fMRI. Since the fMRI signal has a low spatial resolution it is possible that the fMRI signal blurred the fine-grained tuning of neurons at a higher cortical level.

### **Limitation**

The major limitation was the small number of patients in the final analysis. We tested 18 patients, and only nine were included in the end (ref. Methods for details on excluded patients). Another limitation was the presence of primary sensory deficit. Of the nine patients, five had a primary sensory visual deficit, and one had a primary sensory auditory deficit. It is hypothetically possible to fit behavioral data of patients to quantitative descriptive models, and correlate specific parameters to patient lesions and performance. However, the small number of data points from each patient hindered us from fitting the data to such a high-dimensional descriptive model. As such, we benefited from the fMRI findings of previous experiments to provide hints as to what to expect from the

lesions. To investigate fMRI driven predictions, we applied VLSM in the study of the effect of lesions on behavioral parameters on a voxel-by-voxel basis. Nevertheless, due the small number of patients in the final VLSM analysis we refrained from drawing strong inferences regarding the lesion results. As such, we approach the results of this chapter carefully and abstain from drawing strong conclusions and inferences based on the lesions study.

## **Conclusion**

Voxel-based, lesion-symptom mapping is a promising analytical method to understand the effect of lesions on a voxel-by-voxel basis. Moreover, formulating fMRI-driven expectations on the role of specific brain nodes in the cognitive process could help in the understanding of individual patient's deficits. Consequently, such an approach would aid in devising individualized recovery predictions and rehabilitation plans. However, for such analyses to yield conclusive results it is important to have a sufficient number of patients with liberal inclusion criteria.

## **ACKNOWLEDGEMENTS**

This work was supported by the Hermann and Lilly Schilling Foundation, German Research Foundation (DFG) grants WI 4046/1-1 (M.W.). Prof. Dr. Thomas Crozier proof read and edited this manuscript.

## **Contributions**

Ahmad M. Nazzal (A.N.), Melanie Wilke (M.W.), and Carsten Schmidt-Samoa (C.S.) designed the study and interpreted the results. A.N wrote the paper. Manfred Holzgraefe (M.H), Gerhard Wiebold (G.W.), Jonas Koch (J.K.), C.S., and A.N. supervised and/or performed neurophysiological and neuropsychological examinations of the patients. A.N planned, performed and supervised behavioral data collection from the patients and age-matched healthy controls. Mathias Bähr (M.B), and Kai Kallenberg (K.K.) gathered imaging data of patients acquired in other medical centers other than Göttingen. A.N programmed, performed and analyzed behavioral and imaging data. M.W and C.S. provided corrections to the paper. A.N prepared all figures.

## **6. General discussion**

In this manuscript, we explored the neural signatures of auditory and visual perceptual sensory evidence accumulation, confidence in the visual decision, and investigated the effect of cortical and subcortical lesions on auditory and visual spatial perceptual decision-making. In Chapter 1, we introduced a theoretical framework and important terminology, and reviewed the existing literature on perceptual decision-making. In Chapter 2, we reviewed definitions, measures, neuroimaging and animal literature on confidence in decision-making. In Chapter 3, we discussed visual and auditory spatial processing systems and introduced hemispatial neglect as a model for studying spatial perceptual decision-making. We concluded that little is known with regard to how auditory sensory evidence accumulates and leads to the formation of perceptual spatial decisions in the human brain. In Chapter 4, we stated the scope of the manuscript. In Chapter 5, we presented the research performed by ourselves that investigated the correlates of auditory and visual perceptual evidence and confidence in decision. In the first study, we showed that spatially specific sensory evidence accumulated in a modality-specific manner. We demonstrated the presence of visual sensory evidence accumulating signals in occipital regions, while auditory sensory evidence accumulating signals were seen in the superior temporal cortex. Moreover, we showed that activity in frontal and parietal regions is modulated by the level of sensory evidence in a spatially non-specific manner for both visual and auditory modalities; the signal in frontal and

parietal regions was stronger when the level of evidence was low in both modalities suggesting a role of frontal and parietal regions in secondary decision-making processes. In the second study, we were able to disentangle the neural correlates of sensory evidence accumulation from neural correlates of confidence in the decision. We showed that visual sensory evidence accumulates in the occipital cortex. In this study with a different group of subjects, we were able to replicate the major findings from the first study. In addition, we found that the middle frontal region signal fits the criteria proposed for localizing brain activity related to decision-monitoring. In the third study, we investigated the effect of various brain lesions on bias and slope estimates of the auditory and visual spatial perceptual decision-making tasks. We found inconclusive evidence of a causal role of the right parietal cortex in dealing with auditory task performance.

### ***6.1 How the studies are related to each other***

Across all studies, we used the same novel auditory and visual accumulator task. Stimuli were drawn from the same distribution and presented discretely over time and space, and were adjusted for the adaptation dynamics of each modality. Moreover, the participants in all studies gave their response with their right hand by pressing a button after a variable delay period. The reason for the delayed response was to isolate the perceptual component from the motor component, and to prevent participants from forming decision-making strategies. Using

comparable task designs consistently across the fMRI and the patient studies allowed us to formulate a data-driven hypothesis and to test it.

In the first study, we formed a hypothesis based on the results of earlier studies that the frontal and parietal cortex would contain the neural signature of sensory evidence accumulation for different sensory modalities. Interestingly, we found that spatially specific sensory evidence accumulated in a modality-specific manner, i.e. that visual evidence accumulated in the occipital cortex, and auditory evidence accumulated in the superior temporal gyrus. On the other hand, spatially non-specific sensory evidence modulated activity in the frontal and parietal regions with both visual and auditory modalities, i.e. when evidence level was low signal was stronger, suggesting a role of these regions in secondary decision processes such as dealing with task difficulty. Such frontal and parietal activity could be also be interpreted as related to confidence in the decision. Since confidence in the decision is, from a signal detection point of view, the absolute distance between sensory evidence and criterion. Our second study was focused on the visual task and investigated the possibility that frontal and parietal regions code for confidence in the decision. We showed that the signal of sensory evidence accumulation could be dissociated from the signal of decision-monitoring. We found neural correlates of visual sensory evidence accumulation in occipital regions while the neural correlates of decision-monitoring were seen in the middle frontal region. Our finding is consistent with previous neuroimaging and neuropsychology reports of a role of prefrontal



regions in confidence in the decision (ref. Chapter 2). From the first two fMRI studies, we derived an fMRI-driven hypothesis to predict the effect of lesions in specific brain regions. We implemented voxel-based lesion-symptom mapping to establish links between lesion and behavioral measures (Bates et al., 2003). VLSM results suggested a role of the right posterior parietal auditory task performance.

## ***6.2 Relation of our studies to the literature on perceptual decision-making***

We studied the literature on auditory and visual perceptual decision-making and will discuss here the relation of our studies published reports on animal and human perceptual decision-making.

### ***6.2.1 Relation to the literature on perceptual decision-making in rodents***

Our auditory task was inspired by a study by Brunton and co-workers (Brunton et al., 2013), who investigated the possibility that the rat could benefit from sensory information to form perceptual decisions using an accumulation strategy. They found that the rat did use an accumulation strategy to form its perceptual decisions. They also tested the auditory task in human subjects. Our behavioral results with the auditory task represent a successful replication of their results in human. We developed a visual task as a modification of their auditory task by using flickering stimuli instead of clicks. One major difference between our tasks and theirs was that we did not give our subjects any feedback or rewards. This is an important difference, since in their case their aim was to

compare rat behavior to human behavior. In our case, however, it was less important since we only studied performance in humans. Since our results were consistent with their human findings, it seems that offering a reward did not affect behavior. We did give our subjects a monetary compensation at the end of the session, but this did not depend on performance. Nevertheless, the auditory task we implemented in an fMRI environment is, to our knowledge, the first use of an accumulator auditory task in the fMRI. Moreover, we extended the task and added post-decision confidence rating as discussed in the second study. It was shown that rodents were able to opt-out, suggesting that rats are able to monitor their own performance (Kepecs et al., 2008). Interestingly, the rats were more certain when the task was easy and correct, and least certain when the task was incorrect and easy (Kepecs et al., 2008). However, rodents are not closely related to humans evolution-wise. Nevertheless, confidence behavior in our human subjects was similar to that in rats suggesting that confidence in the decision is a phenomenon conserved across species, which illustrates its importance for the survival of a species.

The greatest advantage of using rodents to elucidate neural mechanisms of perceptual decision-making is that rodents are very well suited for the use of cutting-edge breakthroughs in neural measurement and manipulation, such as optogenetics (Hanks & Summerfield, 2017). Several brain nodes in the rat brain, such as the rat posterior parietal cortex (PPC) and frontal orienting fields (FOF), have been shown to exhibit signal-dependent neural buildup during auditory

sensory evidence accumulation. These are homologs of the monkey posterior parietal cortex and frontal eye fields, respectively (Erich, 2015). Inactivation studies of the PPC have shown that it plays no role in sensory evidence accumulation in the rat (Erich, Bialek, & Brody, 2011). Optogenetic studies have shown that inactivation of FOF leads to bias in ipsilateral choices late in the accumulation process but not early on. This suggests more of a motor preparatory role of FOF (Hanks et al., 2015). Thus, it is still debatable which region is the accumulator. We are unaware of any study that recorded the activity of neurons in the sensory cortices while the rats performed such auditory accumulator tasks. We expect our data to motivate researchers using rodents as study animals, to explore the role of the sensory cortices in sensory evidence accumulation.

### ***6.2.2 Relation of studies to the literature on non-human primate perceptual decision-making***

The field of perceptual decision-making benefited from studies investigating the dynamics of decision formation in the monkey (Gold & Shadlen, 2007). Neural correlates of sensory evidence accumulation in the monkey were traditionally proposed to involve parietal and frontal regions (ref. Chapter 1). However, the reign of LIP has been recently challenged with advances in analytical methods and recording technologies (Hanks & Summerfield, 2017). In the literature involving primates, the most popular experimental paradigm is random dot

motion (RDM). In early studies, monkeys were trained to respond using eye movements (saccades) in the RDM. The neural correlates of evidence accumulation were proposed to involve the same oculomotor network encompassing FEF, LIP, SC. Such overlap between the correlates of sensory evidence accumulation and motor network raised concerns that evidence of accumulation neural correlates in the LIP perhaps rather reflected motor preparation. Therefore, later studies attempted to address the possibility that LIP has neural activity related to evidence accumulation regardless of the effector. De Lafuente and colleagues (2015) trained monkeys to perform the RDM task by responding using either with a saccade or a reach (de Lafuente, Jazayeri, & Shadlen, 2015). They recorded from the LIP area as well as from the medial intraparietal (MIP) area, which is considered to be the reach region and not part of the oculomotor system (Andersen & Cui, 2009). They showed that LIP accumulates evidence regardless of the effector modality, while MIP only accumulates for the reaching task. However, it is worth mentioning that they had also trained their monkeys on a saccade task earlier, so it is possible that even though the oculomotor system was not required for the reach trials, information still flowed to that system. Such activity could be interpreted to indicate that the monkeys were still planning saccades even though the desired output was a reaching movement consistent with the intentional framework of the decision-making process. Moreover, such activity could be interpreted as attention, i.e. the monkey was paying attention to a spatial location (Li & Krishnamurthy,

2015). One limitation is the long time required to train a monkey to perform a task. Such long training phases will eventually lead to changes in the network underlying the cognitive processes related to decision-making, such as evidence accumulation. Indeed, it was shown that the training history has a strong effect on the neural responses of the LIP (Law & Gold, 2008). Recent literature examining the causal contribution of LIP in perceptual decision-making tasks found that microstimulation of LIP leads to choice and reaction time biases in an oculomotor decision-making task (Hanks et al., 2006), while unilateral pharmacological inactivation eliminating activity in the LIP had little effect on performance (Katz et al., 2016). Interestingly, reports consistently showed that LIP inactivation resulted in an ipsilesional bias in free saccadic choices (Wardak, Olivier, & Duhamel, 2002; Wilke, Kagan, & Andersen, 2012). Thus recent findings challenge the propositions that LIP has a role in evidence accumulation. They rather suggest its involvement in secondary decision-making processes. Our findings are in line with recent reports which suggest that posterior parietal regions, specifically the inferior parietal lobule, play no role in sensory evidence accumulation, but that the inferior parietal lobule does play a role in secondary decision-making processes.

### ***6.2.3 Relation of studies to literature on human neuroimaging perceptual decision-making***

There is no consensus in the neuroimaging literature whether there are brain regions that are involved in accumulation of sensory evidence regardless of sensory modality (Forstmann., 2016). This study provided a direct answer in this debate. We show that sensory evidence accumulates in modality-specific sensory cortices. Our data is consistent with recent reports suggesting a role of sensory cortices in core decision-making processes such as sensory evidence accumulation, and a role of frontal and parietal regions in secondary decision-making processes (Christophel., 2012; Hebart., 2014; Philiastides & Sajda, 2007). Previous studies have shown that the auditory cortex plays a role in the formation of perceptual decisions (Binder et al., 2004). However, the specific role of the auditory cortex in sensory evidence accumulation had not been explored before this current study. Our study showed that signals in auditory cortex reflect core decision-making processes such as auditory sensory evidence accumulation. In the confidence study, our data agrees with consistent neuroimaging and neuropsychological reports which suggest that the prefrontal cortex plays a role in coding confidence in the decision (Fleming & Frith, 2014). Recent efforts to disentangle the neural correlates of decision from those of confidence in the decision gave different results based on different assumptions as discussed in Chapter 5.2. Our results are consistent with propositions that

confidence emerges as a property of the decision-making network; highly correlated yet localized in different regions of the brain.

### ***6.3 Dealing with the crisis of reproducibility and interpretability***

In recent years, concerns were raised regarding the validity of most published research (Ioannidis, 2005). Several factors could render the findings of seminal studies irreproducible, and the results could have been biased towards finding a true positive. Factors leading to a high incidence of false positives, thereby contributing to the crisis of reproducibility are: small sample size, low prior probability of the effect being true, the large number of statistical tests performed, flexibility in task design analysis, financial and prestige interests in a specific finding, and competition to publish in competitive fields (Ioannidis, 2005). Functional magnetic resonance imaging (fMRI) revolutionized neuroscience, as it made it possible to localize brain signatures of complex cognitive processes in healthy human in a non-invasive way (Logothetis, 2008). Recently, long-time acknowledged concerns regarding the validity of analysis methods in fMRI studies have been raised (Eklund, Nichols, & Knutsson, 2016). Several issues render the field of fMRI studies particularly susceptible to the aforementioned factors contributing to high rates of false positives among which are, i.e. small sample sizes. Another factor is the vast number of statistical comparisons, which leads to a large number of false positives. To manage such large numbers of statistical tests, techniques such as multiple comparison analysis have been proposed. However, it was shown that even one of the most

common approaches for multiple comparison correction, namely family-wise error, could still yield invalid cluster inferences because certain analysis packages used functions that did not follow an assumed Gaussian distribution (Eklund et al., 2016). One other reason for large number of false positives in fMRI is p-hacking (kunda, 1990), which means that the experimenters would simply increase the sample size until the hypothesis was confirmed. Another factor contributing to false positives in fMRI studies is circularity or "double dipping"; voxel selection bias and running statistical tests on already significant voxels. However, the brain is a complex organ, and knowledge about its function is a result of techniques that differ in temporal and spatial resolution (Weber & Thompson-Schill, 2010). Neuroimaging provides a rich amount of data, and therefore, careful task design, proper methods for analysis, and mining databases to establish valid reverse inference is important (Poldrack, 2006).

Fortunately, several solutions have been proposed to investigate reproducibility and improve inference. Among these solutions is replication of findings in independent samples, use of orthogonal contrasts for voxel selection to avoid selection bias, and overcome "double dipping" and the issue of circularity, and usage of data splitting. Lately, an increasing number of studies have applied meta-analysis techniques to improve their inference reliability and validate their results (Wager, Lindquist, & Kaplan, 2007). Meta-analysis can increase the likelihood of true positives and help generalize findings across studies. It relies on summary statistics across studies based on reported values such as the



coordinates of specific contrasts. Techniques such as multi-level kernel density analysis help confirm that the consistency of findings across studies exceeds chance level (Wager u. a., 2007).

In our studies, we dealt with those concerns in the following manner: (1) We managed to reproduce major findings in different samples of subjects. We showed that sensory evidence accumulates in modality-specific sensory cortices in three separate groups of participants. (2) We used ROIs from the first study to investigate correlations with evidence in the second study and found a significant correlation (details in Chapter 5.2). (3) Moreover, we used meta-analysis techniques to confirm the consistency of findings across studies. We applied multi-level kernel density analysis to the difficulty map from three different samples (Wager et al., 2007). We found that, across studies, the frontal and parietal regions were more active when the task was more difficult (**Figure 6.1A Table 6.1**).

**Table 6.1 Coordinates based the meta-analysis of contrast hard > easy across empirical studies**

| Study     | Coordinates |     |     | Coordinate System | Number of subjects | Contrast   | Fixed/Random effects |
|-----------|-------------|-----|-----|-------------------|--------------------|------------|----------------------|
|           | x           | y   | z   |                   |                    |            |                      |
| Pilot     | -3          | 5   | 55  | Tal               | 17                 | Hard >Easy | Random               |
| Pilot     | 27          | -1  | 40  | Tal               | 17                 | Hard >Easy | Random               |
| Pilot     | 24          | -49 | 37  | Tal               | 17                 | Hard >Easy | Random               |
| Pilot     | 36          | -61 | -29 | Tal               | 17                 | Hard >Easy | Random               |
| Pilot     | -30         | -7  | 49  | Tal               | 17                 | Hard >Easy | Random               |
| 1st Study | -6          | 11  | 43  | Tal               | 15                 | Hard >Easy | Random               |
| 1st Study | 42          | 8   | 25  | Tal               | 15                 | Hard >Easy | Random               |
| 1st Study | 36          | -1  | 58  | Tal               | 15                 | Hard >Easy | Random               |
| 1st Study | 45          | -28 | 61  | Tal               | 15                 | Hard >Easy | Random               |
| 1st Study | 3           | 17  | 37  | Tal               | 15                 | Hard >Easy | Random               |
| 1st Study | 39          | -1  | 40  | Tal               | 15                 | Hard >Easy | Random               |
| 1st Study | -24         | -46 | 43  | Tal               | 15                 | Hard >Easy | Random               |
| 1st Study | 24          | -37 | 46  | Tal               | 15                 | Hard >Easy | Random               |
| 2nd Study | 0           | 14  | 46  | Tal               | 12                 | Hard >Easy | Random               |
| 2nd Study | -36         | -49 | 37  | Tal               | 12                 | Hard >Easy | Random               |
| 2nd Study | 48          | 8   | 16  | Tal               | 12                 | Hard >Easy | Random               |

To improve inference, we used a database of 10,000 neuroimaging studies (neurosynth.org) and generated a difficulty map based on the reverse inference from 391 studies (**Figure 6.1B**). From the Neurosynth difficulty term reverse inference map we demonstrated that the medial frontal, prefrontal, parietal, and insula are regions consistently reported in the literature in relation to difficulty.

Therefore, we felt it safe to conclude that regions consistently reported in our studies for the hard > easy contrast reflect dealings with task difficulty.

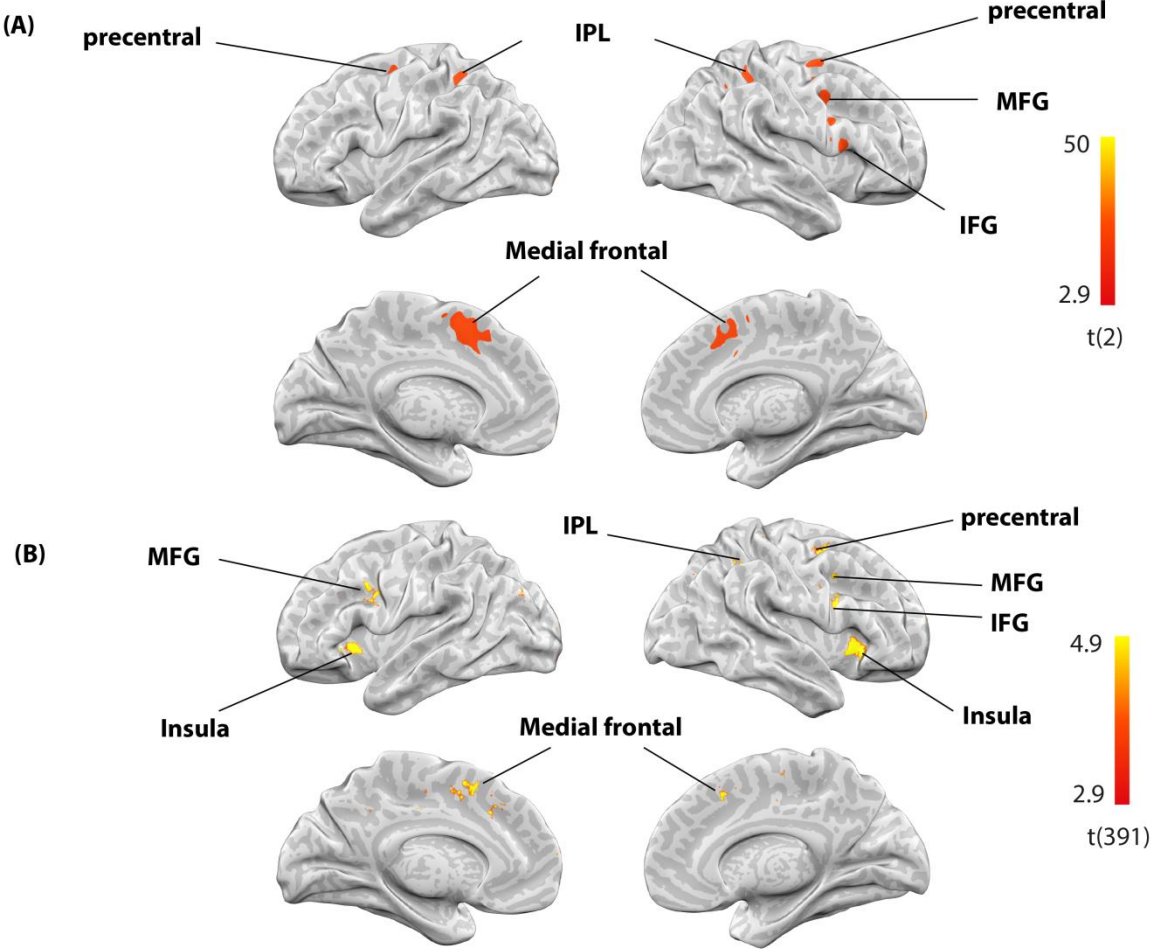


Figure 6.1. **Meta-analysis to prove reproducibly and improve inference.** (A) Results of multi-level kernel density analysis of difficulty contrast (difficult > easy) showing brain regions that are consistently active when the task was difficult in three different group samples. Regions active are consistent with brain regions of the Neurosynth difficulty term map. (B) The brain map of difficulty term from 391 studies shows an effect of task difficulty in medial frontal, precentral, middle frontal gyrus (MFG), inferior frontal gyrus (IFG), insula, and inferior parietal lobule (IPL).

#### ***6.4 General limitations***

fMRI is beneficial for imaging whole brains and investigating healthy human participants in a non-invasive manner. However, it has a limited spatial and temporal resolution. Therefore, it was not possible to regress the fMRI signal to capture the minute dynamics of the accumulation process and benefit from the discreteness of stimuli over time and space. One way to overcome this issue is to take advantage of simultaneous EEG-fMRI recordings.

With regard to the model, due to the small number of data points per subject inside the scanner and small amount of data for each patient it was not possible to fit a separate model for each individual patient or participant. However, since healthy participants had similar psychometric curves, we fitted one model for the data from all participants inside the scanner. Moreover, due to the low temporal resolution of the fMRI, the modeled evidence represented the total evidence accumulated by the end of each trial. It was consequently highly correlated to the stimulus difference between the right and left sides. As such, it is possible to obtain similar accumulator brain maps without use of the modeling part by simply using stimuli difference to parametrically modulate the predictor of interest. However, the beauty of the model is that it contains several parameters that signify various decision-making strategies. Fitting the model to our data from inside the scanner revealed that the participants used an accumulation decision-making strategy in both visual and auditory task.

## ***6.5 Closing remarks and outlook***

There have been exciting breakthroughs in neuroscience in recent years. However, translating those breakthroughs into practical clinical applications takes a long time and great patience. In this manuscript we provided a fresh view of how the brain utilizes sensory information to form perceptual decisions, especially in the auditory domain. We predict that our data will motivate electrophysiologists in the field of perceptual decision-making to record from the regions of interests that we were able to localize in our studies.

It remains interesting to understand the interactions between the brain regions identified in our study as an exciting future prospect. For this reason, it is possible to use dynamic causal modeling and effective connectivity methods to test interactions between frontal, parietal, and sensory regions.

In general, a better understanding of the neural networks underlying complex cognitive behaviors, such as decision-making, will help to devise regimens for the therapy of neuropsychological patients, and perhaps help in the advancement of artificial intelligence research.

## 7. Appendix

### 7.1 Figures list

1. Figure 1.1. Outline for studying perceptual decisions
2. Figure 1.2. Taxonomy of processes in perceptual decision-making
3. Figure 1.3. Tasks in the study of perceptual decision-making
4. Figure 1.4. Signal detection theory framework
5. Figure 1.5. Sequential models
6. Figure 1.6. Architecture of the integrate-and-fire attractor model decision network
7. Figure 1.7. Schematic illustration of the neuronal activity and BOLD signal relationship
8. Figure 1.8. BOLD signal related to difficulty
9. Figure 1.9. Schematic illustration showing an overview of brain regions involved in perceptual decision-making as identified in seminal studies
10. Figure 2.1. The architecture of integrate-and-fire attractor confidence in the decision network.
11. Figure 5.1.1. Behavior of visual and auditory accumulator tasks
12. Figure 5.1.2. Main effect of modality
13. Figure 5.1.3. Main effect of task difficulty
14. Figure 5.1.4. Main effect of space
15. Figure 5.1.5. Signal of visual sensory accumulation in the occipital cortex
16. Figure 5.1.6. Signal of auditory sensory evidence accumulation in the superior temporal gyrus (STG)
17. Figure 5.1.7. Frontal and parietal cortices show spatial non-specific modulation by level of sensory evidence regardless of modality
18. Supplementary Figure 5.1.1. Brain regions showing effect of difficulty (easy > hard).
19. Figure 5.2.1. Visual perceptual task performance
20. Figure 5.2.2. Spatially specific accumulator regions occipital
21. Figure 5.2.3. Spatially specific accumulator regions prefrontal
22. Figure 5.2.4. Non-spatially specific accumulator regions
23. Figure 5.2.4. Accuracy map
24. Figure 5.2.6. Candidate regions of neural correlates of decision-monitoring
25. Supplementary Figure 5.2.1 Accuracy map for delay and motor response periods.
26. Figure 5.3.1. Schematic illustration of fMRI-based predictions of the effect of lesions on auditory and visual perceptual decision-making
27. Figure 5.3.2. Visual and auditory accumulator tasks
28. Figure 5.3.3. Probability maps of lesions
29. Figure 5.3.4. Psychometric curves of patients behavior

30. Figure 5.3.5. Patient VH lesion and behavior in auditory and visual tasks
31. Figure 5.3.6. Patient GB: lesion and behavior in auditory and visual tasks
32. Figure 5.3.7. Patient CT: lesion and behavior in auditory and visual tasks
33. Figure 5.3.8. Auditory group analysis
34. Figure 5.3.9. Colorized depictions of results of permutation tests using Brunner Munzel (BM) rank statistics evaluating effect of patient lesion on slope of each patient on a voxel-by-voxel basis
35. Figure 5.3.10. Colorized depictions of results of permutation tests using Brunner Munzel (BM) rank statistics evaluating effect of patient lesion on bias of each patient on a voxel-by-voxel basis
36. Figure 6.1. Meta-analysis to prove reproducibly and improve inference

## 7.2 Tables list

1. Table 1.1 Neuroimaging studies of sensory evidence accumulation
2. Table 5.1.1. Brain regions showing main effect of task difficulty
3. Table 5.1.2 Three-way interaction (difficulty, space, modality)
4. Table 5.1.3 Visual accumulator regions
5. Table 5.1.4 Auditory accumulator regions
6. Supplementary Table 5.1.1 Model parameters for most relevant parameters to study decision-making strategy based on model fits for each modality
7. Supplementary Table 5.1.2 Modality effect
8. Supplementary Table 5.1.3 Overlap between modalities
9. Supplementary Table 5.1.4 Main effect of space
10. Table 5.2.1 Spatially specific accumulator regions
11. Table 5.2.2 Non-spatially specific accumulator regions (i.e. difficulty)
12. Table 5.2.3 Decision monitoring regions
13. Supplementary Table 5.2.1. Model parameters for the most relevant parameters in the study of decision-making strategy based on model fits.
14. Table 5.3.1 Demographic data
15. Table 5.3.2 Behavioral measures results of individual patients
16. Table 6.1 Coordinates based the meta-analysis of contrast hard > easy across empirical studies

## 8. References

- Adams, R. A., Stephan, K. E., Brown, H. R., Frith, C. D., & Friston, K. J. (2013). The computational anatomy of psychosis. *Frontiers in psychiatry*, *4*(May), 47.  
<https://doi.org/10.3389/fpsy.2013.00047>
- Andersen, R. A., Andersen, K. N., Hwang, E. J., & Hauschild, M. (2014). Optic ataxia: from Balint's syndrome to the parietal reach region. *Neuron*, *81*(5), 967–83.  
<https://doi.org/10.1016/j.neuron.2014.02.025>
- Andersen, R. A., Asanuma, C., Essick, G., & Siegel, R. M. (1990). Corticocortical connections of anatomically and physiologically defined subdivisions within the inferior parietal lobule. *Journal of Comparative Neurology*, *296*(1), 65–113.
- Andersen, R. A., & Cui, H. (2009). Intention, action planning, and decision making in parietal-frontal circuits. *Neuron*, *63*(5), 568–83.
- Arnott. (2004). Assessing the auditory dual-pathway model in humans. *NeuroImage*, *22*(1), 401–408.  
<https://doi.org/10.1016/j.neuroimage.2004.01.014>
- Arnott. (2005). The Functional Organization of Auditory Working Memory as Revealed by fMRI. *Journal of Cognitive Neuroscience*, *17*(5), 819–831.  
<https://doi.org/10.1162/0898929053747612>
- Aron, A. R., Robbins, T. W., & Poldrack, R. A. (2004). Inhibition and the right inferior frontal cortex. *Trends in Cognitive Sciences*, *8*(4), 170–177. <https://doi.org/10.1016/j.tics.2004.02.010>
- Bahrami, B., Olsen, K., Latham, P. E., Roepstorff, A., Rees, G., & Frith, C. D. (2010). Optimally Interacting Minds. *Science*, *329*(5995), 1081. <https://doi.org/10.1126/science.1185718>
- Barrett. (2010). Attention in neglect and extinction: Assessing the degree of correspondence between visual and auditory impairments using matched tasks. *Journal of Clinical and Experimental Neuropsychology*, *32*(1), 71–80. <https://doi.org/10.1080/13803390902838058>
- Bartolomeo, P., Thiebaut De Schotten, M., & Doricchi, F. (2007). Left unilateral neglect as a disconnection syndrome. *Cerebral Cortex*, *17*(11), 2479–2490.  
<https://doi.org/10.1093/cercor/bhl181>



- Bates, E., Wilson, S. M., Saygin, A. P., Dick, F., Sereno, M. I., Knight, R. T., & Dronkers, N. F. (2003). Voxel-based lesion–symptom mapping. *Nature Neuroscience*, 6(5), 448–450. <https://doi.org/10.1038/nm1050>
- Beran, M. J., Smith, J. D., Coutinho, M. V. C., Couchman, J. J., & Boomer, J. (2009). The Psychological Organization of “Uncertainty” Responses and “Middle” Responses: A Dissociation in Capuchin Monkeys (*Cebus apella*). *Journal of experimental psychology. Animal behavior processes*, 35(3), 371–381. <https://doi.org/10.1037/a0014626>
- Binder. (2004). Neural correlates of sensory and decision processes in auditory object identification. *Nature Neuroscience*, 7(3), 295–301. <https://doi.org/10.1038/nm1198>
- Binder, J. R., Liebenthal, E., Possing, E. T., Medler, D. A., & Ward, B. D. (2004). Neural correlates of sensory and decision processes in auditory object identification. *Nature Neuroscience*, 7(3), 295–301. <https://doi.org/10.1038/nm1198>
- Bisiach, E., Cornacchia, L., Sterzi, R., & Vallar, G. (1984). Disorders of perceived auditory lateralization after lesions of the right hemisphere. *Brain : a journal of neurology*, 107 ( Pt 1, 37–52.
- Bray, S., Arnold, A. E. G. F., Iaria, G., & MacQueen, G. (2013). Structural connectivity of visuotopic intraparietal sulcus. *NeuroImage*, 82, 137–145. <https://doi.org/10.1016/j.neuroimage.2013.05.080>
- Brunton. (2013). Rats and Humans Can Optimally Accumulate Evidence for Decision-Making. *Science*, 340(6128), 95–98. <https://doi.org/10.1126/science.1233912>
- Brunton, B. W., Botvinick, M. M., & Brody, C. D. (2013a). Rats and humans can optimally accumulate evidence for decision-making. *Science (New York, N.Y.)*, 340(6128), 95–8. <https://doi.org/10.1126/science.1233912>
- Brunton, B. W., Botvinick, M. M., & Brody, C. D. (2013b). Rats and humans can optimally accumulate evidence for decision-making. *Science (New York, N.Y.)*, 340(6128), 95–8. <https://doi.org/10.1126/science.1233912>

- Carter, C. S., Braver, T. S., Barch, D. M., Botvinik, M., D., N., & Cohen, J. D. (1998). Anterior cingulate cortex, error detection, and the online monitoring of performance. *Science*, 280(May), 747–749.
- Chao, L. L., & Knight, R. T. (1998). Contribution of human prefrontal cortex to delay performance. *Journal of cognitive neuroscience*, 10(2), 167–177. <https://doi.org/10.1162/089892998562636>
- Christophel, T. B., Hebart, M. N., & Haynes, J.-D. (2012). Decoding the Contents of Visual Short-Term Memory from Human Visual and Parietal Cortex. *The Journal of Neuroscience*, 32(38), 12983. <https://doi.org/10.1523/JNEUROSCI.0184-12.2012>
- Cisek, P. (2012). Making decisions through a distributed consensus. *Curr Opin Neurobiol*, 22(6), 927–36. <https://doi.org/10.1016/j.conb.2012.05.007>
- Clifford, C. W., Arabzadeh, E., & Harris, J. A. (2008). Getting technical about awareness. *Trends in cognitive sciences*, 12(2), 54–58.
- Corbetta, M., Kincade, M. J., Lewis, C., Snyder, A. Z., & Sapir, A. (2005). Neural basis and recovery of spatial attention deficits in spatial neglect. *Nature neuroscience*, 8(11), 1603–10. <https://doi.org/10.1038/nn1574>
- Corbetta, M., & Shulman, G. L. (2011). *Spatial neglect and attention networks. Annual review of neuroscience* (Bd. 34). <https://doi.org/10.1146/annurev-neuro-061010-113731>
- de Gardelle, V., & Mamassian, P. (2014). Does Confidence Use a Common Currency Across Two Visual Tasks? *Psychological Science*, 25(6), 1286–1288. <https://doi.org/10.1177/0956797614528956>
- de Lafuente, V., Jazayeri, M., & Shadlen, M. N. (2015). Representation of Accumulating Evidence for a Decision in Two Parietal Areas. *The Journal of Neuroscience*, 35(10), 4306. <https://doi.org/10.1523/JNEUROSCI.2451-14.2015>
- Deco, G., & Rolls, E. T. (2006). Decision-making and Weber’s law: a neurophysiological model. *European Journal of Neuroscience*, 24(3), 901–916. <https://doi.org/10.1111/j.1460-9568.2006.04940.x>

- Dienes. (1995). Unconscious knowledge of artificial grammars is applied strategically. *Journal of Experimental Psychology: Learning, Memory, and Cognition*. <https://doi.org/10.1037/0278-7393.21.5.1322>
- Ding, L., & Gold, J. I. (2012). Separate, Causal Roles of the Caudate in Saccadic Choice and Execution in a Perceptual Decision Task. *Neuron*, *75*(5), 865–874. <https://doi.org/10.1016/j.neuron.2012.07.021>
- Driver, J., & Mattingley, J. B. (1998). Parietal neglect and visual awareness. *Nature neuroscience*, *1*(1), 17–22. <https://doi.org/10.1038/217>
- Dronkers, N. F. (1996). A new brain region for coordinating speech articulation. *Nature*, *384*(6605), 159–161. <https://doi.org/10.1038/384159a0>
- Düzel, E., Bunzeck, N., Guitart-Masip, M., Wittmann, B., Schott, B. H., & Tobler, P. N. (2009). Functional imaging of the human dopaminergic midbrain. *Trends in Neurosciences*, *32*(6), 321–328. <https://doi.org/10.1016/j.tins.2009.02.005>
- Eklund, A., Nichols, T. E., & Knutsson, H. (2016). Cluster failure: Why fMRI inferences for spatial extent have inflated false-positive rates. *Proceedings of the National Academy of Sciences*, *201602413*. <https://doi.org/10.1073/pnas.1602413113>
- Erlich. (2015). Distinct effects of prefrontal and parietal cortex inactivations on an accumulation of evidence task in the rat. *eLife*, *4*, 1–28. <https://doi.org/10.7554/eLife.05457>
- Erlich, J. C., Bialek, M., & Brody, C. D. (2011). A cortical substrate for memory-guided orienting in the rat. *Neuron*, *72*(2), 330–43. <https://doi.org/10.1016/j.neuron.2011.07.010>
- Feldman, H., & Friston, K. J. (2010a). Attention, uncertainty, and free-energy. *Frontiers in human neuroscience*, *4*(December), 215. <https://doi.org/10.3389/fnhum.2010.00215>
- Feldman, H., & Friston, K. J. (2010b). Attention, Uncertainty, and Free-Energy. *Frontiers in Human Neuroscience*, *4*(December), 1–23. <https://doi.org/10.3389/fnhum.2010.00215>
- Fels, M., & Geissner, E. (1996). Neglect-Test (NET).
- Filimon, F. et al. (2013). How Embodied Is Perceptual Decision Making? Evidence for Separate Processing of Perceptual and Motor Decisions. *Journal of Neuroscience*, *33*(5), 2121–2136. <https://doi.org/10.1523/JNEUROSCI.2334-12.2013>

- Fiorillo, C. D., Tobler, P. N., & Schultz, W. (2003). Discrete Coding of Reward Dopamine Neurons. *Science*, 299(March), 1898–1902. <https://doi.org/10.1126/science.1077349>
- Fleming. (2014). How to measure metacognition. *Frontiers in Human Neuroscience*, 8(July), 1–9. <https://doi.org/10.3389/fnhum.2014.00443>
- Fleming, S. M., & Dolan, R. J. (2012). Review. Neural basis of metacognition. *Philosophical Transactions of the Royal Society B Biological Sciences*, 367, 1338–1349. <https://doi.org/10.1098/rstb.2011.0417>
- Fleming, S. M., & Dolan, R. J. (2014). The neural basis of metacognitive ability. *The Cognitive Neuroscience of Metacognition*, 9783642451, 245–265. [https://doi.org/10.1007/978-3-642-45190-4\\_11](https://doi.org/10.1007/978-3-642-45190-4_11)
- Fleming, S. M., & Frith, C. D. (2014). The cognitive neuroscience of metacognition. *The Cognitive Neuroscience of Metacognition*, 9783642451(December 2013), 1–407. <https://doi.org/10.1007/978-3-642-45190-4>
- Forstmann, B. U., Ratcliff, R., & Wagenmakers, E.-J. (2016). Sequential Sampling Models in Cognitive Neuroscience: Advantages, Applications, and Extensions. *Annual review of psychology*, 67, 641–66. <https://doi.org/10.1146/annurev-psych-122414-033645>
- Forstmann, B. U., Ratcliff, R., & Wagenmakers, E.-J. (2016). Sequential Sampling Models in Cognitive Neuroscience: Advantages, Applications, and Extensions. *Annual review of psychology*, 67, 641–66. <https://doi.org/10.1146/annurev-psych-122414-033645>
- Forstmann, B. U., Ratcliff, R., & Wagenmakers, E.-J. (2016). Sequential Sampling Models in Cognitive Neuroscience: Advantages, Applications, and Extensions. *Annual review of psychology*, 67, 641–66. <https://doi.org/10.1146/annurev-psych-122414-033645>
- Frank, M. J. (2005). Dynamic dopamine modulation in the basal ganglia: a neurocomputational account of cognitive deficits in medicated and nonmedicated Parkinsonism. *Journal of cognitive neuroscience*, 17(1), 51–72. <https://doi.org/10.1162/0898929052880093>
- Friston, K. J., Shiner, T., FitzGerald, T., Galea, J. M., Adams, R., Brown, H., ... Bestmann, S. (2012). Dopamine, affordance and active inference. *PLoS Computational Biology*, 8(1). <https://doi.org/10.1371/journal.pcbi.1002327>

- Fritz, J. B., Elhilali, M., David, S. V., & Shamma, S. A. (2007). Auditory attention - focusing the searchlight on sound. *Current Opinion in Neurobiology*, *17*(4), 437–455.  
<https://doi.org/10.1016/j.conb.2007.07.011>
- Gardelle, D., Corre, L., & Mamassian. (2016). Confidence as a common currency between vision and audition. *PLoS ONE*, *11*(1). <https://doi.org/10.1371/journal.pone.0147901>
- Gazzaniga, M. S. (2005). Forty-five years of split-brain research and still going strong. *Nature reviews. Neuroscience*, *6*(8), 653–659. <https://doi.org/10.1038/nrn1723>
- Gehring, W. J., & Fencsik, D. E. (2001). Functions of the medial frontal cortex in the processing of conflict and errors. *The Journal of neuroscience : the official journal of the Society for Neuroscience*, *21*(23), 9430–9437.
- Gherman, S., & Philiastides, M. G. (2015). Neural representations of confidence emerge from the process of decision formation during perceptual choices. *NeuroImage*, *106*, 134–143.  
<https://doi.org/10.1016/j.neuroimage.2014.11.036>
- Gnadt, J. W., & Andersen, R. A. (1988). Memory related motor planning activity in posterior parietal cortex of macaque. *Experimental brain research*, *70*(1), 216–220.
- Gokhale, S., Lahoti, S., & Caplan, L. R. (2013). The neglected neglect: auditory neglect. *JAMA neurology*, *70*(8), 1065–9. <https://doi.org/10.1001/jamaneurol.2013.155>
- Gold, J. I., & Shadlen, M. N. (2007). The neural basis of decision making. *Annu Rev Neurosci*, *30*, 535–574. <https://doi.org/10.1146/annurev.neuro.29.051605.113038>
- Goodale, M. A., & Milner, A. D. (1992). 1 2 Separate Visual Pathways for Perception and Action. *Essential Sources in the Scientific Study of Consciousness*, (I), 175.
- Green, & Swets. (1966). Signal detection theory and psychophysics. *Oxford, England: John Wiley Signal detection theory and psychophysics.*, xi, 455 pp.
- Griffiths. (1998). Right parietal cortex is involved in the perception of sound movement in humans. *Nat Neurosci*, *1*(1), 74–79. <https://doi.org/10.1038/276>
- Gutschalk, A. (2012). Comparison of auditory deficits associated with neglect and auditory cortex lesions. *Neuropsychologia*, *50*(5), 926–938.  
<https://doi.org/10.1016/j.neuropsychologia.2012.01.032>

- Hanes, D. P., & Schall, J. D. (1996). Neural Control of Voluntary Movement Initiation. *Science*, 274(5286), 427. <https://doi.org/10.1126/science.274.5286.427>
- Hanks, T. D., Ditterich, J., & Shadlen, M. N. (2006). Microstimulation of macaque area LIP affects decision-making in a motion discrimination task. *Nature neuroscience*, 9(5), 682–9. <https://doi.org/10.1038/nn1683>
- Hanks, T. D., Kopec, C. D., Brunton, B. W., Duan, C. A., Erlich, J. C., & Brody, C. D. (2015). Distinct relationships of parietal and prefrontal cortices to evidence accumulation. *Nature*, 520(7546), 220–223.
- Hanks, T. D., & Summerfield, C. (2017). Perceptual Decision Making in Rodents , Monkeys , and Humans. *Neuron*, 93(1), 15–31. <https://doi.org/10.1016/j.neuron.2016.12.003>
- Havlicek, M., Roebroeck, A., Friston, K., Gardumi, A., Ivanov, D., & Uludag, K. (2015). Physiologically informed dynamic causal modeling of fMRI data. *NeuroImage*, 122, 355–372. <https://doi.org/10.1016/j.neuroimage.2015.07.078>
- Heathcote, A., & Love, J. (2012). Linear Deterministic Accumulator Models of Simple Choice. *Frontiers in Psychology*, 3(August), 1–19. <https://doi.org/10.3389/fpsyg.2012.00292>
- Heathcote, Wagenmakers, & Brown. (2014). The falsifiability of actual decision-making models. *Psychological Review*, 121(4), 676–678. <https://doi.org/10.1037/a0037771>
- Hebart, M. (2014). On the Neuronal Systems Underlying Perceptual Decision-Making and Confidence in Humans Dissertation.
- Hebart, M. N., Donner, T. H., & Haynes, J.-D. (2012). Human visual and parietal cortex encode visual choices independent of motor plans. *NeuroImage*, 63(3), 1393–1403. <https://doi.org/10.1016/j.neuroimage.2012.08.027>
- Hebart, M. N., Schriever, Y., Donner, T. H., & Haynes, J.-D. (2014). The Relationship between Perceptual Decision Variables and Confidence in the Human Brain. *Cerebral Cortex*, (Dv), bhu181-. <https://doi.org/10.1093/cercor/bhu181>
- Hebscher, M., & Gilboa, A. (2015). A boost of confidence: The role of the ventromedial prefrontal cortex in memory, decision-making, and schemas. *Neuropsychologia*, 90, 46–58. <https://doi.org/10.1016/j.neuropsychologia.2016.05.003>

- Heeger, D. R. and D. J. (2012). NIH Public Access, *100*(2), 130–134.  
<https://doi.org/10.1016/j.pestbp.2011.02.012>.Investigations
- Heekeren. (2004). A general mechanism for perceptual decision-making in the human brain. *Nature*, *431*(7010), 859–862. <https://doi.org/10.1038/nature02966>
- Heekeren. (2008). The neural systems that mediate human perceptual decision making. *Nature Reviews Neuroscience*, *9*(6), 467–479. <https://doi.org/10.1038/nrn2374>
- Heereman, J., Walter, H., & Heekeren, H. R. (2015). A task-independent neural representation of subjective certainty in visual perception. *Frontiers in Human Neuroscience*, *9*(October), 1–12.  
<https://doi.org/10.3389/fnhum.2015.00551>
- Heilman. (1980). Right hemisphere dominance for attention: The mechanism underlying hemispheric asymmetries of inattention(neglect). *Neurology*. <https://doi.org/10.1213/00006123-198030030-00003>
- Heilman, & Valenstein. (1972). Auditory neglect in man. *Archives of Neurology*, *26*(1), 32–35.
- Hilgenstock, R., Weiss, T., & Witte, O. W. (2014). You'd Better Think Twice: Post-Decision Perceptual Confidence. *NeuroImage*, *99*, 323–331.  
<https://doi.org/10.1016/j.neuroimage.2014.05.049>
- Hillis, A. E. (2005). Anatomy of Spatial Attention: Insights from Perfusion Imaging and Hemispatial Neglect in Acute Stroke. *Journal of Neuroscience*, *25*(12), 3161–3167.  
<https://doi.org/10.1523/JNEUROSCI.4468-04.2005>
- Hillis, A. E., Wityk, R. J., Barker, P. B., Beauchamp, N. J., Gailloud, P., Murphy, K., ... Metter, E. J. (2002). Subcortical aphasia and neglect in acute stroke: the role of cortical hypoperfusion. *Brain : a journal of neurology*, *125*(Pt 5), 1094–1104. <https://doi.org/10.1093/brain/awf113>
- Ho, T., & Brown, S. (2009). Domain General Mechanisms of Perceptual Decision Making in Human Cortex, *29*(27), 8675–8687. <https://doi.org/10.1523/JNEUROSCI.5984-08.2009>.Domain
- Horwitz, G. D., & Newsome, W. T. (1999). Separate signals for target selection and movement specification in the superior colliculus. *Science (New York, N.Y.)*, *284*(5417), 1158–1161.  
<https://doi.org/10.1126/science.284.5417.1158>

- Hunt, L. T., Kolling, N., Soltani, A., Woolrich, M. W., Rushworth, M. F. S., & Behrens, T. E. J. (2012). Mechanisms underlying cortical activity during value-guided choice. *Nature Neuroscience*, *15*(3), 470–476. <https://doi.org/10.1038/nn.3017>
- Husain, M., & Kennard, C. (1996). Visual neglect associated with frontal lobe infarction. *Journal of neurology*, *243*, 652–657. <https://doi.org/10.1007/BF00878662>
- Insabato, A., Pannunzi, M., Rolls, E. T., & Deco, G. (2010a). Confidence-Related Decision Making, 539–547. <https://doi.org/10.1152/jn.01068.2009>.
- Insabato, A., Pannunzi, M., Rolls, E. T., & Deco, G. (2010b). Confidence-Related Decision Making, 539–547. <https://doi.org/10.1152/jn.01068.2009>
- Ioannidis, J. P. A. (2005). Why most published research findings are false. *PLoS Medicine*, *2*(8), 0696–0701. <https://doi.org/10.1371/journal.pmed.0020124>
- ISHIKAWA, T., MURAGAKI, Y., MARUYAMA, T., ABE, K., & KAWAMATA, T. (2016). Roles of the Wada Test and Functional Magnetic Resonance Imaging in Identifying the Language-dominant Hemisphere among Patients with Gliomas Located near Speech Areas. *Neurologia medico-chirurgica*, *28–34*. <https://doi.org/10.2176/nmc.0a.2016-0042>
- Jacobs, S., Brozzoli, C., & Farnè, A. (2012). Neglect: a multisensory deficit? *Neuropsychologia*, *50*(6), 1029–44. <https://doi.org/10.1016/j.neuropsychologia.2012.03.018>
- Jansen, A., Menke, R., Sommer, J., Förster, A. F., Bruchmann, S., Hempleman, J., ... Knecht, S. (2006). The assessment of hemispheric lateralization in functional MRI-Robustness and reproducibility. *NeuroImage*, *33*(1), 204–217. <https://doi.org/10.1016/j.neuroimage.2006.06.019>
- Kaas, J. H., & Hackett, T. A. (2000). Subdivisions of auditory cortex and processing streams in primates. *Proc Natl Acad Sci U S A*, *97*(22), 11793–11799. <https://doi.org/10.1159/000013783>
- Kaiser, J., & Lutzenberger, W. (2004). Frontal gamma-band activity in magnetoencephalogram during auditory oddball processing. *NeuroReport*, *15*(14), 2185–2188.
- Karnath, H. O. (2001). Spatial awareness is a function of the temporal not the posterior parietal lobe. *Nature*, *411*(6840), 950–953. <https://doi.org/10.1038/35082075>



- Karnath, H.-O., Fruhmann Berger, M., Küker, W., & Rorden, C. (2004). The anatomy of spatial neglect based on voxelwise statistical analysis: a study of 140 patients. *Cerebral cortex (New York, N.Y. : 1991)*, *14*(10), 1164–72. <https://doi.org/10.1093/cercor/bhh076>
- Katz, L. N., Yates, J. L., Pillow, J. W., & Huk, A. C. (2016). Dissociated functional significance of decision-related activity in the primate dorsal stream. *Nature*, *535*(7611), 285–288.
- Kennerley, S. W., Walton, M. E., Behrens, T. E., Buckley, M. J., & Rushworth, M. F. (2006). Optimal decision making and the anterior cingulate cortex. *Nature Neuroscience*, *9*(7), 940–947.
- Kepecs, A., Uchida, N., Zariwala, H. A., & Mainen, Z. F. (2008). Neural correlates, computation and behavioural impact of decision confidence. *Nature*, *455*(7210), 227–231. <https://doi.org/10.1038/nature07200>
- Kerkhoff, G. (2001). Spatial hemineglect in humans. *Progress in Neurobiology*, *63*(1), 1–27. [https://doi.org/10.1016/S0301-0082\(00\)00028-9](https://doi.org/10.1016/S0301-0082(00)00028-9)
- Kiani, R., & Shadlen, M. N. (2009). Representation of Confidence Associated with a Decision by Neurons in the Parietal Cortex. *Science*, *324*(5928), 759–764. <https://doi.org/10.1126/science.1169405>
- Kilian-hu, N., Valente, G., Vroomen, J., Formisano, E., Kilian-Hütten, N., Valente, G., ... Formisano, E. (2011). Auditory Cortex Encodes the Perceptual Interpretation of Ambiguous Sound. *The Journal of Neuroscience*, *31*(5), 1715–1720. <https://doi.org/10.1523/jneurosci.4572-10.2011>
- Kim, J. N., & Shadlen, M. N. (1999). Neural correlates of a decision in the dorsolateral prefrontal cortex of the macaque. *Nature neuroscience*, *2*(2), 176–185. <https://doi.org/10.1038/5739>
- Kinsbourne, M. (1970). The cerebral basis of lateral asymmetries in attention. *Acta Psychologica*, *33*(C), 193–201. [https://doi.org/10.1016/0001-6918\(70\)90132-0](https://doi.org/10.1016/0001-6918(70)90132-0)
- Koch, C., & Preuschhoff, K. (2007). Betting the house on consciousness. *Nature neuroscience*, *10*(2), 140–141. <https://doi.org/10.1038/nn0207-140>
- Komura, Y., Nikkuni, A., Hirashima, N., Uetake, T., & Miyamoto, A. (2013). Responses of pulvinar neurons reflect a subject's confidence in visual categorization. *Nature neuroscience*, *16*(6), 749–55. <https://doi.org/10.1038/nn.3393>

- Kraftt, C. E., Schwarz, N. F., Chi, L., Li, Q., Schaeffer, D. J., Rodrigue, A. L., ... McDowell, J. E. (2013). The location and function of parietal cortex supporting reflexive and complex saccades, a meta-analysis of a decade of functional MRI data, 9.
- Kravitz, D. J. (2011). A new neural framework for visuospatial processing. *Nature reviews. Neuroscience*, 12(4), 217–230. <https://doi.org/10.1167/11.11.923>
- Kunda1990PsychBulletin.pdf. (o. J.).
- Law, C.-T., & Gold, J. I. (2008). Neural correlates of perceptual learning in a sensory-motor, but not a sensory, cortical area. *Nat Neurosci*, 11(4), 505–513. <https://doi.org/10.1038/nn2070>
- Lewis, J. W., Beauchamp, M. S., & DeYoe, E. A. (2000). A comparison of visual and auditory motion processing in human cerebral cortex. *Cerebral Cortex*, 10(9), 873–88. <https://doi.org/10.1093/cercor/10.9.873>
- Li, Y., & Krishnamurthy, K. (2015). Is There a General Role for the Monkey Oculomotor System in Perceptual Decision-Making? *Journal of Neuroscience*, 35(27), 9783–9785. <https://doi.org/10.1523/JNEUROSCI.1818-15.2015>
- Liu, T., & Pleskac, T. J. (2011). Neural correlates of evidence accumulation in a perceptual decision task. *Journal of neurophysiology*, 106(5), 2383–98. <https://doi.org/10.1152/jn.00413.2011>
- Logothetis, N. K. (2008). What we can do and what we cannot do with fMRI. *Annual review of neuroscience*, 24(7197), 869–878. <https://doi.org/10.1038/nature06976>
- Macko, K. A., Jarvis, C. D., Kennedy, C., Miyaoka, M., Shinohara, M., Sokoloff, L., & Mishkin, M. (1982). Mapping the Primate Visual System with [<sup>14</sup>C]Deoxyglucose. *Science*, 218(4570), 394–397. <https://doi.org/10.1126/science.7123241>
- Macmillan, & Creelman. (2005). Detection theory: A user's guide (2nd ed.). *New York: Psychological Press*.
- Maeder, P. P., Meuli, R. a, Adriani, M., Bellmann, a, Fornari, E., Thiran, J. P., ... Clarke, S. (2001). Distinct pathways involved in sound recognition and localization: a human fMRI study. *NeuroImage*, 14(4), 802–16. <https://doi.org/10.1006/nimg.2001.0888>
- Mamassian, P. (2016). Visual Confidence. *Annual Review of Vision Science*, 2(1), annurev-vision-111815-114630. <https://doi.org/10.1146/annurev-vision-111815-114630>

- Masalski, M., & Kręcicki, T. (2013). Self-Test Web-Based Pure-Tone Audiometry: Validity Evaluation and Measurement Error Analysis. *Journal of Medical Internet Research*, *15*(4), e71. <https://doi.org/10.2196/jmir.2222>
- Metcalfe, J. E., & Shimamura, A. P. (1994). Metacognition: Knowing about knowing. *The MIT Press*.
- Mulder, M. J., van Maanen, L., & Forstmann, B. U. (2014). Perceptual decision neurosciences – A model-based review. *Neuroscience*, *277*, 872–884.  
<https://doi.org/10.1016/j.neuroscience.2014.07.031>
- Nagata, S. I., Uchimura, K., Hirakawa, W., & Kuratsu, J. I. (2001). Method for quantitatively evaluating the lateralization of linguistic function using functional MR imaging. *American Journal of Neuroradiology*, *22*(5), 985–991.
- Newsome, W., Britten, K., & Movshon, J. (1989). Neuronal correlates of a perceptual decision. *Nature*. <https://doi.org/doi:10.1038/341052a0>
- Newsome, W., & Pare, E. (1988). A selective impairment of motion perception following lesions of the middle temporal visual area (MT). *The Journal of Neuroscience*, *8*(6), 2201.
- Parton, A., Malhotra, P., & Husain, M. (2004). Hemispatial neglect. *Journal of Neurology, Neurosurgery, and Psychiatry*, *75*(1), 13–21.
- Pearson, J. M., Watson, K. K., & Platt, M. L. (2014). Decision making: the neuroethological turn. *Neuron*, *82*(5), 950–65. <https://doi.org/10.1016/j.neuron.2014.04.037>
- Pedersen, M. L. (2015). Evidence accumulation and choice maintenance are dissociated in human perceptual decision making. *PLoS ONE*, *10*(10), 1–20.  
<https://doi.org/10.1371/journal.pone.0140361>
- Pedersen, M. L., Endestad, T., & Biele, G. (2015). Evidence accumulation and choice maintenance are dissociated in human perceptual decision making. *PLoS ONE*, *10*(10), 1–20.  
<https://doi.org/10.1371/journal.pone.0140361>
- Persaud, N., McLeod, P., & Cowey, A. (2007). Post-decision wagering objectively measures awareness. *Nat Neurosci*, *10*(2), 257–261. <https://doi.org/10.1038/nn1840>

- Philiastides, M. G., Auksztulewicz, R., Heekeren, H. R., & Blankenburg, F. (2011). Causal role of dorsolateral prefrontal cortex in human perceptual decision making. *Current Biology*, *21*(11), 980–983. <https://doi.org/10.1016/j.cub.2011.04.034>
- Philiastides, M. G., & Sajda, P. (2007). EEG-informed fMRI reveals spatiotemporal characteristics of perceptual decision making. *Journal of Neuroscience*, *27*(August), 13082–13091. <https://doi.org/10.1523/JNEUROSCI.3540-07.2007>
- Philiastides, M. G., & Sajda, P. (2007). EEG-informed fMRI reveals spatiotemporal characteristics of perceptual decision making. *Journal of Neuroscience*, *27*(August), 13082–13091. <https://doi.org/10.1523/JNEUROSCI.3540-07.2007>
- Philiastides, M. G., & Sajda, P. (2007). EEG-informed fMRI reveals spatiotemporal characteristics of perceptual decision making. *Journal of Neuroscience*, *27*(August), 13082–13091. <https://doi.org/10.1523/JNEUROSCI.3540-07.2007>
- Phillips, D. P., Quinlan, C. K., & Dingle, R. N. (2012). Stability of central binaural sound localization mechanisms in mammals, and the Heffner hypothesis. *Neuroscience and biobehavioral reviews*, *36*(2), 889–900. <https://doi.org/10.1016/j.neubiorev.2011.11.003>
- Pierce, C. S., & Jastrow, J. (1884). On small differences in sensation. *Memoirs of the National Academy of Science*, *3*, 75-83. *Memoirs of the National Academy of Science*, *3*, 75–83.
- Pleger, B., Ruff, C. C., Blankenburg, F., Bestmann, S., Wiech, K., Stephan, K. E., ... Dolan, R. J. (2006). Neural coding of tactile decisions in the human prefrontal cortex. *The Journal of Neuroscience*, *26*(48), 12596–601. <https://doi.org/10.1523/JNEUROSCI.4275-06.2006>
- Pleskac, T. J., & Busemeyer, J. R. (2010). Two-stage dynamic signal detection: A theory of choice, decision time, and confidence. *Psychological Review*, *117*(3), 864–901. <https://doi.org/10.1037/a0019737>
- Poldrack, R. A. (2006). Can cognitive processes be inferred from neuroimaging data? *Trends in Cognitive Sciences*, *10*(2), 59–63. <https://doi.org/10.1016/j.tics.2005.12.004>
- Ptak, R. (2012). The Frontoparietal Attention Network of the Human Brain: Action, Saliency, and a Priority Map of the Environment. *The Neuroscientist*, *18*(5), 502–515. <https://doi.org/10.1177/1073858411409051>

- Purcell, B. A., Heitz, R. P., Cohen, J. Y., Schall, J. D., Logan, G. D., & Palmeri, T. J. (2010). Neurally constrained modeling of perceptual decision making. *Psychological review*, *117*(4), 1113–43. <https://doi.org/10.1037/a0020311>
- Ramsøy, T. Z., & Overgaard, M. (2004). Introspection and subliminal perception. *Phenomenology and the Cognitive Sciences*, *3*(1), 1–23. <https://doi.org/10.1023/B:PHEN.0000041900.30172.e8>
- Ratcliff, R. (1978). A theory of memory retrieval. *Psychological Review*, *85*(2), 59–108. <https://doi.org/10.1037/0033-295X.85.2.59>
- Ratcliff, & McKoon. (2008). The Diffusion Decision Model: Theory and Data for Two-Choice Decision Tasks. *Neural Computation*, *20*(4), 873–922.
- Ratcliff, & Smith. (2004). A Comparison of Sequential Sampling Models for Two-Choice Reaction Time. *Psychological Review*, *Vol 111*(2), 333–367.
- Rohe, T., & Noppeney, U. (2015). Cortical Hierarchies Perform Bayesian Causal Inference in Multisensory Perception. *PLOS Biology*, *13*(2), e1002073–e1002073. <https://doi.org/10.1371/journal.pbio.1002073>
- Roitman, J. D., & Shadlen, M. N. (2002). Response of neurons in the lateral intraparietal area during a combined visual discrimination reaction time task. *Journal of Neuroscience*, *22*(21), 9475–89. [https://doi.org/10.1016/S0377-2217\(02\)00363-6](https://doi.org/10.1016/S0377-2217(02)00363-6)
- Rolls, E. T., Grabenhorst, F., & Deco, G. (2010). Choice, difficulty, and confidence in the brain. *NeuroImage*, *53*(2), 694–706. <https://doi.org/10.1016/j.neuroimage.2010.06.073>
- Rolls, & Deco. (2010). The Noisy Brain: Stochastic Dynamics as a Principle of Brain Function. *Animal Behaviour*, *80*(1), 171. <https://doi.org/10.1016/j.anbehav.2010.04.019>
- Romanski, L. M., Tian, B., Fritz, J., Mishkin, M., Goldman-Rakic, P. S., & Rauschecker, J. P. (1999). Dual streams of auditory afferents target multiple domains in the primate prefrontal cortex. *Nature neuroscience*, *2*(12), 1131–6. <https://doi.org/10.1038/16056>
- Romo. (1998). Somatosensory discrimination based on cortical microstimulation. *Nature*, *392*(6674), 387–390. <https://doi.org/10.1038/32891>
- Rorden, C., Karnath, H.-O., & Bonilha, L. (2007). Improving lesion-symptom mapping. *Journal of cognitive neuroscience*, *19*(7), 1081–1088. <https://doi.org/10.1162/jocn.2007.19.7.1081>

- Rounis, E., Maniscalco, B., Rothwell, J. C., Passingham, R. E., & Lau, H. (2010). Theta-burst transcranial magnetic stimulation to the prefrontal cortex impairs metacognitive visual awareness. *Cognitive Neuroscience*, *1*(3), 165–175.  
<https://doi.org/10.1080/17588921003632529>
- Sandberg. (2010). Measuring consciousness: Is one measure better than the other? *Consciousness and Cognition*, *19*(4), 1069–1078. <https://doi.org/10.1016/j.concog.2009.12.013>
- Schneider, G. E. (1969). System Adversely, (February).
- Schultz. (1998). Predictive Reward Signal of Dopamine Neurons, 1–27.
- Schultz, W., Dayan, P., & Montague, P. R. (1997). A Neural Substrate of Prediction and Reward. *Science*, *275*(5306), 1593–1599. <https://doi.org/10.1126/science.275.5306.1593>
- Schwartenbeck. (2015). The dopaminergic midbrain encodes the expected certainty about desired outcomes. *Cerebral Cortex*, *25*(10), 3434–3445. <https://doi.org/10.1093/cercor/bhu159>
- Shadlen, M. N., & Kiani, R. (2013). Decision making as a window on cognition. *Neuron*, *80*(3), 791–806. <https://doi.org/10.1016/j.neuron.2013.10.047>
- Sharath Bennur and Joshua I. Gold. (2011). NIH Public Access, *72*(2), 181–204.  
<https://doi.org/10.1038/nature13314.A>
- Silver, M. A., & Kastner, S. (2009). Topographic maps in human frontal and parietal cortex. *Trends in cognitive sciences*, *13*(11), 488–95. <https://doi.org/10.1016/j.tics.2009.08.005>
- Steinberg, E. E., Keiflin, R., Boivin, J. R., Witten, I. B., Deisseroth, K., & Janak, P. H. (2013). A causal link between prediction errors, dopamine neurons and learning. *Nat Neurosci*, *16*(7), 966–973. <https://doi.org/10.1038/nn.3413>
- Stone. (1960). Models for choice reaction time. *Psychometrika*, *25*, 251–260.
- Teodorescu, & Usher. (2013). Disentangling decision models: From independence to competition. *Psychological Review*, *Vol 120*(1), 1–38.
- Thiebaut de Schotten, M., ffytche, D. H., Bizzi, A., Dell'Acqua, F., Allin, M., Walshe, M., ... Catani, M. (2011). Atlasing location, asymmetry and inter-subject variability of white matter tracts in the human brain with MR diffusion tractography. *NeuroImage*, *54*(1), 49–59.  
<https://doi.org/10.1016/j.neuroimage.2010.07.055>

- Thompson, S. K., von Kriegstein, K., Deane-Pratt, A., Marquardt, T., Deichmann, R., Griffiths, T. D., & McAlpine, D. (2006). Representation of interaural time delay in the human auditory midbrain. *Nat Neurosci*, *9*(9), 1096–1098. <https://doi.org/10.1038/nn1755>
- Tournier. (2016). Review of safety and mobility issues among older pedestrians. *Accident Analysis and Prevention*, *91*, 24–35. <https://doi.org/10.1016/j.aap.2016.02.031>
- Tsunada, J., Lee, J. H., & Cohen, Y. E. (2011). Representation of speech categories in the primate auditory cortex. *Journal of neurophysiology*, *105*(6), 2634–2646. <https://doi.org/10.1152/jn.00037.2011>
- Uchida, N., & Mainen, Z. F. (2003). Speed and accuracy of olfactory discrimination in the rat. *Nat Neurosci*, *6*(11), 1224–1229. <https://doi.org/10.1038/nn1142>
- Usher, M., & McClelland, J. L. (2001). The time course of perceptual choice: the leaky, competing accumulator model. *Psychological review*, *108*(3), 550–592. <https://doi.org/10.1037/0033-295X.108.3.550>
- Uttenweiler. (1980). Dichotischer Diskriminationstest für Kinder. *Sprache Stimme Gehör*, (4), 107–111.
- Vallar, G., & Perani, D. (1986). The anatomy of unilateral neglect after right-hemisphere stroke lesions. A clinical/CT-scan correlation study in man. *Neuropsychologia*, *24*(5), 609–622. [https://doi.org/10.1016/0028-3932\(86\)90001-1](https://doi.org/10.1016/0028-3932(86)90001-1)
- Vesia, M., & Crawford, J. D. (2012). Specialization of reach function in human posterior parietal cortex. *Experimental Brain Research*, *221*(1), 1–18. <https://doi.org/10.1007/s00221-012-3158-9>
- Vickers, D., & Packer, J. (1982). Effects of alternating set for speed or accuracy on response time, accuracy and confidence in a unidimensional discrimination task. *Acta Psychologica*, *50*(2), 179–197. [https://doi.org/10.1016/0001-6918\(82\)90006-3](https://doi.org/10.1016/0001-6918(82)90006-3)
- Vossel, S., Eschenbeck, P., Weiss, P. H., Weidner, R., Saliger, J., Karbe, H., & Fink, G. R. (2011). Visual extinction in relation to visuospatial neglect after right-hemispheric stroke: quantitative assessment and statistical lesion-symptom mapping. *Journal of neurology, neurosurgery, and psychiatry*, *82*, 862–868. <https://doi.org/10.1136/jnnp.2010.224261>

- Wager, T. D., Lindquist, M., & Kaplan, L. (2007). Meta-analysis of functional neuroimaging data: Current and future directions. *Social Cognitive and Affective Neuroscience*, 2(2), 150–158. <https://doi.org/10.1093/scan/nsm015>
- Wang. (2002). Probabilistic decision making by slow reverberation in cortical circuits. *Neuron*, 36(5), 955–968. [https://doi.org/10.1016/S0896-6273\(02\)01092-9](https://doi.org/10.1016/S0896-6273(02)01092-9)
- Wang. (2008). Decision making in recurrent neuronal circuits. *Neuron*, 60(2), 215–34. <https://doi.org/10.1016/j.neuron.2008.09.034>
- Wardak, C., Olivier, E., & Duhamel, J.-R. (2002). Saccadic target selection deficits after lateral intraparietal area inactivation in monkeys. *The Journal of neuroscience : the official journal of the Society for Neuroscience*, 22(22), 9877–84.
- Warren, J. D., Zielinski, B. A., Green, G. G. R., Rauschecker, J. P., & Griffiths, T. D. (2002). Perception of sound-source motion by the human brain. *Neuron*, 34(1), 139–148. [https://doi.org/10.1016/S0896-6273\(02\)00637-2](https://doi.org/10.1016/S0896-6273(02)00637-2)
- Weber, M. J., & Thompson-Schill, S. L. (2010). Functional neuroimaging can support causal claims about brain function. *Journal of cognitive neuroscience*, 22(11), 2415–6. <https://doi.org/10.1162/jocn.2010.21461>
- Wilke, M., Kagan, I., & Andersen, R. A. (2012). Functional imaging reveals rapid reorganization of cortical activity after parietal inactivation in monkeys. <https://doi.org/10.1073/pnas.1204789109/-/DCSupplemental.www.pnas.org/cgi/doi/10.1073/pnas.1204789109>
- Williams, G. V., & Goldman-Rakic, P. S. (1995). Modulation of memory fields by dopamine D1 receptors in prefrontal cortex. *Nature*. <https://doi.org/10.1038/376572a0>
- Woldorff, M. G., Tempelmann, C., Fell, J., Tegeler, C., Gaschler-Markefski, B., Hinrichs, H., ... Scheich, H. (1999). Lateralized auditory spatial perception and the contralaterality of cortical processing as studied with functional magnetic resonance imaging and magnetoencephalography. *Human brain mapping*, 7(1), 49–66.



Zatorre, R. J., & Penhune, V. B. (2001). Spatial localization after excision of human auditory cortex.

*The Journal of neuroscience : the official journal of the Society for Neuroscience*, 21(16),

6321–8. <https://doi.org/21/16/6321> [pii]

## 9. Curriculum Vitae

Ahmad M. Nazzal

### **Personal:**

Place and Date of Birth: Amman Jordan | 25. Nov 1986

Email: nazzal2009@gmail.com

### **Education:**

- (2013- 2017) Ph.D. in neuroscience, University of Göttingen, Germany.
- (August 2013) Completed first year of the M.Sc. /Ph.D. Neurosciences program, university of Goettingen, Germany.
- (June 2011) Doctor of Medicine (M.D), University of Jordan.

### **Scholarships:**

- (2013-2014) Ph.D. Stipend from the German Primate center (DPZ).
- (Oct-Jan 2013) Ph.D. bridging stipend from Göttingen Graduate School for Neurosciences, Biophysics, and Molecular Biosciences (*GGNB*).
- (2012–2013) Stipend of the Excellence Foundation for the Promotion of the Max Planck Society.
- (2005–2011) Scholarship from her Royal Majesty Queen Rania Al-Abdullah for studying Medicine at the University of Jordan, Amman, Jordan
- (2004–2005) Academic excellence scholarship for studying computer engineering at H.R.H. Princess Sumaya University for Technology, Amman, Jordan
- (2001–2004) Full Scholarship Al-Mashrek International School, Amman, Jordan

### **Travel grants:**

- (July 2016) Forum of European neuroscience conference Copenhagen, Denmark.
- (November 2016) Society of neuroscience conference San Diego, USA.
- (June 2015) Model based neuroscience school university of Amsterdam.

## **Publications:**

- (2017) *Reach and grasp deficits following damage to the dorsal pulvinar. Melanie Wilke, Lukas Schneider, Adan-Ulises Dominguez-Vargas, Yuranny Cabral-Calderin, Carsten Schmidt-Samoa<sup>1</sup>, Kristina Miloserdov, Ahmad Nazzal, Peter Dechent, Hansjörg Scherberger<sup>2</sup>, Igor Kagan, Mathias Bähr. submitted*
- (2017) *Dissociated neural signature of sensory evidence accumulation and decision-monitoring. A. Nazzal, Y. Liao, C. Schmidt Samoa, J. Erlich, M. Wilke. In prep*
- (2016) *Modality-specific neural signature of evidence accumulation in sensory cortices. A. Nazzal, C. Schmidt Samoa, J. Erlich, M. Wilke. In prep*
- (2016) Poster: Modality-specific neural signature of evidence accumulation in sensory cortices. A. Nazzal, C. Schmidt Samoa, J. Erlich, M. Wilke FENS Copenhagen Denmark
- (2016) Poster: Modality-specific neural signals of evidence accumulation for spatial decisions in healthy and hemispatial neglect patients. A. Nazzal, C. Schmidt Samoa, M. Holzgraefe, M. Bähr, J. Erlich, M. Wilke SfN San Diego USA

## **Lab Experience:**

- (May-Jul 2013) Transcranial static magnetic stimulation effect on implicit learning neurophysiology department university hospital of Goettingen.
- (March-May 2013) Central Pontine Myelinolysis animal model for Multiple Sclerosis, neuropathology department university hospital Goettingen.
- (Jan-Mar 2013) Study the effect of Myelin deficiency on acute electrophysiology auditory cortex in Shiverers, Neurogenetics department MPI-EM.

## **Training courses:**

- (February 2016) Clinical training in neurology in neurology department university of Göttingen.
- (March 2015) Theory and practice of transcranial brain stimulation department of clinical neurophysiology university medical center of Goettingen.
- (June 2015) Model-based neuroscience school university of Amsterdam.

**Supervision:**

(2015-2016) Yian Liao Confidence in visual and auditory decision making, master thesis.

(2014-2015) Marie Dewenter Visual spatial perceptual decision making in healthy participants, fMRI Study, bachelor thesis.

**Teaching:**

(2015-2016) Curriculum tutorial of the MSc/PhD Neuroscience Program of the International Max Planck Research School "Reward and Decision Making/Consciousness" (4x4h/year)

**Languages:**

Native Arabic speaker.

Fluent English speaker and writer.

Professional German language command (B2).

Matlab programming language.